5-2019

Cool and Warm Season Climate Signals in Tree Rings from North America

Max Carl Arne Torbenson
University of Arkansas, Fayetteville

Cool and Warm Season Climate Signals in Tree Rings from North America

A dissertation submitted in partial fulfillment
of the requirements for the degree of
Doctor of Philosophy in Geosciences

by

Max Torbenson
Queen's University Belfast
Bachelor of Science in Archaeology-Palaeoecology, 2011
University of Minnesota
Master of Arts in Geography, 2014

May 2019
University of Arkansas

This dissertation is approved for recommendation to the Graduate Council.

_____
David Stahle, Ph.D.
Dissertation Director

_____
Malcolm Cleaveland, Ph.D.
Committee Member

_____
Song Feng, Ph.D.
Committee Member

_____
Frederick Paillet, Ph.D.
Committee Member

Abstract

Earlywood (EW) and latewood (LW) ring-width chronologies have become an increasingly important proxy in paleoclimate reconstructions. These subannual variables can provide estimates of past hydroclimate variability for seasonal windows that total ring-widths cannot resolve. The strength of the relationship between EW and LW series may influence what type of paleoclimate information is embedded within the tree-ring series. High correlations (> 0.70) between EW and LW are recorded for much of the continent but the magnitude of correlation varies greatly across space and species boundaries. Using four LW chronologies from shortleaf pine, the North American conifer species displaying the lowest EW-LW correlation, a reconstruction of summer atmospheric moisture balance spanning the years 1685-2015 was produced for the central United States. A second reconstruction, based on ten EW and total-ring width chronologies from three other species, estimates May soil moisture for the same period. The relationship between reconstructions displays strong decadal swings in both instrumental and reconstructed data that could potentially improve forecasting skill of summer rainfall. The Atlantic Multidecadal Oscillation (AMO) appears to dictate the changing persistence in seasonal hydroclimate and the reconstructions suggest that this ocean-atmosphere forcing has been a stable feature of North American climate dynamics over the past 300 years. Finally, this dissertation investigates the temporal stability of El Niño-Southern Oscillation (ENSO) signals in the North American tree-ring network in relation to AMO phasing. Numerous reconstructions of ENSO have been produced relying on tree-ring chronologies from the American Southwest as predictors, however, the teleconnection between ENSO and local hydroclimate has varied in strength and spatial expression during the 20th and early 21st century. There is a significant loss of tree-ring records exhibiting significant correlations with ENSO during subperiods associated

with the negative phase of the AMO. A new reconstruction, relying solely on a subset of chronologies with time-stable ENSO signals, was produced. When compared to the North American Drought Atlas for the past 350 years, similar expansions and retractions of ENSO influence from the core region of northern Mexico and the border states of the United States seen in the instrumental period/data are recorded.

Acknowledgements

First and foremost, my thanks go out to my advisor, Dr. David Stahle. My time as his PhD student has been filled with a lot of laughter, more than one nickname, great conversations (as well as a few disagreements), and several stints of fieldwork in several different states and countries. More than anything though, my years in the Tree-Ring Laboratory has been filled with learning. Dr. Stahle is the main reason I have become a better field worker (arguably), analysist (arguably), writer (arguably), and person (highly arguably). I am also grateful for the continuous support and advice from my committee members Drs. Malcolm Cleaveland, Song Feng, and Frederick Paillet. Ian Howard has provided help, input, and collaboration since the day we both joined the lab. I also acknowledge the Department of Geosciences for financial support to attend conferences, and in particular Dr. Christopher Liner for extending this support to publication costs.

I am thankful to a large number of scientists from other institutions that have provided help during parts or throughout my dissertation work, including Drs. Dorian Burnette, Ed Cook, Daniel Griffin, Michael Stambaugh, José Villanueva-Díaz, and Park Williams. My thanks also go out to Dr. Ana Carolina Barbosa and (past and present) members of the tree-ring lab at the Universidad Federal de Lavras (Brazil), Drs. Ricardo Villalba and Lidio Lopez (CONICET, Argentina), and Dr. Jochen Schöngart (INPA, Brazil).

Outside the confinement of the Fayetteville campus, a large number of people have been instrumental in keeping me focused, including but not limited to Justin Allison, Hans Dennenfelser, Steve Dickerson, James Gates, Enrique Irigoyen, Mackenzie Lea, Keith Warford, and Brian and Sharon Waters. Finally, I would like to express my gratitude for the continuous support from my parents. Without them I would not be where I am today.

Dedication

To my parents.

Table of Contents

Chapter 1..... 1

Introduction

Chapter 2..... 16

The relationship between earlywood and latewood ring-growth across North America

References..... 32

Tables..... 37

Figures..... 40

Chapter 3..... 48

The relationship between cool and warm season moisture balance over the central United States, 1685-2015

References..... 72

Tables..... 79

Figures..... 82

Chapter 4..... 90

Multidecadal modulation of the ENSO teleconnection to precipitation and tree growth over subtropical North America

References..... 110

Tables..... 115

Figures..... 117

Chapter 5..... 125

Conclusions

References..... 129

List of Published Papers

Chapter 2:
Torbenson, M.C.A., D.W. Stahle, J. Villanueva Díaz, E.R. Cook, and D. Griffin, 2016. The relationship between earlywood and latewood ring-growth across North America. *Tree-Ring Research* **72**: 53-66.

Chapter 3:
Torbenson, M.C.A., and D.W. Stahle, 2018. The relationship between cool and warm season moisture over the central United States, 1685-2015. *Journal of Climate* **31**: 7909-7924.

Chapter 4:
Torbenson, M.C.A., D.W. Stahle, I.M. Howard, D.J. Burnette, J. Villanueva Díaz, E.R. Cook, and D. Griffin (accepted) Multidecadal modulation of the ENSO teleconnection to precipitation and tree growth over subtropical North America. *Paleoceanography and Paleoclimatology*.

CHAPTER 1

INTRODUCTION

Our current observations of precipitation and temperature are often too short to provide robust analyses on long-term climate change and variability (Bradley 1985). The instrumental period may not encompass the full natural variability of the climate system and some strong dynamical forcings on North American hydroclimate are decadal to multi-decadal in scale, which means that even 120 years of instrumental data may only cover two or three full cycles of oscillation. Climate models of the past millennium suggest that droughts more severe and sustained than any witnessed during the 20th and 21st centuries, so-called megadroughts, have occurred in the recent past (Ault et al. 2018). Proxy records used to extend our temporally-limited instrumental record come in many forms, including historical records (e.g. Rodrigo et al. 2001; Therrell and Trotter 2011), lake sediments (e.g. Brauer et al. 1999), ice cores (e.g. Kobashi et al. 2007), and tree rings (e.g. Fritts 1965; Stahle et al. 2009). Each type of proxy has advantages and limitations, however, due to the widespread spatial distribution of trees and the annual resolution of their growth layers, tree rings are considered the pinnacle for reconstructing climate variability over the most recent millennium.

The principal behind cross-dating, a common growth response to climate across a stand of trees, also allows for the reconstruction of past climate variability (Fritts 1965). In cold environments, such as high latitudes and high altitudes, the climate variable that limits growth is usually growing-season temperature (e.g. Jacoby and D'Arrigo 1989; Esper et al. 2002; Salzer et al. 2009). In arid environments, such as the American Southwest, tree growth is mainly limited by moisture availability during growth (Fritts 1976). Depending on the seasonality of the local climate, trees can record pre-growing season rainfall, precipitation during the growing season, or both. Blue oak chronologies from California have an exceptionally strong winter precipitation

signal (e.g. Stahle et al. 2013), and the growth of many conifer species in Mexico, and the US Southwest, are also correlated with winter or spring rainfall (e.g. Fritts 1966; Stahle and Cleaveland 1988; D'Arrigo and Jacoby 1991; Villanueva-Díaz et al. 2007). In eastern United States, where winter rainfall does not make up as large portion of the annual precipitation total as in the West, tree-ring chronologies tend to be correlated higher with spring and/or summer moisture. Bald cypress (*Taxodium distichum*) records have been used to reconstruct summer drought conditions over 1500 years back in time (Stahle et al. 1988).

The North American Drought Atlas (NADA; Cook et al. 1999) is a 0.5 x 0.5 gridded reconstruction of summer Palmer Drought Severity Index (PDSI, Palmer 1965) and represents one of the most important contributions to paleoclimatology in the past two decades. The transition from reconstructing individual time-series of local and/or regional climate variability to gridded networks has allowed paleoclimate data to become increasingly relevant for the wider climate science, historical, and archaeological communities. The NADA has been used extensively in climate modeling (e.g. Herweijer et al. 2007; Cook et al. 2011), ecology (Speer et al. 2001; McKenzie et al. 2004), and climate-social interactions (DeMenocal 2001; Guyette et al. 2002; Stahle and Dean 2011). The high prescribed month-to-month persistence in PDSI facilitates reconstruction on continental scale, without too much compromise on any regional scale. However, due to differences in regional climatology and species used, the NADA contains diverse seasonal precipitation signals across its spatial domain (St. George et al. 2010). These discrete seasonal tree-ring proxies could be used to produce separate estimates of the cool and warm season moisture balances over much of subtropical and temperate North America.

The following dissertation is part of a larger effort to produce gridded reconstructions of seasonal precipitation under the NSF P2C2 award #AGS-1266014. Each chapter investigates a

different aspect of paleoclimate reconstruction, including evaluation of the characteristics of tree-ring chronology relationships, the development of new predictors and new regional reconstructions, and the examination of ocean-atmosphere teleconnections on predictor signal stability. The nuances in hydroclimate signals embedded in tree rings from across North America will allow for separately reconstructed estimates of cool and warm season precipitation, offering seasonal information that cannot be obtained from the NADA and its long-term persistent PDSI estimates.

Subannual measurements of growth and their potential in seasonal dendroclimatology

Total ring widths (TRW) has been the vastly dominant variable of growth used in tree-ring studies since the modern foundation of the field (Douglass 1920; Glock 1937; Douglass 1941; Fritts et al. 1965). The division of the annual ring into earlywood (EW) and latewood (LW) widths was rare for most of the 20th century, however, studies that explored these subannual growth variables showed that additional information could be extracted (e.g. Douglas 1919; Paul and Marts 1931; Schulman 1942; Cleaveland 1986). Dendroclimatology has seen an increase in the application of EW and LW measurements over the past 20 years (e.g. Watson and Luckman 2004; Stahle et al. 2009; Crawford et al. 2015), utilizing the seasonal climate signal that often is embedded in EW and/or LW widths.

The introduction of adjusted LW measurements (LW_a), produced from regressing LW on EW, has provided a new subannual variable with LW variance independent from the EW (Meko and Baisan 2001). The second chapter of this dissertation explores the relationship between EW and LW growth across North America, using 197 pairs of chronologies from a wide range of species. Differences in LW-EW persistence, EW-LW correlation, and changing variance, will likely affect how tree ring variables record climate variability. Understanding how the

characteristics of EW and LW change across space and species boundaries could therefore lead to better approaches when selecting predictors for climate reconstruction.

The traditional TRW variable correlated with traditional climate season windows (St. George 2014) is mapped for a network of 1427 chronologies in **Figure 1**. Spearman rank-order correlations were calculated for each standard chronology and the closest CRU TS v.4.01 grid point (Harris et al. 2014) precipitation data for a range of averaged seasonal windows. Distinct geographical features can be distinguished, associated with the regional climatology and species differences. Lagged summer signals (precipitation from the year prior to growth affecting current year's growth) is present in the Northeast, around the Great Lakes, and the Pacific Northwest (**Figure 1a**). The US Southwest, which is home to the largest number of chronologies in the network, displays the largest number of significant correlations during cool months (e.g. SON, **Figure 1b**; DJF, **Figure 1c**; MAM, **Figure 1d**). A similar seasonal response can be found in California, however, here most chronologies do not record precipitation variability for the prior SON window. Chronologies from Mexico also appear to have a later response, perhaps mainly confined to DJF.

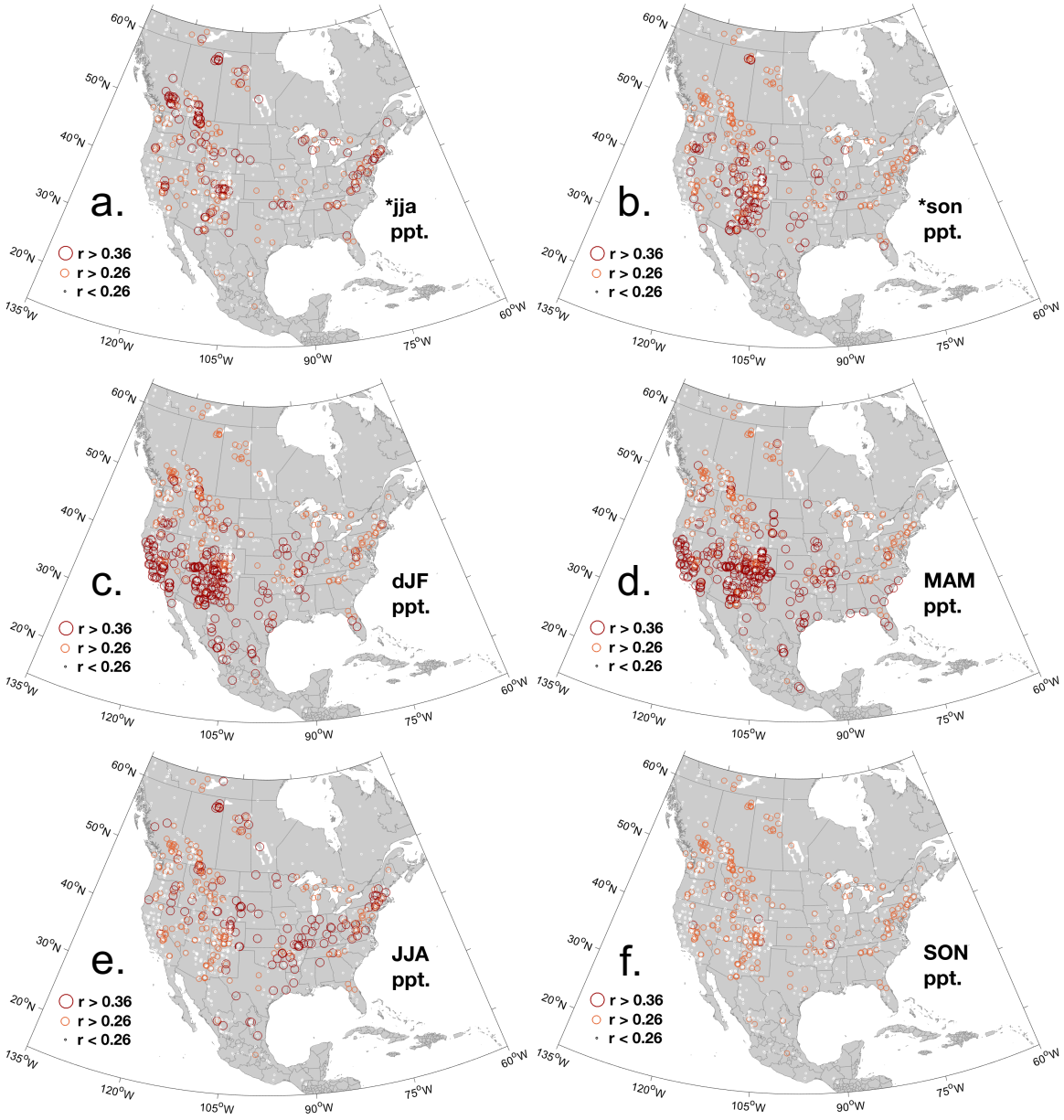

Figure 1. Levels of significance (r > 0.26 = $p < 0.05$; r > 0.36 = $p < 0.01$) for correlations between seasonal precipitation and the TRW for 1928-1979, for seasonal windows (a) prior JJA; (b) prior SON; (c) dJF; (d) MAM; (e) JJA; and (f) SON. Note that only five of 1427 chronologies display highly significant correlations with current SON precipitation.

Identifying target windows for seasonal hydroclimate reconstructions require several considerations. It is clear from the spatial evolution of climate signals presented in **Figure 1** that compromises are needed to produce continental reconstructions for uniform seasonal windows. Because many of the chronologies are significantly correlated with more than one of the traditional three-month season, extending the target to a longer window yields better results (i.e. a higher number of significant chronologies and their distribution across space), which is also the reason why summer PDSI was chosen for the NADA (Cook et a. 1999). Counts of TRW chronologies significantly correlated with cool and warm season precipitation totals are presented in **Table 1**. Extending the cool season from prior December to current May produces the highest number of potential predictors. However, to provide new information from the NADA one must also consider the season-to-season relationship in the instrumental data.

Table 1. Counts of TRW chronologies from the North American tree ring network (n = 1427) displaying significant correlations (1928-78) with local precipitation for different seasonal windows.

	Overall		**Discrete**	
	p < 0.05	*p < 0.01*	*p < 0.05*	*p < 0.01*
dJFMA	521	427	265	290
MJJ	496	349	242	212
dJFMAM	577	477	366	387
JJ	375	229	167	139
dJFMAM	577	477	453	424
JJA	260	157	138	104

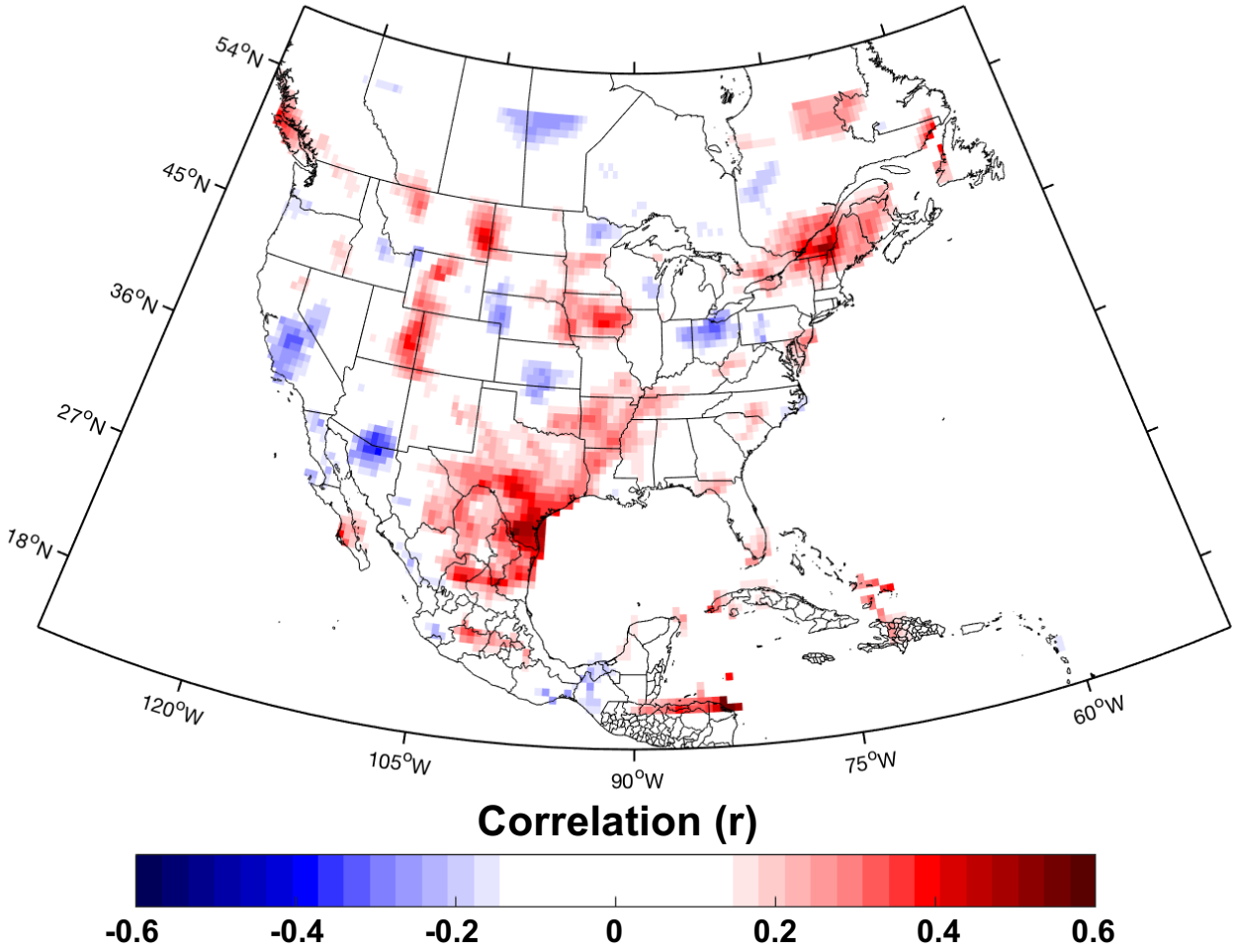

Figure 2. Correlation between CRU gridded dJFMA and MJJ precipitation across North America, for the period 1928-78.

Although there is some persistence between cool and warm season precipitation across North America (**Figure 2**), there is a risk of inflating this relationship by including chronologies that record both cool and warm season precipitation signals. If only considering chronologies that are significantly correlated with precipitation for a single seasonal window (correlated with the cool season but not the warm season, or vice versa), the number of potential predictors lowers drastically. This test to identify *discrete* predictors is especially affecting the predictor counts for the dJFMAM/JJ seasonal configuration (**Table 1**).

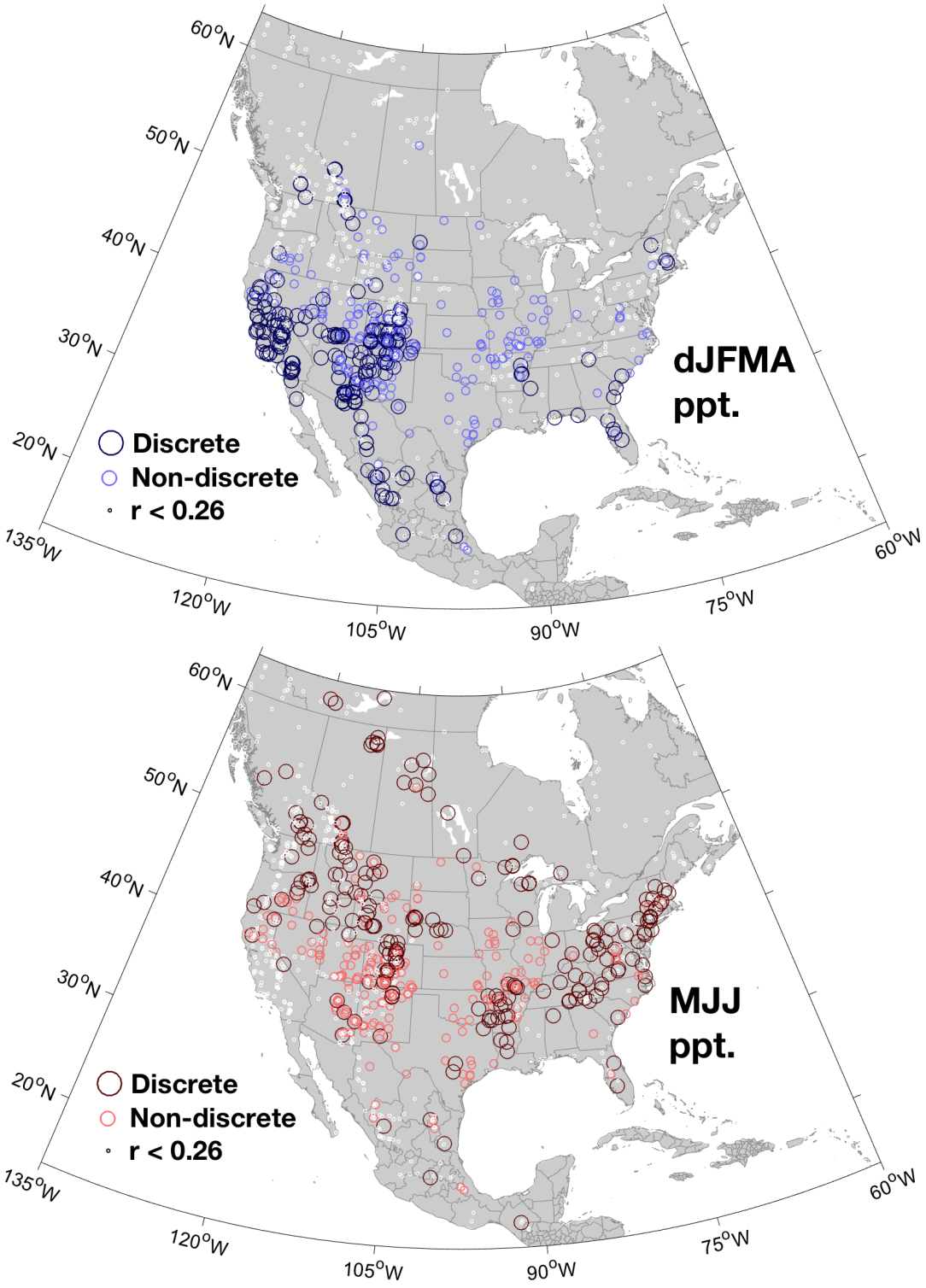

Figure 3. Location of TRW chronologies that display statistically significant ($p < 0.05$) correlations with local dJFMA (top) and MJJ (bottom) precipitation for the period 1928-1978, with discrete ($p < 0.05$ with target season and $p > 0.05$ with alternate season) in darker color and non-discrete ($p < 0.05$ with both target and alternate season) in lighter color.

The number of discrete TRW predictors are most even between seasons when allowing the month of May to be considered as a warm season component (**Table 1**). In total, 18.6% of TRW chronologies are discretely ($p < 0.05$) correlated with dJFMA precipitation and 17% are discretely correlated with MJJ precipitation. The distribution of discrete dJFMA and MJJ predictors across North America (**Figure 3**) is also better than for other seasonal configurations (not shown). Western United States and Mexico are still dominated by cool season predictors, and the majority of predictors in eastern United States are chosen for the warm season, but all of subtropical North America have significant discrete predictors within a 500-km search radius for both seasons.

It is worth noting that the results reported above are for standard ARSTAN chronologies (Cook 1985). When residual chronologies are analyzed, the list of chronologies with discrete signals is significantly different (not shown). However, the relative number of chronologies remain the most even between seasons for the dJFMA and MJJ seasonal configurations. Furthermore, the closest CRU grid point may not necessarily represent the local precipitation variability at the site of the tree-ring chronology. Correlating the tree-ring data with the closest grid point *and* the surrounding eight grid points, or using a Queen's Case smoothing approach on the center grid point (Lloyd 2010), is likely to produce higher numbers of discrete predictors for both seasons.

Table 2. Counts of EW/LW/LW_a chronologies from the North American tree ring network (n = 372) displaying significant correlations (1928-78) with local precipitation for different seasonal windows.

	Overall		**Discrete**	
	p < 0.05	*p < 0.01*	*p < 0.05*	*p < 0.01*
dJFMA	187	148	116	110
MJJ	199	161	152	132
dJFMAM	206	171	174	155
JJ	185	139	161	130
dJFMAM	206	171	172	159
JJA	171	124	145	111

The addition of subannual chronologies to the analysis greatly increases the number of potential predictors for both seasons (**Table 2**), underlining the seasonal division of both tree growth and climate signals that EW and LW chronologies represent. For a site to count towards both seasons in **Table 2**, EW *and* LW/LW_a chronologies would need to be discretely correlated for *different* seasons (e.g. both EW and LW could not be considered for the same season). The Douglas-fir chronologies from Bear Canyon, Arizona, represents an example of the seasonal potential in subannual measurements. The EW chronology displays high correlation with dJFMA (r = 0.627) and low correlation with MJJ (r = 0.028) making it a discrete cool season predictor. The LW is significantly correlated with both seasons (r = 0.394 for dJFMA and r = 0.432 for MJJ), failing the discretion test. However, the LW_a chronology is discrete with MJJ (r = 0.092 and 0.564 respectively), and the site thus provides discrete predictors for both seasons. A higher percentage of chronologies from the EW/LW/LW_a qualify as discrete predictors than for the TRW network. Out of the 372 EW and LW chronology pairs, 116 (31.2%) are discretely correlated with the dJFMA cool season and 152 (40.9%) with the MJJ warm season (**Figure 4**).

Of the 116 cool season predictors, 101 are EW chronologies. Of the 152 warm season predictors, 136 are either LW or LW_a chronologies.

The seasonal windows identified for continental-wide reconstruction of precipitation are not necessarily optimal for all regions across North America. The role May precipitation plays in growing season conditions is evident in chronology count comparisons between dJFMA/MJJ and dJFMAM/JJ (or dJFMAM/JJA), especially so for total-ring width chronologies. There is significant potential for increasing not just the number of predictors, but also the signal strength of predictors, by confining the spatial coverage of the reconstructions. Shortleaf pine (*Pinus echinata*) displays the lowest average correlation between EW and LW of any conifer species in North America (Torbenson et al. 2016), suggesting that the uniquely strong JJA precipitation signal originally identified by Schulman (1942) is truly independent from biological persistence recorded in other regions (e.g. Griffin et al. 2013). The third chapter presents two seasonally discrete reconstructions of May self-calibrated PDSI and June-through-August (JJA) atmospheric moisture for the central United States, utilizing the summer signal in shortleaf pine.

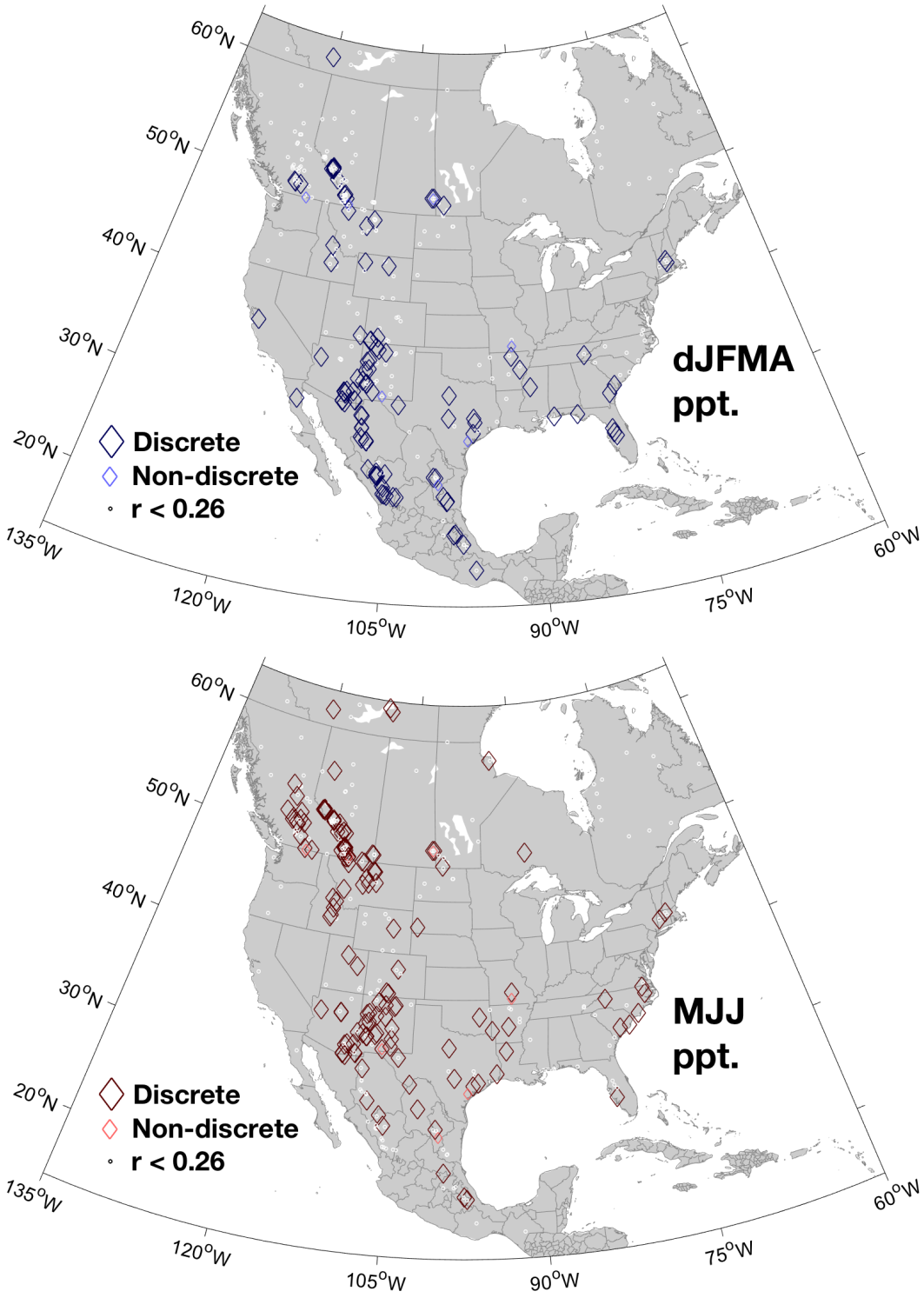

Figure 4. Location of subannual chronologies that display statistically significant ($p < 0.05$) correlations with local dJFMA (top) and MJJ (bottom) precipitation for the period 1928-1978. Markers can indicate more than one discrete chronology from each site (e.g. EW and LW).

Reconstructing teleconnections to North American hydroclimate

The role of teleconnections in North American precipitation and temperature variability is well studied (e.g. Allan et al. 1996). Similar to our temporally limited observational records of local climate, teleconnection indices are constrained to the period from the late 19th century to present. Tree ring-based proxy reconstructions of ENSO (e.g. Stahle et al. 1998; D'Arrigo et al. 2005; Li et al. 2013), the Atlantic Multidecadal Oscillation (AMO, Gray et al. 2004); the North Atlantic Oscillation (NAO, Cook et al. 2002; Trouet et al. 2009); and the Pacific Decadal Oscillation (PDO; D'Arrigo et al. 2001; MacDonald and Case 2005) have extended the instrumental indices and provided additional information about the variability of these important ocean-atmosphere processes. However, such reconstructions are highly sensitive to predictor selection and past estimates of the same teleconnection index often disagree on magnitude and even sign for individual years or longer periods (e.g. Gergis and Fowler 2009; Kipfmueller et al. 2012).

The fourth chapter of this dissertation explores the role ENSO plays in the variability of winter precipitation, and subsequent tree growth, across subtropical North America. The strongest correlations between ENSO and North American climate are recorded for northern Mexico and southwestern United States (Allan et al. 1996), where El Niño conditions bring cooler and wetter conditions and La Niña conditions are associated with warmer and drier conditions. However, as previously showed by Cole and Cook (1999), ENSO forcing on summer soil moisture is not uniform over time and space across the US Southwest. This time-dependent signal also appears to be recorded by tree-ring chronologies from the same region. Two reconstructions of ENSO influence are produced, one that excludes chronologies with non-stable ENSO signals (i.e. when ENSO correlations are only significant for subperiods of the full

instrumental period) and one that does not discriminate predictors based on signal stability. Comparisons of the two reconstructions indicate that the inclusion of tree-ring chronologies with non-stable ENSO signals greatly degrades the skill of past estimates, perhaps most so in the low-frequency periodicities.

CHAPTER 2

THE RELATIONSHIP BETWEEN EARLYWOOD AND LATEWOOD RING-GROWTH ACROSS NORTH AMERICA

M. C. A. TORBENSON[1], D. W. STAHLE[1], J. VILLANUEVA DÍAZ[2], E. R. COOK[3], and **D. GRIFFIN[4]**

[1]Department of Geosciences, University of Arkansas, AR, USA

[2]INIFAP, Gómez Palacio, Durango, Mexico

[3]Lamont-Doherty Earth Observatory, Columbia University, NY, USA

[4]Department of Geography, Environment and Society, University of Minnesota, MN, USA

ABSTRACT

The relationship between earlywood width (EW) and latewood width (LW) is investigated using 197 tree-ring collections representing several tree species from across the North American continent. Chronologies of LW have limited paleoclimate value when they have low variance or very high correlation with EW from the same site. The correlation of LW and EW can be removed by taking the residuals from linear regression to provide a chronology of discrete latewood growth free from the carryover effects of prior EW (the so-called adjusted latewood chronology, LW_a). The correlation between EW and LW, along with LW_a variance, varies dramatically across North America. The lowest correlations between EW and LW chronologies can be found in *Pseudotsuga menziesii* in the summer monsoon region of northwestern Mexico. Low correlations between EW and LW chronologies are also noted for *Pinus echinata* and *Quercus stellata* in the south-central United States. *Q. stellata* also displays the highest LW_a

variance among any species in the dataset. For three conifer species, correlations between EW and LW appear to increase with the biological age of the tree. An age-related decline in LW_a variance was also detected for Douglas-fir, bald cypress and ponderosa pine older than 200 years. These results imply that heavy sampling to produce "age-stratified" chronologies based on trees ≤ 200 years in age throughout the record may produce the best quality LW chronologies with the highest variance and most discrete growth signal independent from EW.

Keywords: Dendrochronology, earlywood, latewood, North America, seasonal growth.

INTRODUCTION

Tree-ring records are among the most important proxy archives of past climate (Bradley 1985) and are widely used as a dating tool in the fields of ecology (Schweingruber 1996), archaeology (Baillie 1982), and geomorphology (Stoffel and Bollschweiler 2008). Total ring-width (TRW) is the most common of the many different growth variables that can be measured and thousands of TRW chronologies have been developed over the past 100 years (Grissino-Mayer and Fritts 1997; St. George 2014). The relationship between climate variability and TRW has facilitated regional to hemispheric scale reconstructions of temperature and soil moisture balance (Cook *et al*. 1999; Esper *et al*. 2002), which have provided valuable perspectives of past social and environmental change (Villalba *et al*. 1994; Watson and Luckman 2004; Stahle *et al*. 2007; Buckley *et al*. 2010).

The network of earlywood width (EW) and latewood width (LW) chronologies covering large parts of North America has been developed over several decades but has seen a rapid increase in numbers in recent years. These growth variables may contain discrete subannual climate information and have been used for seasonal climate reconstructions (*e.g.* Stahle *et al*. 1998; Meko and Baisan 2001; Villanueva Díaz *et al*. 2007). In general, EW records display high correlations with climate for months prior to or during the early part of the growing season (Villanueva Díaz *et al*. 2007; Stahle *et al*. 2009; Meko *et al*. 2013; Dannenberg and Wise 2016) whereas LW chronologies tend to show higher correlations with climate during the later stages of the growing season (Meko and Baisan 2001; Stahle *et al*. 2009; Griffin *et al*. 2013). However, the correlation between EW and LW is often high and this very strong coupling may prevent registration of any discrete climate signal in LW independent of the climate effect on EW (Meko and Baisan 2001; Griffin *et al*. 2011). The strength of the correlation between EW and LW may

vary because of (1) spatial and temporal variability in climate and timing of wood production through growth of cambial meristem, (2) species-specific differences, and (3) age-related effects. In this paper, we examine the empirical inter-relationship of subannual ring-width chronologies across North America in order to better understand seasonal tree growth variation across time and space, and to identify the ideal age classes of trees for development of LW chronologies with the highest variance and most discrete environmental signals independent of the strong natural correlation between EW and LW.

The density of wood formed in most temperate conifer species varies over the growing season (Hoadley 1990). The earlywood (or springwood) is formed during the initial growth and consists of larger cells with thinner walls, but as the season progresses resources are instead allocated towards thicker walls at the expense of cell diameter and thus the LW (or summerwood) is formed (Glock 1937; Zahner 1963; Larson, 1969). The increase in density over the growing season and abrupt decrease in the next season usually allow for visual identification of annual growth rings in many conifers and in numerous hardwoods (Aloni 1987). In some species, the boundary between earlywood and latewood is also abrupt (Figure 1), and the width of these seasonal growth bands has attracted scientific interest since the earliest days of dendrochronology (Douglass 1919).

EW and LW tend to be very highly correlated in the few areas that it has been investigated (Meko and Baisan 2001; Stahle *et al*. 2009; Griffin *et al*. 2011; Brice *et al*. 2013). However, there is some independent variability in EW and LW, which can reflect seasonal climate signals. Experiments on longleaf pine (*Pinus palustris* Mill.) in the 1920's suggested that the amount of latewood produced could be enhanced through irrigation towards the end of the growing season (Paul and Marts 1931). Early analysis of tree-ring densitometry suggested

that the formation of latewood might be governed by climatic factors other than those influencing the earlywood (Cleaveland 1986). More recently, Meko and Baisan (2001) used simple regression to remove the influence of EW variability on the LW series, with the resulting time series known as adjusted latewood width (LW_a). Adjusted LW chronologies have become a standard tree ring variable in dendroclimatology and have been shown to contain separate information than that recorded by EW (Griffin *et al*. 2011; Griffin *et al*. 2013). LW and LW_a in Douglas-fir (*Pseudotsuga menziensii* (Mirb.) Franco) and ponderosa pine (*Pinus ponderosa* Douglas ex C. Lawson) have been used as indicators of summer rainfall in southwestern United States (Meko and Baisan 2001; Stahle *et al*. 2009; Faulstich *et al*. 2013; Griffin *et al*. 2013; Woodhouse *et al*. 2013). Distinct spring and summer climate signals have also been detected in Douglas-fir in the northern Rocky Mountains (Watson and Luckman 2002; Crawford *et al*. 2015). Although the recent advances have shed light on some aspects of the relationship between EW and LW, these studies have been restricted to select species and regions, and do not portray the full variance across the climate provinces of the North American continent.

We analyze the largest dataset to date of seasonal growth records from North America. In total, 197 paired chronologies of EW and LW were studied to estimate the persistence and partitioning of growth forcing during the current and preceding year over time, space, and species-boundaries. Our goal is to gain insight into how these two growth increments are related and to identify how the discrete seasonal growth signal might be examined.

MATERIAL AND METHODS

A total of 228 tree-ring collections with paired chronologies of EW and LW from locations distributed across North America were available for analysis (Figure 2; Supplementary Table 1). The majority of chronologies were obtained from the International Tree-Ring Data Bank

(ITRDB, Grissino-Mayer and Fritts 1997), however, a number of records are yet to be publically available. Chronologies were constructed using a range of standardization approaches by the various contributors, but all analyses below are based on standardized mean ring-width index chronologies without autoregressive modeling to remove low-order growth persistence from the time series (*e.g.* Meko 1981; Cook 1985). Most chronologies are at least 300 years long but the longest records cover the past two millennia. A common period spanning 1800-1979 was selected for analysis, based on a compromise between the maximum number of chronologies and length of time available for analysis. The 197 records that cover this 1800-1979 common period include 79 *Pseudotsuga*, 55 *Picea*, 28 *Pinus*, 23 *Taxodium*, and 12 chronologies of other genera (including six *Quercus* records). Each pair of chronologies was correlated to estimate the dependency of LW on EW within the same growing season. For each site, an adjusted latewood (LW_a) chronology was produced by regressing the site level LW chronology on the site level EW chronology (*per* Meko and Baisan (2001)). In addition, the EW chronologies were also correlated with 1-year lagged EW and LW_a chronologies (EW_{t-1} and $LW_{a(t-1)}$) to examine EW dependency on both spring and summer tree growth in the prior year. LW variance in particular appears to have a large effect on intercorrelation between EW and LW (Meko and Baisan 2001). Therefore, the variance of each EW and LW_a chronology was computed for the common period and used in the analysis of inter-seasonal growth dependence in North American tree species.

For a subset of the data, the actual raw measurements of both EW and LW were available for the individual trees and radii included in each chronology. These include 38 site collections of Douglas-fir (3074 measured radii for both EW and LW), 20 site collections of bald cypress (*Taxodium distichum* (L.) Rich.) and Montezuma bald cypress (*Taxodium mucronatum* Ten.) (1122 radii), and 15 site collections of ponderosa pine (936 radii). The individual measurements

in these subsets were processed using the tree-ring chronology development program ARSTAN (Cook 1985; Cook and Krusic 2005) with a 100-year cubic spline (Cook and Peters 1981) used to both remove the age-dependent effects on radial growth and to stabilize the variance of the derived EW and LW series. Between-series mean correlations (RBAR, Wigley *et al*. 1984) for the period 1800-1979 were computed for each collection for which individual measurements were available. Correlations between standardized EW and LW for individual radii, as well as correlations over individual 50- and 100-year segments, were computed for all series. The residuals from regression of LW on EW for each radius from the same tree produced individually-adjusted latewood series when these measurements were available. The variance of all standardized EW, LW, and LW_a series was also computed, both for the full period and for non-overlapping segments of 50 years.

RESULTS

Pearson correlations between EW and LW chronologies for the period 1800-1979 range from r = 0.166 to 0.891. There is considerable variability in correlation across space and between species (Figure 3; Table 1). Most low correlations ($r < 0.5$) between EW and LW chronologies are located in Mexico, and low correlations are more common in *Pseudotsuga* than in the other genera. The seven lowest correlations between EW and LW chronologies from the same sites are of Douglas-fir in the summer monsoon region of Mexico. Other relatively low correlations between EW and LW chronologies were computed for shortleaf pine in the continental United States and post oak in central Texas (Figure 3). These relatively low correlations may imply potential for reconstruction of discrete seasonal climate using those particular subannual ring-width chronologies.

For most chronologies, correlations between EW and prior year's LW_a are lower than the correlations between EW and prior year's EW (Figure 4; Table 2). Most high correlations between EW_t and EW_{t-1} are found in *Picea* chronologies from northern United States and Canada. Low lag-1 correlations were observed for EW_t and EW_{t-1} in the southeastern United States and Mexico, where many of the correlations are negative (Figure 4a). Because low-order growth persistence has not been removed from these EW and LW chronologies, the low EW_t and EW_{t-1} correlations of Douglas-fir in particular over Mexico may reflect regional climate differences between Mexico and the Douglas-fir stands in western United States.

The mean variance in the EW chronologies is higher than in the LW_a chronologies for all conifer species, but for the only hardwood species analyzed (post oak, *Quercus stellata* Wangenh.) the variance in LW_a is significantly higher than for EW (Table 3; Figure 5). Mean EW variance is below 0.05 in *Picea* but above 0.10 in *Pseudotsuga*, *Pinus*, and *Taxodium*. Similarly, the mean variance in LW_a for *Pseudotsuga*, *Pinus*, and *Taxodium* is above 0.05, but for *Picea* it is below 0.02. The variance of the EW and LW_a chronologies have a large, but opposite, effect on the intercorrelation between these subannual ring-width chronologies. EW variance is positively correlated with the intercorrelation between EW and LW, but LW_a variance is negatively related to this intercorrelation (Figure 6; Figure 7). The strongest effect of LW_a variance on the correlation between EW and LW was computed for *Taxodium* (Figure 7).

The coherence of subannual ring-width variability at a site, as measured by RBAR and believed to reflect the climate sensitivity of the trees, does not show a significant linear relationship with the degree of correlation between EW and LW in the available Douglas-fir, bald cypress, or ponderosa pine collections investigated in this study ($p > 0.1$ for all three species). Correlations between EW and LW for the individual radii by age class in Douglas-fir,

bald cypress, and ponderosa pine are lower in the first 50- to 100-years of growth (Figure 8). In subsequent 50-year windows there are little or no significant changes in correlations and it appears that age does not play a role in the relationship between EW and LW for trees of ages greater than 100 years. Variance in LW_a from individual trees and radii tends to decline after 200 years in age for the three species investigated (Figure 8). Variance in the LW_a for Douglas-fir and ponderosa pine appears to peak in the 150-200 year age range, and declines thereafter, but there is a steady decline in LW_a variance in bald cypress (Figure 8). These age-based correlations between EW and LW, and the age-related changes in variance suggest that age-stratified techniques, where younger trees are preferentially sampled throughout the time spanned by the available trees, might lead to enhanced summer-season environmental signals in adjusted latewood chronologies.

DISCUSSION

The analysis of 197 tree-ring collections indicates that the correlation between EW and LW is generally high across all of North America for the several species studied. The lowest correlations between EW and LW were computed for Douglas-fir in the monsoon region of Mexico. But at the same time, some of the highest correlations were computed for Douglas-fir in the Four Corners region of the southwestern United States. This steep gradient in the correlation between EW and LW in Douglas-fir is clearly evident when the results for just Douglas-fir are mapped (Figure 9a). The change in EW and LW correlations across the United States and Mexico might arise in part from (1) the north-south temperature gradient and later onset of the growing season in the Four Corners area, and/or (2) the earlier onset of the summer rains in northwestern Mexico after the pre-monsoon dry period. Previous studies using subannual ring-width data from Douglas-fir have linked LW production to the availability of soil moisture in

summer (Meko and Baisan 2001; Therrell *et al*. 2002; Stahle *et al*. 2009; Griffin *et al*. 2013). Because of an earlier arrival of the monsoon precipitation in Mexico (Douglas *et al*. 1993; Adams and Comrie 1997), the late-season moisture source is available to the trees for a longer part of the growing season, and it is possible that this regional climate mechanism effectively decouples LW from EW. Despite the high correlation between EW and LW in Douglas-fir from southern Arizona and southern New Mexico, the LW_a variance is still relatively high in many of these collections (Figure 9b) and is likely to explain the success of summer precipitation reconstructions for the region (*e.g.* Griffin *et al*. 2013).

The influence of prior growth on current year EW also differs between the Four Corners region and northern Mexico (Figure 9c and d). In the Four Corners region, the correlation between prior summer adjusted latewood ($LW_{a(t-1)}$) and earlywood during the current year (EW_t) is among the highest of all collections analyzed (Figure 4b; Table 2). In contrast, many chronology pairs in Mexico show negative correlation between the two variables. The same pattern is observed for correlations between prior spring earlywood (EW_{t-1}) and EW_t. The traditional explanation of low-order autocorrelation in trees is that an accumulation of food during the latter stages of the growing season is stored during winter (Fritts 1976). Such food storage appears to be significantly less important, even non-existent, in several Douglas-fir stands growing in northwestern Mexico. The difference in resource allocation throughout the range of the species may, again, be caused by differences in local hydroclimate.

Shortleaf pine (*Pinus echinata* Mill.) displays the lowest mean correlation between EW and LW of any conifer species (Table 1). Shortleaf pine is also the only conifer species for which the mean LW_a variance is higher than the mean EW variance (this holds true for 7 of the 9 site chronology pairs; Table 3). Shortleaf pine in Arkansas was the subject of one of the pioneer

studies on seasonal growth by Schulman (1942), who identified July-September precipitation as a potential driver of LW variability. Removing the LW dependency of EW in shortleaf pine might enhance the correlation between LW_a and late summer precipitation or soil moisture conditions.

The mean EW-LW correlations for post oak, an angiosperm, is lower than in any of the gymnosperms. As measured in the oak collections included in this study, EW is the part of the annual growth ring made up of large-diameter vessels. In these particular datasets, interannual variation in vessel size and number is miniscule compared with the width of the latewood component of the ring (Figure 1). Therefore, the variation in total ring width is almost entirely dominated by LW. The variance in post oak EW is significantly lower than in LW or LW_a (Table 3), which is in agreement with the findings of other studies on the genus *Quercus* (Nola 1996; Yang 1997; García-González and Eckstein 2003). Earlier studies on EW and LW variability in oaks have recorded high correlation between (unadjusted) LW_{t-1} and EW_t (r = 0.25-0.49 (Nola 1996); r = 0.67 (García-González and Eckstein 2003)), which has been explained by the timing of wood formation in relation to photosynthetic activity in oaks. Starches stored from prior summer and autumn may support earlywood xylem production prior to or during leaf-out (Wareing 1951; Aloni 1995; LeBlanc and Terrell 2011). The mean correlation between LW_{t-1} and EW_t in the six post oak collections is < 0.1, and just marginally higher for $LW_{a(t-1)}$ and EW.

The difference between post oak and other oak species may be caused by the relatively arid growing environments of the former. The limited correlation between EW and LW, in addition to high LW_a variance, indicates that additional climate information might be gained from the seasonal growth components of this species. In fact, this analysis of post oak, although

based on only six collections, may suggest that there is dendroclimatic potential for subannual tree-ring variables in other drought-stressed oak species elsewhere in North America.

The correlation between EW and LW is extremely high in bald cypress. The rings, particularly in multi-century aged individuals, are dominated by earlywood tracheids with only a handful of tracheids (and low variability in the number) in the latewood. Nevertheless, previous research has shown that it is possible to produce discrete climate reconstructions from bald cypress LW_a records (Stahle *et al*. 2012), despite the high correlation between EW and LW. Only two Montezuma bald cypress collections were analyzed, but these display the lowest correlations (r = 0.574 and 0.646) between EW and LW within the genus. Total ring-width of Montezuma bald cypress has been used for millennium-length reconstructions of June soil moisture conditions (Stahle *et al*. 2011) and the relatively weak relationship between EW and LW growth suggests that its rings may contain discrete seasonal climate information. However, LW variance in Montezuma bald cypress is often low so that the potential for LW chronology development may be limited for this species.

The highest correlation of prior and current-year EW is found in *Picea* collections (Table 1; Figure 4a). Significant autocorrelation in Engelmann spruce (*Picea engelmannii* Parry ex Engelm.) and white spruce (*P. glauca* (Moench) Voss) total ring-width (TRW) has previously been reported (Parker and Henoch 1971; Adams and Kolb 2005; Tardif *et al*. 2008), which may muddle any climate signal in the chronologies if left untreated (D'Arrigo *et al*. 1992). Our results suggest that the autocorrelation recorded in spruce TRW is mainly driven by EW, perhaps more so in white spruce than in Engelmann spruce or black spruce (*P. mariana* (Mill.) Britton).

A low correlation between EW and LW growth, or a stronger decoupling of the two, is thought to indicate potentially discrete climate signals in the respective growth variables. The

strong negative relationship between EW-LW correlations and LW_a variance (Figure 7) suggests that a greater amount of LW_a variance can be retained in trees with decoupled growth. Increased year-to-year variability in tree-growth is usually assumed to be caused by a stronger climatic forcing (*e.g.* Fritts *et al*. (1965)), and is therefore desirable from a dendroclimatological standpoint. Other factors could influence correlations and the variance of the seasonal growth components. Choices made during the processing of measurements could have an effect on the relationship between EW and LW, and regression to produce LW_a chronologies can impact the variance of the latter. Griffin *et al*. (2011) recommend that adjustments should be made at the radii level rather than after chronology construction because of the large differences in correlations within stands. Tree age has also been suggested as having an effect on the usefulness of independent seasonal growth variables (Meko and Baisan 2001; Stahle *et al*. 2009; Griffin *et al*. 2011).

Our analyses of the age effect based on individual measurements from a subset of data indicate an increase in correlation between EW and LW for Douglas-fir, bald cypress and Montezuma bald cypress, and ponderosa pine within the first 100 years of estimated tree age (Figure 8). Because inner-ring dates in these measurements are likely an underestimate of the true tree establishment dates, the effect of estimated tree age on correlation may be even stronger than suggested by our results and may extend out to the first 150 years of absolute tree age. Similar age-dependent trends are apparent in LW_a variance, which tend to decrease after *ca*. 200 years of growth for the three main conifer species studied (Figure 8). Meko and Baisan (2001) noted that the interannual variability in the latewood for five Douglas-fir records from Arizona decreased after the first 250 years of growth. This notion seems to hold true when extending the analysis to 38 sites and over 3000 radii (Figure 8). Although using only tree-ring series younger

than 100 or 150 years old would impose significant constraints on the number of acceptable samples and most likely shorten the period of climate reconstruction, such a sampling strategy may enhance the seasonal climate signal present in the adjusted latewood chronologies. Age-stratified sampling and chronology construction have recently been used to improve the climate signal of riparian trees for streamflow reconstructions, as younger trees appear more sensitive to hydroclimate in some settings (Meko *et al*. 2015).

CONCLUSIONS

The simple correlations of same-site EW and LW chronologies from across North America are often very high ($r > 0.7$). Nonetheless, several recent studies indicate that adjusted latewood, where the dependency of EW has been removed, can contain discrete climate information otherwise unavailable from TRW. The decoupling between EW and LW is strongest in Douglas-fir chronologies from the monsoon region of northern Mexico but relatively low correlations of EW and LW can also be observed in post oak and shortleaf pine from southcentral United States, which may also arise from seasonal climate patterns. Our analyses also indicate that the lowest correlations of EW and LW are typically found in the first 200 years of growth for three major conifer species in North America.

The measurement of EW and LW has not been a routine practice within dendrochronology in the past, however as already demonstrated by Schulman (1942) and others, the simple optical measurement can be made objectively and with great reproducibility. This paper shows that there can be major differences in the interannual variability in EW and LW, differences that are likely caused by varying seasonal distribution of precipitation. The seasonal climate response of EW, LW, and LW_a chronologies described in this paper will be investigated in a follow-on study,

as well as the potential benefits of using strict age-stratified chronologies to reconstruct discrete seasonal climate from EW and LW_a.

ACKNOWLEDGMENTS

The data used are listed in the references, supplementary table, and can be accessed through the International Tree-Ring Data Bank (http://www.ncdc.noaa.gov/data-access/paleoclimatology-data/datasets/tree-ring). We thank the many contributors to the International Tree-Ring Data Bank at NOAA, especially Fritz Schweingruber, Julian Cerano-Paredes, Brian Luckman, Jordan Burns, and Connie Woodhouse. We also appreciate the constructive and insightful comments by two anonymous reviewers. The National Science Foundation (grant #AGS-1266014) and Inter-American Institute for Global Change Research (CRN #2047) funded this study. DG was supported by a NOAA Climate & Global Change Fellowship. Lamont-Doherty Earth Observatory contribution no. 8020.

REFERENCES CITED

Adams, D. K., and A. C. Comrie, 1997. The North American Monsoon. *Bulletin of the American Meteorological Society* 78:2197–2213.

Adams, H. D., and T. E. Kolb, 2005. Tree growth response to drought and temperature in a mountain landscape in northern Arizona, USA. *Journal of Biogeography* **32**: 1629–1640.

Aloni, R., 1987. Differentiation of vascular tissues. *Annual Review of Plant Physiology* 38:179–204.

Aloni, R., 1991. Wood formation in deciduous hardwood trees. In *Physiology of Trees*, edited by A. S. Raghavendera, pp. 175–197. John Wiley & Sons, New York, NY.

Baillie, M. G. L., 1982. *Tree-Ring Dating and Archaeology*. Croom Helm, London, UK.

Bradley, R. S., 1985. *Quaternary Paleoclimatology: Methods of Paleoclimatic Reconstruction*. Chapman and Hall, London, UK.

Brice, B., K. K. Lorion, D. Griffin, A. K. Macalady, C. H. Guiterman, J. H. Speer, L. R. Benakoun, A. Cutter, M. E. Hart, M. P. Murray, S. E. Nash, R. Shepard, A. K. Stewart, and H. Wang, 2013. Signal strength in sub-annual tree-ring chronologies from *Pinus ponderosa* in northern New Mexico. *Tree-Ring Research* 69:81–86.

Buckley, B. M., K. J. Anchukaitis, D. Penny, R. Fletcher, E. R. Cook, M. Sano, L. C. Nam, A. Wichienkeeo, T. T. Minh, and T. M. Hong, 2010. Climate as a contributing factor in the demise of Angkor, Cambodia. *Proceedings of the National Academy of Sciences* 107:6748–6752.

Cleaveland, M. K., 1986. Climatic response of densitometric properties in semiarid site tree rings. *Tree-Ring Bulletin* 46:13–29.

Cook, E. R., 1985. *A Time Series Analysis Approach to Tree-Ring Standardization*. Ph.D. dissertation, The University of Arizona, Tucson.

Cook, E. R., D. M. Meko, D. W. Stahle, and M. K. Cleaveland, 1999. Drought reconstructions of the continental United States. *Journal of Climate* 12:1145–1162.

Cook, E. R., and P. J. Krusic, 2005. *Program ARSTAN, A Tree-Ring Standardization Program Based on Detrending and Autoregressive Time Series Modeling with Interactive Graphics*. Tree-Ring Laboratory Lamont Doherty Earth Observatory of Columbia University, New York.

Cook, E. R., and K. Peters, 1981. The smoothing spline: A new approach to standardizing forest interior tree-ring width series for dendroclimatic studies. *Tree-Ring Bulletin* 41:45–53.

Crawford, C. J., D. R. Griffin, and K. F. Kipfmueller, 2015. Capturing season-specific precipitation signals in the northern Rocky Mountains, USA, using earlywood and latewood tree rings. *Journal of Geophysical Research–Biogeosciences* 120:428–440.

D'Arrigo, R, D., G. C. Jacoby, and R. M. Free, 1992. Tree-ring width and maximum density at the North American tree line: Parameters of climatic change. *Canadian Journal of Forest Research* 22:1290–1296.

Dannenberg, M. P., and E. K. Wise, 2016. Seasonal climate signals from multiple tree ring metrics: A case study of *Pinus ponderosa* in the upper Columbia River Basin. *Journal of Geophysical Research –Biogeosciences* 121:1178–1189.

Douglas, M. W., R. A. Maddox, K. Howard, and S. Reyes, 1993. The Mexican Monsoon. *Journal of Climate* 6:1665–1677.

Douglass, A. E., 1919. *Climatic cycles and tree growth, volume I*. Carnegie Institute of Washington, Washington, DC.

Esper, J., E. R. Cook, and F. H. Schweingruber, 2002. Low-frequency signals in long tree-ring chronologies for reconstructing past temperature variability. *Science* 295: 2250–2253.

Faulstich, H. L., C. A. Woodhouse, and D. Griffin, 2013. Reconstructed cool- and warm-season precipitation over the tribal lands of northeastern Arizona. *Climatic Change* 118:457–468.

Fritts, H. C., 1976. *Tree Rings and Climate*. Academic Press, London, UK.

Fritts, H. C., D. G. Smith, J. W. Wardis, and C. A. Budelsky, 1965. Tree-ring characteristics along a vegetation gradient in northern Arizona. *Ecology* 46:393–401.

García-González, I., and D. Eckstein, 2003. Climatic signal of earlywood vessels of oak on a maritime site. *Tree Physiology* 23:497–504.

Glock, W. S., 1937. *Principles and Methods of Tree-Ring Analysis*. Carnegie Institution of Washington, Washington, D.C.

Griffin, D. R., D. M. Meko, R. Touchan, S. W. Leavitt, and C. A. Woodhouse, 2011. Latewood chronology development for summer-moisture reconstruction in the US Southwest. *Tree-Ring Research* 67:87–101.

Griffin, D. R., C. A. Woodhouse, D. M. Meko, D. W. Stahle, H. L. Faulstich, C. Carrillo, R. Touchan, C. L. Castro, and S. W. Leavitt, 2013. North American monsoon precipitation reconstructed from tree-ring latewood. *Geophysical Research Letters* 40:954–958.

Grissino-Mayer, H. D., and H. C. Fritts, 1997. The International Tree-Ring Data Bank: An enhanced global database serving the global scientific community. *The Holocene* 7:235–238.

Hoadley, B., 1990. *Identifying Wood: Accurate Results with Simple Tools*. Taunton Press, Newton, CT.

LeBlanc, D. C., and M. A. Terrell, 2011. Comparison of growth-climate relationships between white oak and northern red oak across eastern North America. *Canadian Journal of Forest Research* 41:1936–1947.

Meko, D.M., 1981. *Applications of Box-Jenkins Methods of Time-Series Analysis to Reconstruction of Drought from Tree Rings*. Ph.D. dissertation, The University of Arizona, Tucson.

Meko, D.M., and C. H. Baisan, 2001. Pilot study of latewood-width of conifers as an indicator of variability of summer rainfall in the North American monsoon region. *International Journal of Climatology* 21:697–708.

Meko, D. M., R. Touchan, J. Villanueva Díaz, D. Griffin, C. A. Woodhouse, C. L. Castro, C. Carillo, and S. W. Leavitt, 2013. Sierra San Pedro Martir, Baja California, cool-season precipitation reconstructed from earlywood width of *Abies concolor* tree rings. *Journal of Geophysical Research–Biogeosciences* 118:1660–1673.

Meko, D. M., J. M. Friedman, R. Touchan, J. R. Edmondson, E. R. Griffin, and J. A. Scott, 2015. Alternative standardization approaches to improving streamflow reconstructions with ring-width indices of riparian trees. *The Holocene* 25:1093–1101.

Nola, P., 1996. Climatic signal in earlywood and latewood of deciduous oaks from northern Italy. In *Tree Rings, Environment and Humanity*, edited by J. S. Dean, D. M. Meko and T. W. Swetnam, pp. 249–258. Radiocarbon, University of Arizona, Tucson.

Parker, M. L., and W. E. S. Henoch, 1971. The use of Engelmann spruce latewood density for dendrochronological purposes. *Canadian Journal of Forest Research* 1:90–98.

Paul, B. H., and R. O. Marts, 1931. Controlling the proportion of summerwood in longleaf pine. *Journal of Forestry* 29:784–796.

St. George, S., 2014. An overview of tree-ring width records across the Northern Hemisphere. *Quaternary Science Reviews* 95:132–150.

Schulman, E., 1942. Dendrochronology in pines of Arkansas. *Ecology* 23:309–318.

Schweingruber, F. H., 1996. *Tree Rings and Environment: Dendroecology*. Paul Haupt, Bern, Switzerland.

Stahle, D. K., D. J. Burnette, and D. W. Stahle, 2013. A moisture balance reconstruction for the drainage basin of Albemarle Sound, North Carolina. *Estuaries and Coasts* 36:1340–1353.

Stahle, D. W., D. J. Burnette, J. Villanueva Diaz, F. K. Fye, R. D. Griffin, M. K. Cleaveland, D. K. Stahle, J. R. Edmondson, and K. Perkins, 2012. Tree-ring analysis of ancient baldcypress trees and subfossil wood. *Quaternary Science Reviews* 34:1–15.

Stahle, D. W., M. K. Cleaveland, H. Grissino-Mayer, R. D. Griffin, F. K. Fye, M. D. Therrell, D. J. Burnette, D. M. Meko, and J. Villanueva-Diaz, 2009. Cool- and warm-season precipitation reconstructions over western New Mexico. *Journal of Climate* 22:3739–3750.

Stahle, D. W., R. D. D'Arrigo, P. J. Krusic, M. K. Cleaveland, E. R. Cook, R. J. Allan, J. E. Cole, R. B. Dunbar, M. D. Therrell, D. A. Gay, M. D. Moore, M. A. Stokes, B. T. Burns, J. Villanueva-Diaz, and L. G. Thompson, 1998. Experimental dendroclimatic reconstructions of the Southern Oscillation. *Bulletin of the American Meteorological Society* 79:2137–2152.

Stahle, D. W., F. K. Fye, and E. R. Cook, 2007. Tree-ring reconstructed megadroughts over North American since AD 1300. *Climatic Change* 83:133–149.

Stoffel, M., and M. Bollschweiler, 2008. Tree-ring analysis in natural hazards research – An overview. *Natural Hazards Earth System Sciences* 8:187–202.

Tardif, J. C., F. Conciatori, and S. W. Leavitt, 2008. Tree rings, $\delta^{13}C$ and climate in *Picea glauca* growing near Churchill, subarctic Manitoba, Canada. *Chemical Geology* 252:88–101.

Therrell, M. D., D. W. Stahle, M. K. Cleaveland, and J. Villanueva-Diaz, 2002. Warm season tree growth and precipitation over Mexico. *Journal of Geophysical Research* 107: ACL6-1–ACL6-8.

Villalba, R., Veblen, T. T., and J. Ogden, 1994. Climatic influences on the growth of subalpine trees in the Colorado front range. *Ecology* 75:1450–1462.

Villanueva Díaz, J., D. W. Stahle, B. H. Luckman, J. Cerano-Paredes, M. W. Therrell, M. K. Cleaveland, and E. Cornejo-Oviedo, 2007. Winter-spring precipitation reconstructions from tree rings from northeast Mexico. *Climate Change* 83:117–131.

Wareing, P. F., 1951. Growth studies in woody species. IV. The initiation of cambial activity in ring-porous species. *Physiologia Planatarum* 4:546–562.

Watson, E., and B. Luckman, 2002. The dendroclimatic signal in Douglas-fir and ponderosa pine tree-ring chronologies from the southern Canadian Cordillera. *Canadian Journal of Forest Research* 32:1858–1874.

Watson, E., and B. Luckman, 2004. Tree-ring based reconstructions of precipitation for the southern Canadian Cordillera. *Climatic Change* 65:209–241.

Wigley, T. M. L., K. R. Briffa, and P. D. Jones, 1984. On the average value of correlated time series, with applications in dendroclimatology and hydrometeorology. *Journal of Climate and Applied Meteorology* 23:201–213.

Woodhouse, C. A., D. M. Meko, D. Griffin, and C. L. Castro, 2013. Tree rings and multiseason drought variability in the lower Rio Grande Basin, USA. *Water Resources Research* 49:844–850.

Yang, S. Y., 1997. Variations and correlations of various ring width and ring density features in European oak: Implications in dendroclimatology. *Wood Science and Technology* 31:63–72.

Zahner, R., 1963. Internal moisture stress and wood formation in conifers. *Forest Products Journal* 13:240–247.

TABLES

Table 1. Summary statistics of Pearson correlations between EW and LW chronologies for the common period 1800-1979. Significant correlations ($p < 0.01$) are indicated by an asterisk.

Genus	Species	*n*	mean r	min r	max r	median r
Pseudotsuga		**79**	**0.629***	**0.166**	**0.891***	**0.642***
Picea		**55**	**0.631***	**0.349***	**0.868***	**0.646***
	engelmannii	20	0.633*	0.366*	0.821*	0.662*
	glauca	20	0.667*	0.370*	0.868*	0.680*
	mariana	12	0.556*	0.349*	0.770*	0.563*
Pinus		**28**	**0.658***	**0.360***	**0.856***	0.668*
	echinata	9	0.547*	0.360*	0.715*	0.523*
	ponderosa	16	0.724*	0.430*	0.856*	0.736*
Taxodium		**23**	**0.773***	**0.574***	**0.873***	0.791*
Other		**12**	**0.635***	**0.417***	**0.870***	0.601*
	Quercus stellata	6	0.537*	0.417*	0.620*	0.543*

Table 2. Summary statistics of Pearson correlations between (1) current earlywood width (EW) and prior year earlywood (pEW), and (2) EW and prior year adjusted latewood (pLW_a), chronologies computed for the common period 1800-1979. Significant correlations ($p < 0.01$) are indicated by an asterisk.

			EW vs. pEW			EW vs. pLWa		
Genus	**Species**	***n***	**mean r**	**min r**	**max r**	**mean r**	**min r**	**max r**
Pseudotsuga		**79**	**0.229***	**-0.126**	**0.522***	**0.221***	**-0.084**	**0.406***
Picea		**55**	**0.422***	**0.048**	**0.844***	**0.173**	**-0.127**	**0.484***
	engelmannii	20	0.328*	0.049	0.669*	0.217*	-0.031	0.405*
	glauca	20	0.487*	0.048	0.844*	0.131	-0.127	0.484*
	mariana	12	0.458*	0.163	0.668*	0.168	-0.003	0.285*
Pinus		**28**	**0.334***	**0.043**	**0.643***	**0.179**	**-0.017**	**0.343***
	echinata	9	0.503*	0.432*	0.643*	0.154	0.023	0.305*
	ponderosa	16	0.275*	0.043	0.480*	0.186	-0.017	0.343*
Taxodium		**23**	**0.105**	**-0.133**	**0.408***	**0.070**	**-0.098**	**0.250***
Other		**12**						
	Quercus stellata	6	0.020	-0.191	0.220*	0.102	0.058	0.219*

Table 3. Summary statistics of EW and LW_a variance during the common period 1800-1979.

			Earlywood			Latewood (adjusted)		
Genus	**Species**	***n***	**mean var**	**min var**	**max var**	**mean var**	**min var**	**max var**
Pseudotsuga		**79**	**0.108**	**0.019**	**0.302**	**0.067**	**0.011**	**0.175**
Picea		**55**	**0.035**	**0.019**	**0.082**	**0.015**	**0.006**	**0.040**
	engelmannii	20	0.031	0.021	0.046	0.008	0.014	0.040
	glauca	20	0.041	0.019	0.082	0.014	0.006	0.031
	mariana	12	0.031	0.019	0.049	0.015	0.009	0.023
Pinus		**28**	**0.110**	**0.042**	**0.230**	**0.086**	**0.021**	**0.183**
	echinata	9	0.063	0.051	0.100	0.118	0.047	0.183
	ponderosa	16	0.131	0.042	0.230	0.067	0.021	0.139
Taxodium		**23**	**0.143**	**0.082**	**0.220**	**0.053**	**0.014**	**0.187**
Other		**12**	**0.0502**	**0.016**	**0.087**	**0.128**	**0.013**	**0.221**
	Quercus stellata	6	0.033	0.016	0.054	0.217	0.127	0.326

FIGURES

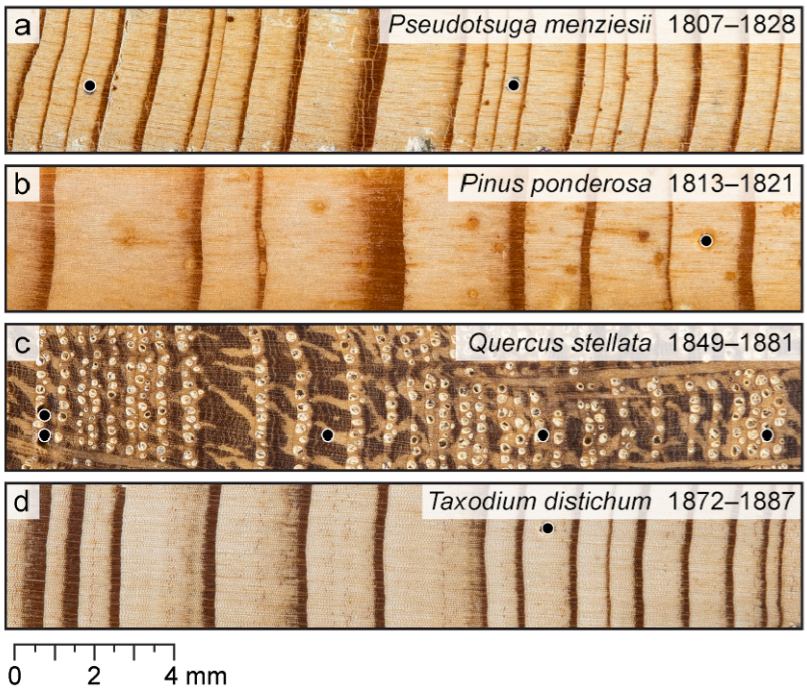

Figure 1. Photomicrographs of earlywood and latewood growth in (a) *Pseudotsuga menziesii* (MAN51A, Mancos River, CO), (b) *Pinus ponderosa* (SIE68B, Sierra Grande, NM), (c) *Quercus stellata* (WIL05A, Wilson Cabin Corinth, TX), and (d) *Taxodium distichum* (BSK06, Bearskin Lake, AR). Note the relatively wide latewood bands in year 1816 for (a) and (b), in years 1858-1860 in (c), and year 1873 in (d), independent from the earlywood variability. One dot represents the year of a decade; two dots represent the year 1850, according to conventional dendrochronological practices.

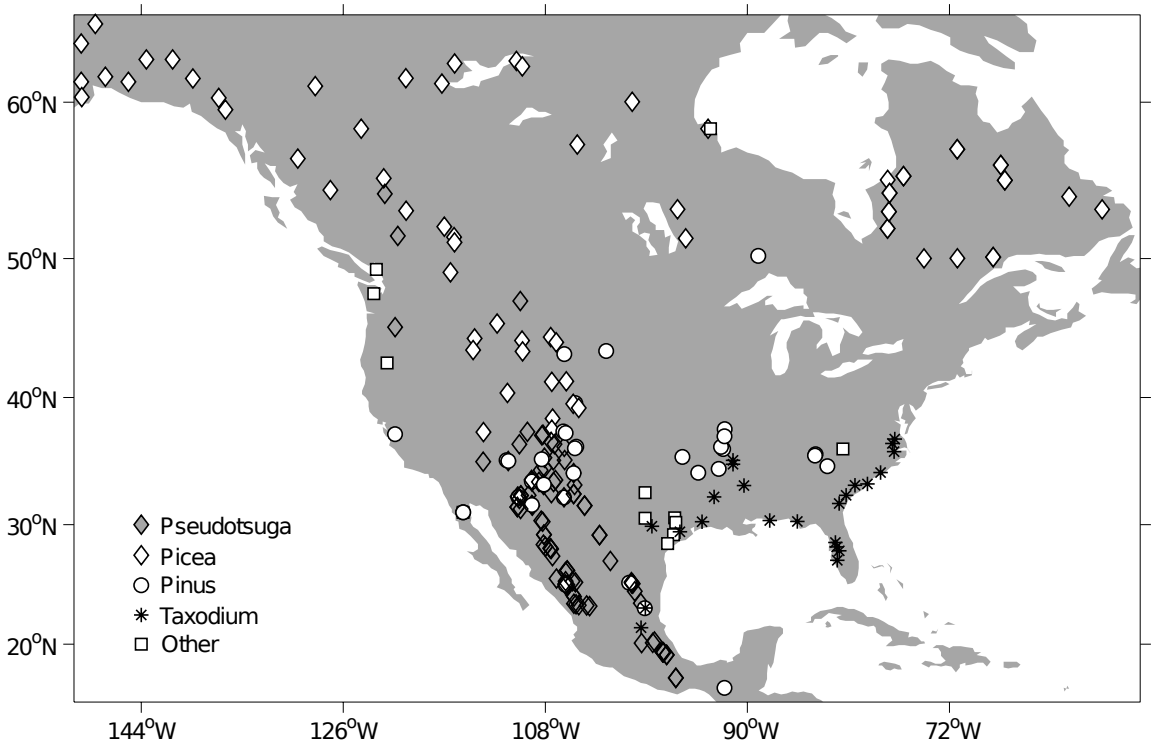

Figure 2. The spatial distribution of tree-ring records derived from several genera and used in this study is illustrated.

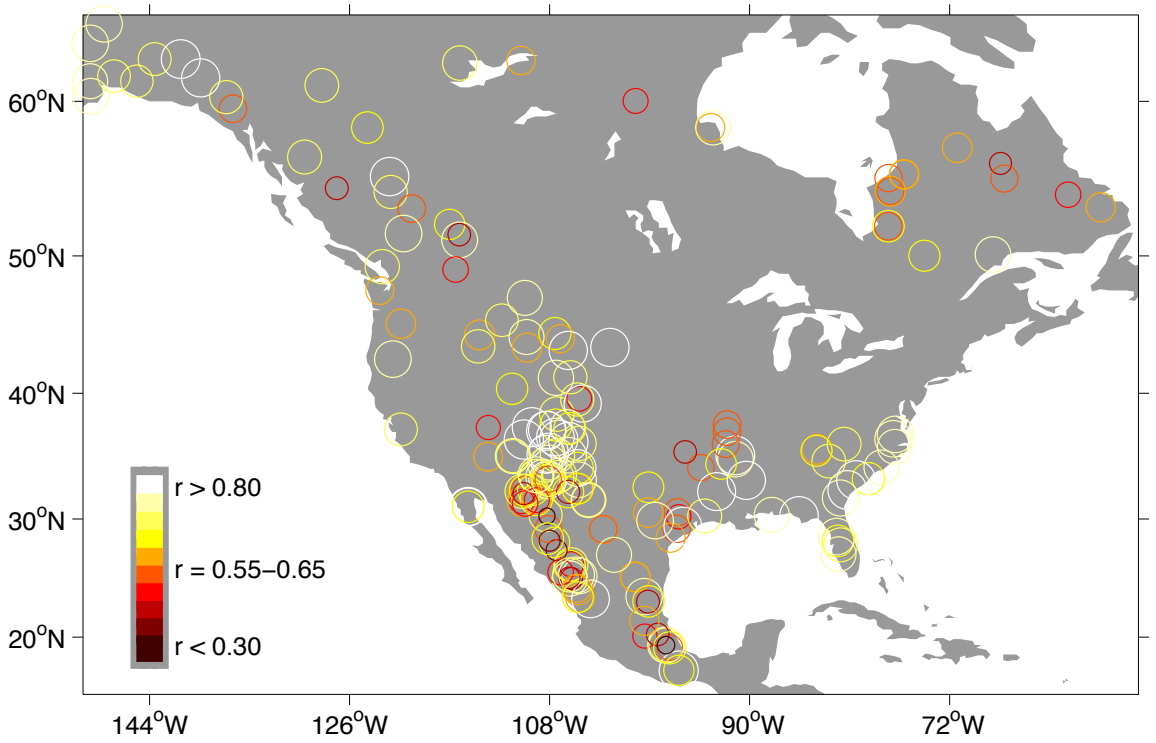

Figure 3. The correlation between EW and LW chronologies is computed and scaled, based on data drawn from the same trees at 197 tree-ring sites across North America. All correlations were computed for the common period 1800-1979.

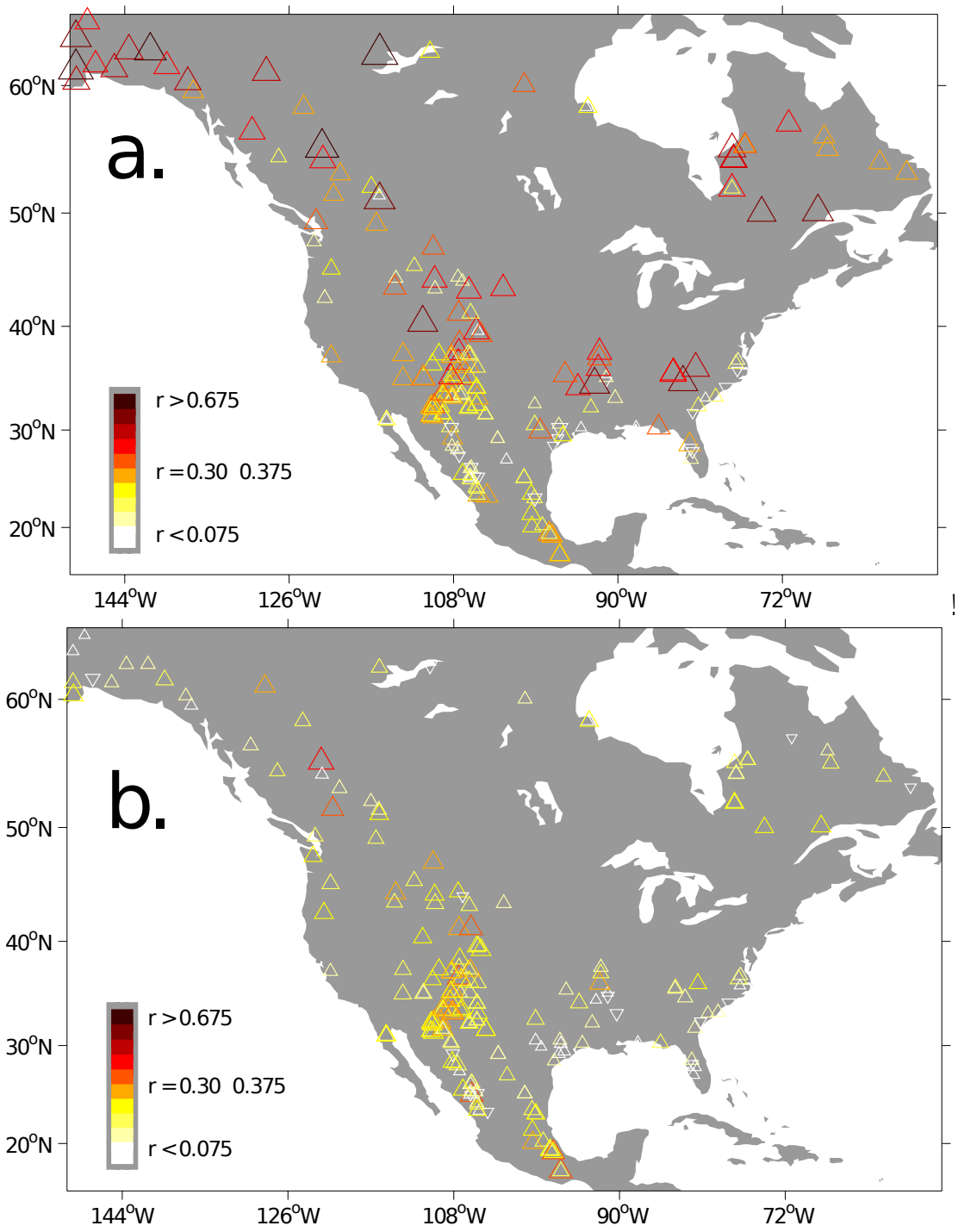

Figure 4. Maps illustrating correlations between current earlywood (EW_t) and prior year earlywood (EW_{t-1}, a); and EW_t and prior year adjusted latewood ($LW_{a(t-1)}$, b), chronologies computed for the common period 1800-1979. The negative correlations (down-pointing triangles) between EW_t and EW_{t-1} are primarily restricted to bald cypress in the southeastern United States and to Douglas-fir in Mexico. Negative correlations between EW_t and $LW_{a(t-1)}$ are not common, but are computed for bald cypress, Douglas-fir, and spruce.

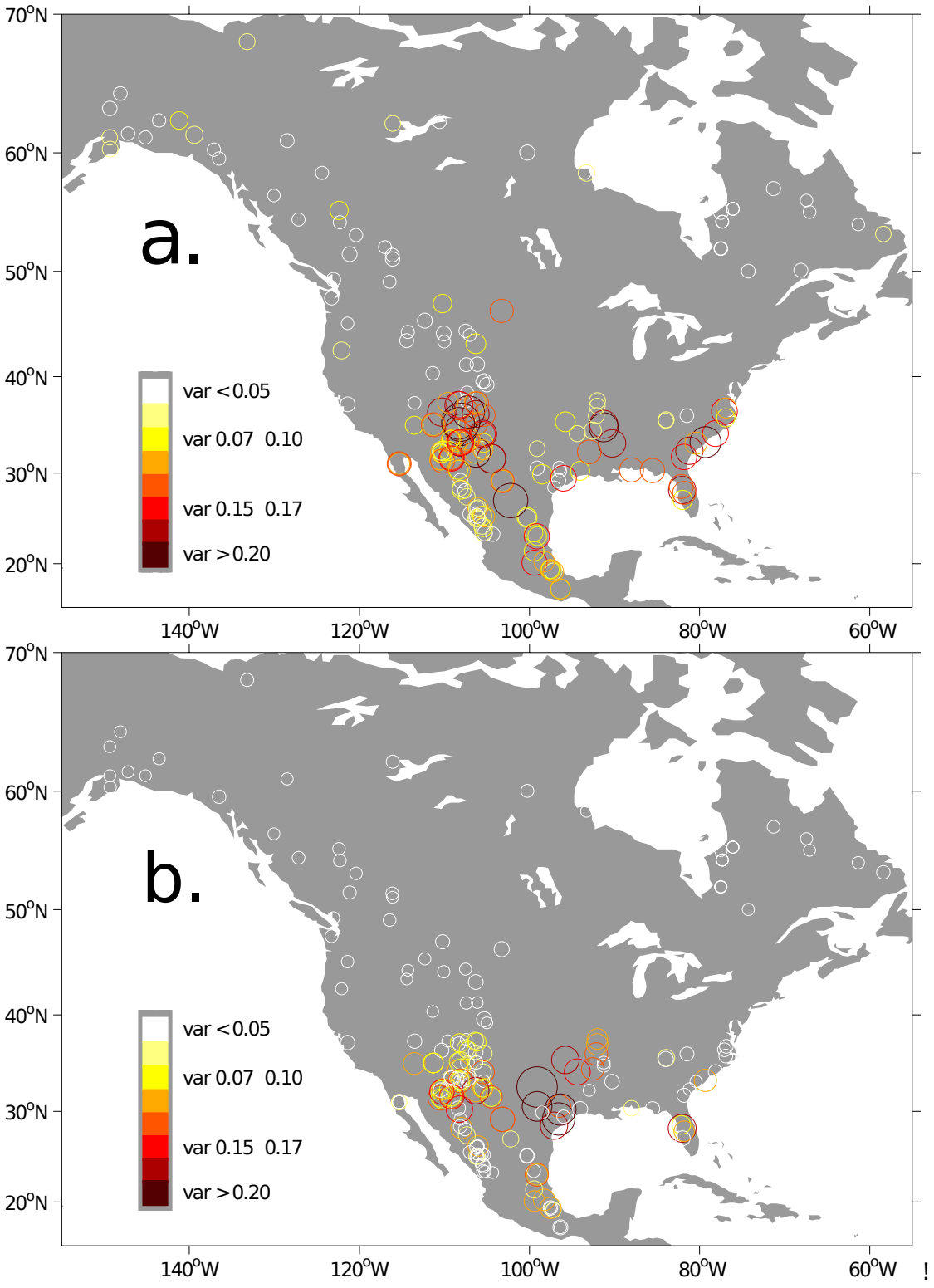

Figure 5. The variance of the EW (a) and LW_a (b) chronologies is scaled and mapped for 197 sites and several species across North America. LW_a variance exceeds EW variance only for a few series, mainly shortleaf pine and post oak in the southcentral United States.

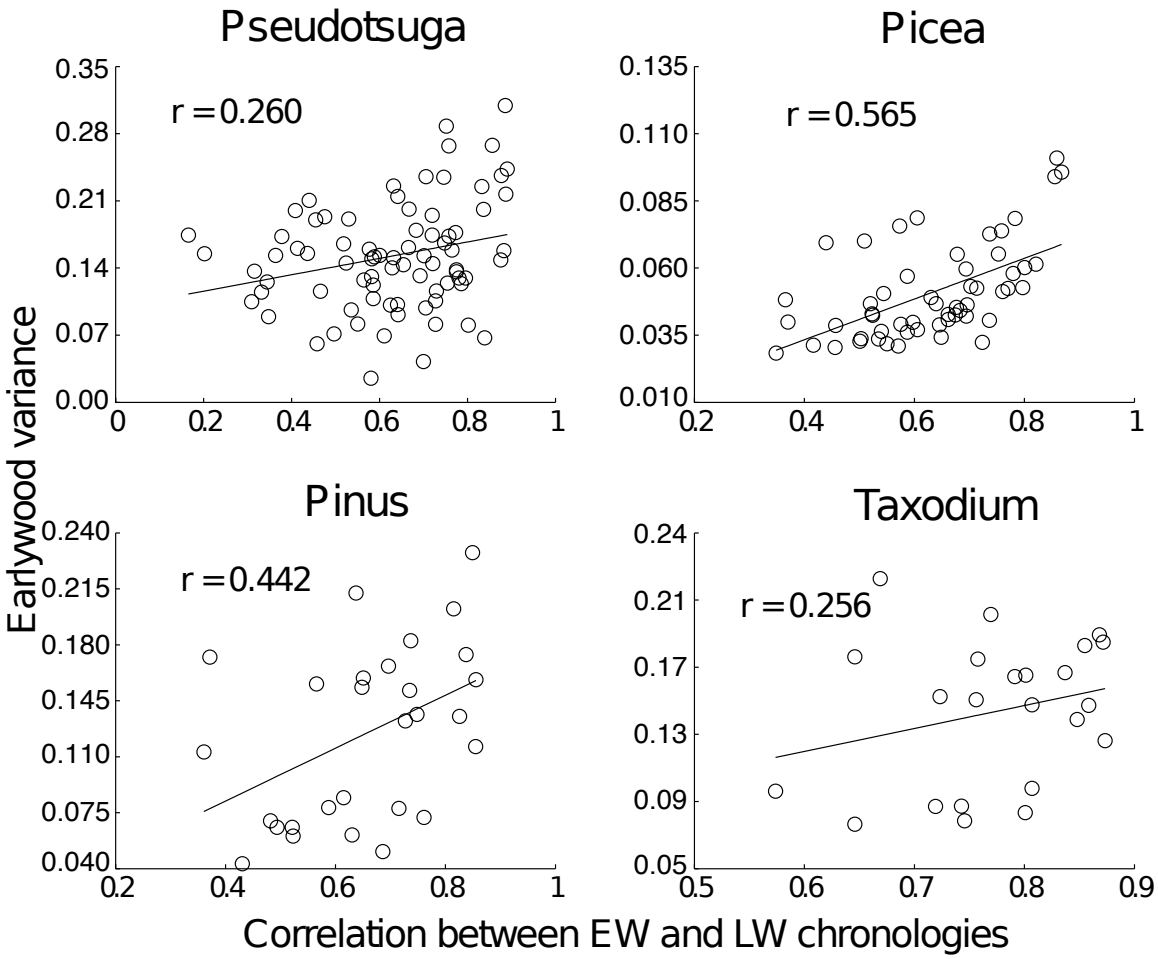

Figure 6. Scatterplots between EW variance and the correlation coefficients computed for EW and LW for each chronology pair by genera.

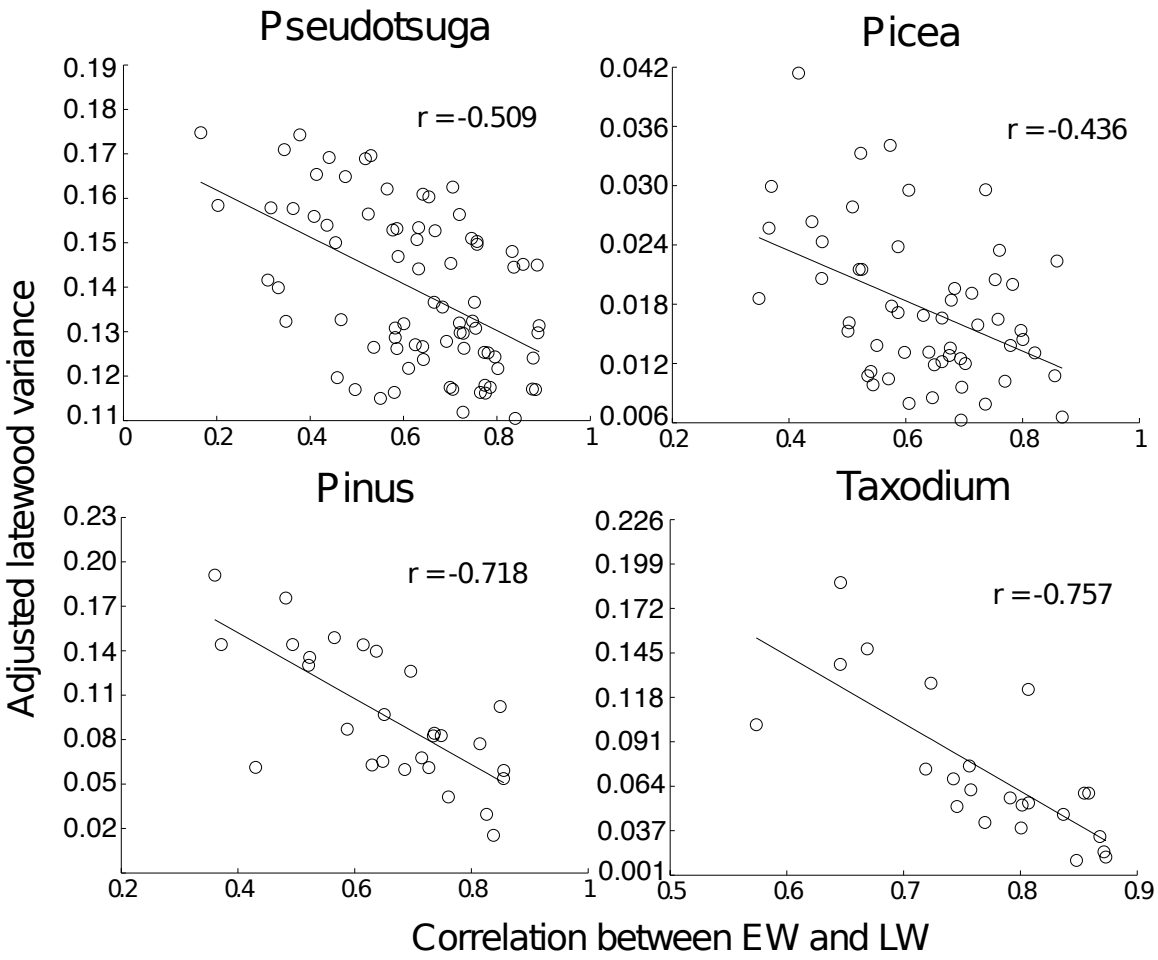

Figure 7. Scatterplots between LW_a variance and the correlation coefficients computed for EW and LW for each chronology pair by genera.

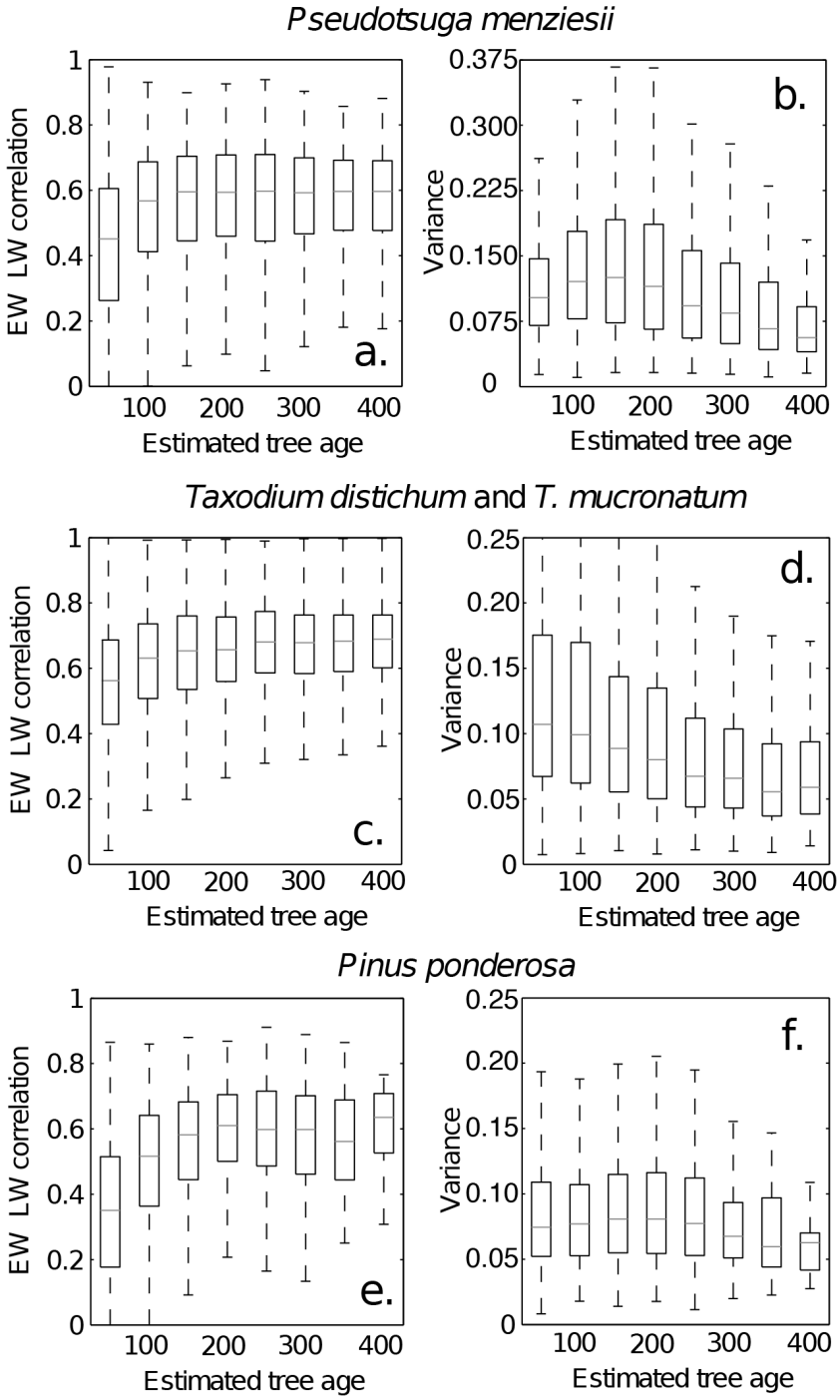

Figure 8. The effect of "tree age" on the intercorrelation between EW and LW (a,c,e) and on LW_a chronology variance (b,d,f) is illustrated for non-overlapping 50-year periods using box plots of the median, 25th and 75th percentile, and the minimum and maximum values. The sample size of individual age classes varies from (3016 to 118) for Douglas-fir, (1122 to 305) for bald cypress and Montezuma bald cypress, and (936 to 73) for ponderosa pine. Note the generally lower correlations typical for the first 50- to 100-years of growth, and the general decline in LW_a variance after 200 years for all three species.

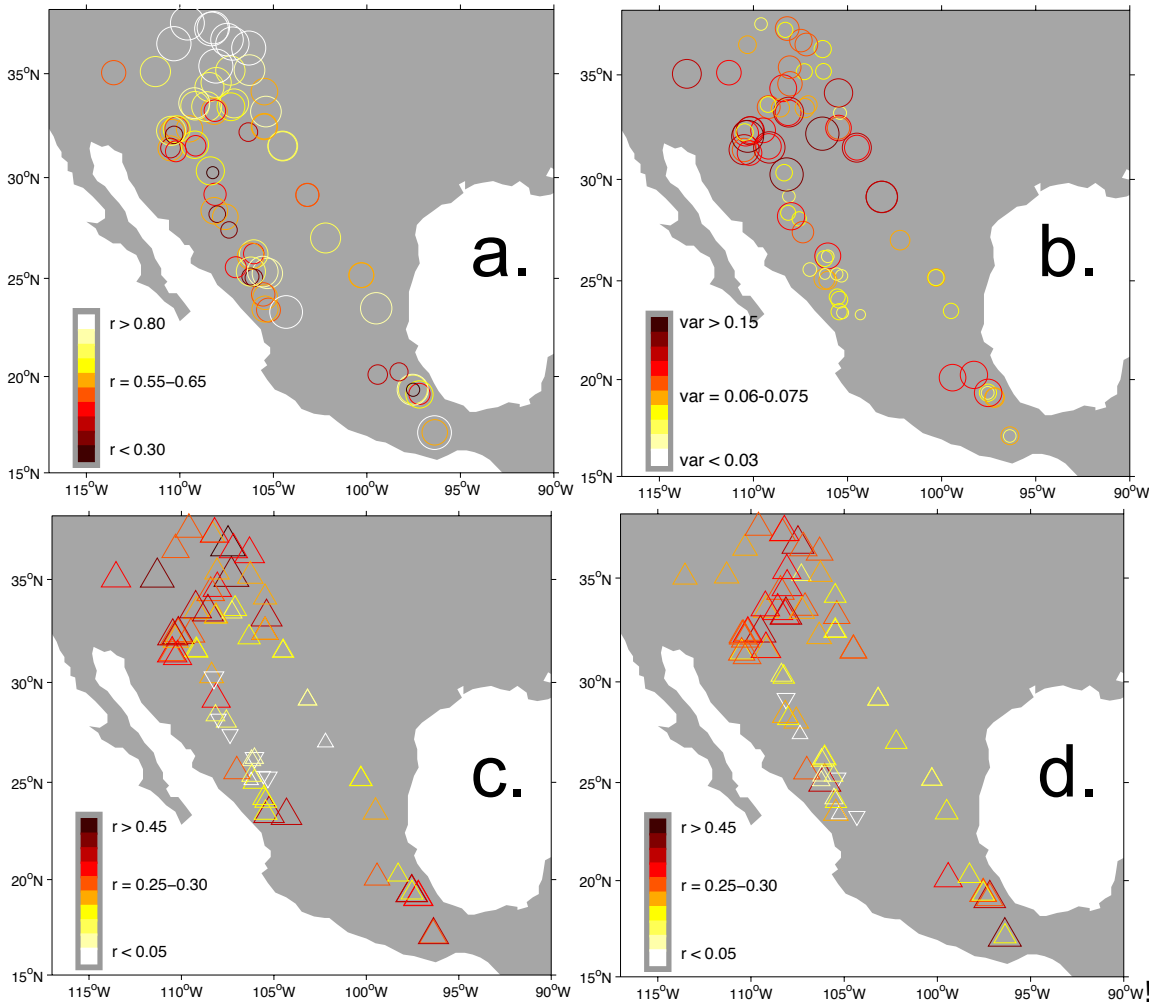

Figure 9. Statistics of seasonal growth for 78 Douglas-fir chronology pairs in the southwestern United States and Mexico: correlation between EW and LW (a); LW_a variance (b); correlation between EW_{t-1} and EW_t (c); and correlation between $LW_{a(t-1)}$ and EW_t (d).

CHAPTER 3

The relationship between cool and warm season moisture over the central United States, 1685-2015

Max C.A. Torbenson[1,2]*, David W. Stahle[1]

[1] Department of Geosciences, University of Arkansas, Fayetteville, Arkansas, United States.

[2] Departamento de Ciências Florestais, Universidade Federal de Lavras, Lavras, Minas Gerais, Brazil.

* Corresponding author: mtorbens@uark.edu

ABSTRACT

Land-surface feedbacks impart a significant degree of persistence between cool and warm season moisture availability in the central United States. However, the degree of correlation between these two variables is subject to major changes that appear to occur on decadal to multidecadal time scales, even in the relatively short 115-year instrumental record. Tree-ring reconstructions have extended the limited observational record of long-term soil moisture levels but such reconstructions do not resolve the seasonal differences in moisture conditions. We present two separate 331-year long seasonal moisture reconstructions for the central United States, based on sensitive subannual and annual tree-ring chronologies that have strong and separate seasonal moisture signals: an estimate of the long-term May soil moisture balance and a second estimate of the short-term June to August atmospheric moisture balance. The predictors used in each seasonal reconstruction are not significantly correlated with the alternate season target. Both reconstructions capture over 70% of the interannual variance in the instrumental data for the calibration period and also share significant decadal and multidecadal variability with the

instrumental record in both the calibration and validation periods. The instrumental and reconstructed moisture levels are both positively correlated between spring and summer, strongly enough to have potential value in seasonal prediction. However, the relationship between spring and summer moisture exhibits major decadal changes in strength and even sign that appear to be related to large scale ocean-atmosphere dynamics associated with the Atlantic Multidecadal Oscillation.

INTRODUCTION

Monthly timescale persistence of drought and wetness can play an important role in the forecasting of seasonal moisture levels (Preisler and Westerling 2007; Mason and Badour 2008; Hao et al. 2014). Spring moisture conditions in the central United States have some skill in predicting the baseline probability of summer drought (Lyon et al. 2012; Otkins et al. 2015). A nationwide perspective on the correlation between spring soil moisture and the atmospheric moisture balance during the following summer is presented in **Figure 1**. The self-calibrated Palmer Drought Severity Index (scPDSI; Palmer 1965; Wells *et al*. 2004) for the month of May is correlated with Palmer's Z index (which is calculated without prescribed persistence) for June-August (JJA), and the highest correlations are computed in the Mediterranean climate of California and southern Oregon. The weakest spring to summer moisture correlations are computed in the monsoon climate of the southwestern United States. A zone of high inter-seasonal correlation is also present in the central United States, extending from the coast of Texas to central Minnesota (**Figure 1**). The seasonal climatology can explain the presence or absence of seasonal persistence in California, the Pacific Northwest, and the Southwest, but in the central United States land-surface feedbacks and possibly large-scale ocean atmospheric forcing may be responsible and could therefore provide a degree of useful forecast potential (Lyon et al. 2012; Otkins et al. 2015).

One consequence of the persistence in moisture levels from spring to summer is that spring drought is unlikely to be terminated during the following summer months (Karl et al. 1987). However, the usefulness of seasonal persistence in climate forecasting is dependent on temporal stability. A weakening of the moisture correlation from spring to summer can be observed on decadal timescales in instrumental records, greatly degrading the skill in simple

persistence-based forecasts. Large-scale ocean atmospheric variability may be responsible for some changes in the strength of seasonal moisture persistence. Identifying the factors involved in the change is persistence may lead to improved forecasting. Longer proxy records of persistence, extending beyond the period of observational data, may be helpful in understanding the seasonal evolution of drought and wetness regimes.

Long, exactly dated tree-ring chronologies have been used to extend the temporally limited instrumental record of drought and wetness on regional (e.g. Blasing et al. 1988; Watson and Luckman 2002) and continental scales (Cook et al. 1999; Cook et al. 2007, 2015; Palmer et al. 2015). These reconstructions have been valuable for investigations of large-scale ocean-atmospheric forcing and regional climate (Herweijer et al. 2007; Graham et al. 2008; Seager et al. 2009), interactions between climate and ecology (Speer et al. 2001; Woodhouse et al. 2002), and the societal responses to climatic extremes (DeMenocal 2001; Stahle and Dean 2011). These high-quality tree-ring reconstructions have identified decadal regimes of drought and wetness in the past 500 to 1000 years that were more extreme than those experienced in the instrumental period (Herweijer et al. 2006; Cook et al. 2011; Stahle et al. 2011).

Most North American tree-ring chronologies are correlated with the long-term soil moisture balance integrating conditions prior to and during the spring-summer growing season (Fritts 1965). PDSI is an excellent model of the integrated multi-season moisture signal embedded in many tree-ring chronologies and has been widely used for reconstructions (e.g. Cook et al. 1999; 2007). Reconstructions of strict single-season moisture conditions from tree rings, especially for the summer (JJA) season over the continental United States, are considerably rarer. As a result, there are few annually resolved proxy records of summer moisture that are not also correlated with antecedent conditions during the winter and/or spring.

This is an important distinction because the climate dynamics responsible for interannual to decadal variability of drought can change from the cool to warm season (Seager et al. 2009; Coats et al. 2015; Pu et al. 2016). The impact of multi-season droughts will also tend to be more severe than anomalies confined to a single season (e.g., Stahle et al. 2009; Griffin et al. 2013) and with the overestimation of seasonal persistence, the potential predictability of summer conditions from soil moisture during the preceding season cannot be evaluated with tree-ring reconstructions.

The two most extreme decadal droughts of the 20th century in North America differed across space but also in seasonality, and appears to have involved different climate forcings. In the southcentral United States, the Dust Bowl drought of the 1930s was most intense during summer and developed in part due to a combination of global sea surface temperature (SSTs) anomalies and regional land surface feedbacks (Cook et al. 2011; Cook and Seager 2013). The 1950s drought was most severe over some sectors of the United States during the winter-spring when La Niña conditions prevailed in the equatorial Pacific (Hoerling et al. 2009; Seager and Hoerling 2014; Pu et al. 2016). If separate seasonal signals, mirroring the relationship in the instrumental data, can be recovered from a subset of the available tree-ring chronologies then it may be possible to use these high-quality climate proxies to gain a greater understanding of the complex seasonal variability and persistence of droughts and pluvials.

In this paper we describe the development of new sub-annual tree-ring chronologies of latewood width for shortleaf pine (*Pinus echinata*) that have strong signals of full summer (JJA) moisture conditions (without being excessively correlated with any preceding season). The derived reconstruction of the summer moisture balance is then compared with an equally strong reconstruction of the soil moisture during the preceding winter-spring based on earlywood width

and total ring-width chronologies of post oak (*Quercus stellata*), eastern red cedar (*Juniperus virginiana*), and baldcypress (*Taxodium distichum*) that are only correlated with cool season conditions. These two reconstructions are used to separately describe the history of cool and warm season moisture variability over the southcentral United States for the past 330-years, including the co-occurrence of cool and warm season extremes. The persistence of drought from spring to summer is estimated in both the instrumental and reconstructed indices, and periods when the relationship between spring and summer seasonal moisture weakens and even reverses sign are identified. These variations in inter-seasonal persistence appear to be related to anomalies in large-scale ocean-atmospheric forcing and Atlantic sea surface temperatures (SSTs), which may provide an empirical basis for improving seasonal forecasts based only on persistence.

METHODS

Tree-ring data collected by the University of Arkansas Tree-Ring Laboratory from 14 old growth forest locations in southcentral United States were used in this study (**Table 1**). Each collection is made up of 40-80 increment core specimens and/or cross-sections from living or dead trees, and the annual rings (**Figure 2**) on all specimens were exactly dated to their calendar year of formation with dendrochronological methods (Stokes and Smiley 1968). These collections include samples from shortleaf pine, post oak, bald cypress, and eastern cedar. Most of these species exhibit a sharp distinction between earlywood and latewood portions of the annual ring (also known as springwood and summerwood), and interannual variability in these subannual ring components may contain useful proxy information on both cool and warm season climate conditions (e.g. Schulman 1942; Meko and Baisan 2001; Griffin et al. 2013). The dated tree rings from the 14 sites were measured for earlywood width (EWW), latewood width (LWW),

and total ring width (TRW) with a precision of 0.001 mm on a stage micrometer. Several different methods of standardization to remove age-related effects on radial growth and to stabilize the variance of each right with series were evaluated. The signal free method of detrending and standardization (Melvin and Briffa 2008; Cook et al. 2014), using age-dependent splines, was chosen due to its ability to retain low and medium frequency variability. The EWW, LWW, and TRW measurements were first power transformed and then an age-dependent spline (Cook and Peters 1981; Melvin et al. 2007) that allowed for a positive asymptote was fitted to each measurement series. The width indices were calculated as residuals from the fitted curve values and then averaged to produce master chronologies of EWW, LWW, and TRW for each collection, which represent the mean radial growth conditions at each collection site.

The various types of ring width chronologies were correlated with the closest grid point of monthly moisture balance indices (scPDSI and *Z* index; Williams et al. 2015) based on PRISM data (Daly et al. 2004) for the common period 1921-1980 to identify the season of highest association between hydroclimate and tree-growth. The 14 chronologies include ten that were mainly correlated with cool season moisture and four that were mainly correlated with the warm season. Principal component analysis (PCA; Jolliffe 2002) was performed on the ten EWW and TRW chronologies displaying correlations above r = 0.30 with local May scPDSI. This group of EWW and TRW chronologies is referred to as the cool season network. PCA was also performed on a separate group of four shortleaf pine LW chronologies that are all highly correlated with the moisture balance in the three summer months (JJA), referred to as the warm season network. Because none of the chronologies used in either seasonal network is correlated higher with the alternate climate season (**Table 2**), or higher than the range of inter-correlation

between the instrumental data (see below), it was possible to develop two separate cool and warm season moisture reconstructions for our study region.

a. Cool-season reconstruction

The first principal component time series (PC1) of the cool season chronology network is correlated the highest with observed May scPDSI data (**Figure 3a**). The scPDSI uses instrumental precipitation and temperature to estimate available soil moisture (Palmer, 1965) and is calibrated with local climate data to allow for comparisons of drought and wetness intensity across space (Wells *et al*. 2004). The index prescribes a strong month-to-month persistence term of 0.897 and has been a standard for calculating long-term meteorological drought in climatology (Heim, 2002) and paleoclimatology (Cook et al. 2007). Based on the spatial pattern of correlations between the first principal component of the cool season chronology network and scPDSI, a regional time-series was computed by averaging scPDSI from grid points within a bounding box covering 32.75-38.25°N and 90.25-98.25°W.

Forward stepwise regression between the tree-ring predictors (i.e. PC1 in year t, t_{-1}, and t_{+1}) and May scPDSI was computed. The coefficients of the regression model were used to estimate May drought severity back to 1685. The predictor PC1 time series computed from the cool season network was calibrated with the predictand May scPDSI for the period 1941-1980, and the reconstruction was verified on independent instrumental data for the period 1895-1940. Standard regression and statistical metrics were used to quantify the agreement between reconstructed and instrumental May PDSI at interannual time scales, including the calibration period explained variance, the square of the Pearson correlation coefficient, the reduction of error (RE), and coefficient of efficiency (CE) during the validation period (Fritts 1976; Cook et al. 1999). The instrumental May scPDSI variance lost in regression was restored to the

reconstruction so that the instrumental data could be used to extend the full estimate from 1685 to 2015 (331-years) using both reconstructed and instrumental data. Spectral coherence analysis (Percival and Constantine 2006) was employed to estimate how well the reconstruction and instrumental data of May scPDSI agree on timescales greater than the interannual. The similarity of the time series' periodogram (Bloomfield 2000) was compared to standard Gaussian noise using bootstrap simulations (n = 10,000). Singular spectrum analysis (SSA; Ghil et al. 2002; St. George and Ault 2011) was performed to decompose the reconstructions into temporal eigenvectors in order to estimate the relative importance of variability at different periodicities.

b. Warm-season reconstruction

PC1 of the warm season chronology network displays the highest correlation with the JJA *Z* index (**Figure 3b**). Unlike scPDSI, no month-to-month persistence is included in the calculation of the *Z* index (Palmer 1965; Heim 2002). Therefore, any correlation between May scPDSI and the subsequent summer moisture balance represented by the JJA Z-index would be due to persistence in the physical climate system and would not arise from the statistical design of the indices. Furthermore, we only use shortleaf pine LWW chronologies to estimate the JJA Z-index. These LWW chronologies are not significantly correlated with the winter-spring scPDSI and there can be no physiological persistence between the cool and warm season proxies, which are based on separate chronologies from different species. Precipitation dictates a large portion of the variability in summer *Z* index in our study region, with more than 70% of the variance in JJA *Z* index explained by JJA precipitation. The first PC time series of the warm season network was used to reconstruct the regional average JJA *Z* index for the central U.S. from 1685-1980, and updated to 2015 with the instrumental *Z* indices for summer, using the

same regional domain, calibration, and validation procedures that were used estimate May scPDSI (above).

c. Analysis of the possible persistence between cool- and warm-season moisture

Running correlations between instrumental May scPDSI and JJA *Z* index for a 25-year moving window, advancing in one-year increments, were computed to examine the stability of the relationship between cool- and warm-season moisture availability over time. The same analyses were performed on the reconstructed data. Spectral coherence analysis (Ghil et al. 2002, St. George and Ault 2011) was used to identify any frequency band-limited coherence between reconstructed cool and warm season moisture from 1685 to 2015. Each year in the reconstructions was also ranked according to the severity of spring and summer drought respectively. To estimate the persistence in inter-seasonal moisture conditions, the absolute difference in rank between spring and summer was computed. The reconstructions and rank difference time series were compared to the Atlantic Multidecadal Oscillation index (AMO; Enfield et al. 2001) for the period 1871-2015.

RESULTS

The results for each reconstruction will first be described, followed by a discussion of annual and decadal extremes, confirmation of selected extremes with historical information, analysis of the frequency and characteristics of moisture reversals, and analyses of the time dependency in the potential predictability of summer moisture based on conditions during spring.

a. Reconstruction of May scPDSI

The PC1 time series based on the ten cool season chronologies in year t makes up the predictor of May scPDSI in the forward regression for the 1941-1980 calibration period. The transfer function used for the reconstruction of regional May scPDSI is simply:

$$\hat{Y}_t = 0.01 + 0.634X_t \quad (1)$$

where $\hat{Y}_t$ is the estimated May scPDSI value for year *t* and X_t is the value for the cool season PC1 time series also in year *t*. The transfer function explains 70.4% of the interannual variability in May scPDSI during the calibration period (1941-1980; **Table 3**, **Figure 4a**). This strong empirical relationship between cool season PC1 and May scPDSI weakens somewhat in the validation period (1895-1940), but even during the statistically independent early 20th century the reconstruction is still representing over 50% of the variance in the instrumental May scPDSI (r = 0.728, **Table 3**). An alternative calibration period, using the full instrumental data, reaffirms the strong hydroclimate signal that exists in the ten cool season chronologies. The reconstruction passes the reduction of error (RE = 0.486) and the coefficient of efficiency (CE = 0.449) tests, indicating that the reconstruction provides a skillful estimation of the independent moisture balance data (Cook and Kairiukstis, 1990). The scPDSI values in the instrumental data (**Figure 4b**) and the reconstructed time series (**Figure 4c**) are both normally distributed (Lilliefors test ($p > 0.05$); Conover, 1980) but the more numerous reconstructed values are more symmetrical around the mean. The reconstruction and instrumental data are highly correlated (r = 0.79) over the full overlapping period (1895-1980), and the scatter plot indicates only a slight deviation from linearity in the point cloud (**Figure 4d**). The results of the spectral coherence analysis indicate that the instrumental and reconstructed May scPDSI time series share significant

common variability at all frequencies, including decadal and multi-decadal time scales (**Figure 4e**).

b. Reconstruction of JJA Z index

The PC1 time series based on the four shortleaf pine LWW chronologies in year t was entered as a potential predictor in a regression with the summer Z index for the central United States for 1941-1980. The transfer function for reconstructing the regional JJA *Z* index is:

$$\hat{Y}_t = 0.076 + 0.593X_t \quad (2)$$

where $\hat{Y}_t$ is the estimated JJA *Z* index for year *t* and X_t is the value of PC1 of the four LWW chronologies in year *t*. The instrumental data for 1895-1940 were withheld for independent statistical verification of the reconstruction. The transfer function explains 74.2% of the interannual variability in JJA *Z* index during the calibration period (1941-1980; **Figure 5a**). Similar to the reconstruction of May scPDSI, the strong relationship during the calibration period weakens only a little when the reconstruction is compared with independent *Z* indices during the validation period 1895-1940 (r = 0.797). The distribution of instrumental *Z* index values (**Figure 5b**) is largely in agreement with the reconstructed time series (**Figure 5c**), and both instrumental and reconstructed data are normally distributed.

c. Persistence between May scPDSI and JJA Z index

The correlation between the regionally averaged spring scPDSI and summer Z index in the instrumental data is statistically significant for the study area (r = 0.38 for 1895-2015, $p < 0.01$; r = 0.43 for 1895-1980, $p < 0.01$). The central United States is one of few regions in North America where simple persistence of these seasonal moisture balances could have some modest value in climate forecasts (**Figure 1**). However, the correlation between the two variables shows

great variability over the instrumental era. The period 1978-2002 displays the weakest relationship between spring and summer hydroclimate, with the correlation falling below 0.0, while other 25-year periods reach correlations above 0.60.

The relationship between the reconstructed indices mimics the varying correlation between the instrumental data (r = 0.24, 1895-1980, no statistical difference from the correlation of the instrumental data for the same period ($p > 0.05$); Fisher 1921). The correlation for the full period of reconstruction (1685-2015; r = 0.33, **Figure 6ab**) is not statistically different from the correlation of instrumental data for 1895-2015 (r = 0.38), and as with the instrumental data, the relationship between spring and summer moisture varies significantly over time. For some periods the running correlation exceeds 0.7 and for shorter intervals it falls below zero. The overall correlation between the reconstructions is slightly lower than for the instrumental data for the overlapping period (1895-1980) but is not statistically different, and the running correlations fluctuate in a similar way (**Figure 7a**). Notable breakdowns in the correlation are found in the 1980s and 1990s, around 1900, in the 1860s and 1820s, and periods of high correlations are noted for the 1950s, 1880s and the second half of the 18th century. During the last 145 years of available instrumental data (1871-2015), the AMO was in the negative phase for 81 years and in the positive phase for 64 years. Testing the rank differences of the two AMO phases with Welch's t-test (Welch 1947) reveals a significant ($p = 0.0078$) difference in the sample populations, with greater similarity (or persistence) between spring and summer ranks during years of positive AMO (**Figure 8ab**), likely to explain the time-dependent relationship seen in the running correlation (**Figure 7a**).

DISCUSSION

The strong reconstructions of spring and summer moisture presented in this paper offer new insights into the hydroclimatic history of the central United States for the past 331 years. Cool season precipitation, and its effect on spring soil moisture, has a defining impact on radial growth of post oak, bald cypress, and eastern red cedar (e.g. Blasing et al. 1988; Stahle and Cleaveland 1988) and tree-ring chronologies from these species therefore represent excellent proxies of May scPDSI. Extended periods of drought and pluvials are prominent in the reconstruction (**Figure 6a**), with the 1980s and 90s standing out as the wettest sustained spring conditions of the past 330 years. The decade of lowest reconstructed values is recorded for 1855-1864 (mean scPDSI: -1.33), which has previously been dubbed the 'Civil War Drought' (Stahle and Cleaveland 1988; Woodhouse and Overpeck 1998; Fye et al. 2003; Herweijer et al. 2006). These low-frequency swings are apparent in the spectral properties of the record and the first reconstructed components of the SSA fall around 16 years, explaining more than 20% of the variance in May scPDSI.

The strong statistics for the JJA Z index reconstruction is based on the LW width chronologies of shortleaf pine. Schulman (1942) first discovered the remarkable summer moisture signal embedded in the latewood of this species but little work has been done since to further utilize the proxy climate information in this subannual ring width variable. Because tree-ring chronologies from North America tend to be correlated mainly with long-term integrated cool and warm season hydroclimate variables, records of only summer conditions are rare (St. George 2014). Shortleaf pine also displays some of the lowest correlation between earlywood and latewood width of any conifer species on the continent (Torbenson et al. 2016), suggesting that on average there is little climate information shared between earlywood and latewood. Similar to the decadal- to bi-decadal variability recorded in the spring scPDSI reconstruction, the

first reconstructed components of the summer Z index reconstruction fall around 16 years. The 1930s Dust Bowl drought stands out as the lowest estimates of summer drought period in the record but individual years of greater severity are recorded in the pre-instrumental era (**Figure 6b**).

We note that there is a modest positive trend in the May scPDSI since the mid-19th century (**Figure 6a**) that might be consistent with the increase in both streamflow and precipitation in the instrumental record for the northcentral United States (Lettenmaier et al. 1994; Lins and Slack 1999; Hirsch and Ryberg 2012). No significant trend is present in the summer Z index reconstruction over this interval. However, the early 20th century pluvial (Woodhouse et al. 2005, Cook 2011) is strongly expressed in the summer atmospheric moisture balance reconstruction (**Figure 6b**), in fact more so than in the May scPDSI estimate.

a. Historical validation of the reconstructions

The reliability and strength of both reconstructions is further supported by historical sources, which validate many of the years and periods of extreme values recorded by the proxy records. The lowest pre-instrumental value in the May scPDSI reconstruction occurs in 1855, a year that in previous studies have been described as the "driest summer of the past 500 years", or the Kiowa "sitting summer" of drought so severe that their horses were too weak to ride (Mooney 1979; Stahle et al. 2007). Although the reconstructed May soil moisture balance indicates very dry conditions in our study region in 1855, the JJA Z reconstruction shows just above average conditions (Z = 0.21). In fact, using the Karl et al. (1987) thresholds for drought termination and amelioration, the reconstructed Z index value for 1855 suggests that the summer conditions would have ameliorated the anteceding spring drought. The presence of average summer rainfall in 1855 is also supported by historical records (Hickmon 1920).

The lowest single-year value in the summer reconstruction is recorded for 1838, when the estimated JJA Z index was -2.65. Period accounts from Arkansas suggest that it was the most disastrous drought ever experienced, despite average spring conditions, and that the corn harvest averaged less than half of what was generally expected (Hickmon 1920). During 1838, the United States government initiated the forceful removal of the Cherokee nation from the land in present-day Georgia, what is known as the 'Trail of Tears' (Perdue and Green, 2007). The estimated number of deaths on the journey to Oklahoma totaled at least 4,000 (Knight 1954) but the true number may have been considerably higher (Thornton 1984). Drought is said to have been so bad in the southeastern United States that the migration had to be halted during the early summer of 1838. By that time, however, three detachments of Cherokee had already been sent by June 17th (Perdue and Green 2007). These parties travelled through some of the worst summer conditions the southcentral United States have experienced in the past 330 years, and the lack of moisture in 1838 undoubtedly added to the traumatic conditions the Cherokee had to endure.

b. The relationship between spring soil moisture and the subsequent atmospheric moisture balance in summer

Running correlation analyses suggest that the relationship between spring and summer hydroclimate over the central United States is subject to strong decadal modulation, due in part to large-scale ocean-atmospheric variability. The running correlation between instrumental May scPDSI and JJA Z index is plotted from 1895-2015 (**Figure 7a**) and documents major changes in the magnitude of seasonal persistence. The running correlation for the instrumental spring and summer data exceeded r = 0.7 during the 1970s, but then became negative below r = -0.3 during the 1990s. The running correlation between reconstructed May scPDSI and reconstructed summer Z index is also plotted in **Figure 7a** and largely reproduces the changes in magnitude

seen in the instrumental data. In fact, the reconstructions indicate that strong multi-decadal changes in the correlation between spring and summer moisture have been a significant reoccurring feature of the seasonal hydroclimate variability over central United States since 1685. The running correlation was above 0.7 for several decades after 1750 and showed negative values around 1825, the 1850s and 1860s, and around 1900. During these phases, the chance of summer rainfall to mitigate spring drought is significantly lessened.

The coupling between soil moisture in spring and the atmospheric moisture balance in the following months is likely due in part to land-surface feedbacks and the recycling of moisture through evapotranspiration and precipitation (Betts et al. 1996). These processes are the strongest over midcontinent regions for the summer months (Brubaker et al. 1993; Koster et al. 2000) and correlations between May and August soil moistures in our study region have been found to range from 0.2 to 0.5 in models and instrumental data (Huang et al. 1996; Maurer et al. 2002). Our results, using both instrumental and reconstructed scPDSI and Z index, fall within these reported correlations.

Land-surface feedbacks have been shown to play a significant role in the amount of memory imparted from spring to summer moisture conditions but the impact is thought to be greater during years of drought (Hu and Feng 2004). However, there does not appear to be any preference towards dry years in the relationship between spring and summer conditions in the instrumental nor the reconstructed data in our study. The decadal to multi-decadal modulation of the correlation between spring and summer moisture further indicates that land-surface feedbacks may not be the sole driver of seasonal persistence. The reconstructions suggest a few episodes of strong association when 25% of the variance in the summer moisture balance may be

explained by antecedent spring soil moisture conditions. During the 1750s and 1950s the relationship may have exceeded 40% of the variance (**Figure 7a**).

This regime-like relationship between spring and summer moisture raises important questions about potential teleconnections that may be involved. Certainly, land-surface feedbacks must be considered, but ocean-atmosphere processes appear to have some impact on the relationship. Other research has suggested that SSTs may influence the amount of persistence imparted on seasonal precipitation in parts of North America (Mo and Paegle 2000; Feng et al. 2011). If the breakdowns in correlation have a dynamical component that can be identified, then the potential usefulness for forecasting could be strengthened. Below, we hypothesize on one such possible component; the Atlantic Multidecadal Oscillation.

c. The possible influence of SSTs on seasonal moisture balance persistence

North Atlantic SSTs have been highlighted as a possible predictor in forecasting North American climate (Sutton and Allen 1997), and drought variability in the central United States has previously been linked to the AMO (Enfield et al. 2001; Rogers and Coleman 2003; McCabe et al. 2004). The reconstructed time series of ranked differences between spring and summer (**Figure 6c**) displays significant negative correlation with cool-season (October through March) SSTs in the waters south and southeast of Greenland, as well as weaker but significant negative correlations with the North Pacific (**Figure 8a**). This pattern is similar to the spatial pattern of the AMO (Xie and Tanamoto 1998; Enfield et al. 2001; Ting et al. 2009; Deser et al. 2010). The positive (warm) phase of the AMO is strongly associated with fall season precipitation deficits in the central United States (Knight et al. 2006) and significant deficits are also recorded for spring and summer (Nigam et al. 2011), resulting in interseasonal drought persistence during years of positive AMO. Warmer North Atlantic SSTs are thought to drive moisture transport south across

the continent and reduce the amount of precipitation coming from the Gulf of Mexico (Nigam and Ruiz-Barradas 2006; Nigam et al. 2011). This multi-season impact could, at least in part, explain the stronger correlation between May scPDSI and JJA Z index in our study region during periods of positive AMO. However, the relationship between warmer North Atlantic SSTs and seasonal moisture persistence in our study area is not confined solely to years of drought.

In the instrumental era, the highest rank differences occur in the first decade of the 20th century (**Figure 6c**). Not surprisingly, this period displays the lowest extended correlation between May scPDSI and JJA Z index and it coincides with a strong negative excursion in the AMO index (**Figure 8**). The 1950s and early 60s are characterized by low rank differences and also occur during one of the warmest periods of observational SSTs south of Greenland (Dijkstra et al. 2006). A sharp decrease in the running correlation is recorded during the decades of cold North Atlantic SST following 1970. The AMO has been in a positive phase during the most recent 15-20 years, and although the window length of the running correlation only allows for an upwards trend, the rank differences have been below the mean for most years since 2000 (**Figure 6c**).

Models suggest that the AMO has been a stable feature of North Atlantic climate variability in periods prior to the instrumental record (Grosfeld et al. 2007; Feng et al. 2008; Ting et al. 2011) and the reconstructions indicate that the time-dependent coupling between spring and summer moisture during the 20th and early 21st century may be part of the long-term climate dynamics of the region in the pre-instrumental era as well. Gray et al. (2004) produced a 12-month averaged AMO index based on tree-ring chronologies from eastern United States, western Europe, and north Africa that extends from 1567 to 1990. The running correlation between reconstructed May scPDSI and JJA Z index exhibits similar multidecadal variability with the

Gray et al. (2004) AMO reconstruction (**Figure 7**). The relationship is not perfect, perhaps partly due to the different seasonal window for the AMO, but the lowest extended period of correlation between spring soil moisture and the subsequent summer atmospheric moisture balance is recorded for the decades after 1900, the longest negative spell of the AMO in the instrumental data. Similarly, a breakdown in correlation between May scPDSI and JJA Z index occurred during the most negative period of the AMO reconstruction (the 1810s and 1820s), and negative AMO values and low correlations can also be found in the 1720s. Periods of exceptionally strong correlation between spring and summer moisture over the past 300 years appear to occur during times when the reconstruction of the AMO index is in a positive phase.

CONCLUSIONS

The new reconstructions of spring and summer moisture each represent over 70% of the instrumental moisture variability during the calibration period and provide high quality records of seasonal moisture variability over the central United States from 1685-2015. The reconstructions indicate major differences between cool and warm season moisture regimes since 1685, including the 1850-60s when the cool season suffered severe sustained dryness but the warm season was near normal. During the 1880's the warm season was dry but the cool season was relatively wet.

Similar to the instrumental data, the cool and warm season reconstructions are weakly but significantly correlated and can be used to examine decadal variations in seasonal persistence over the past 330-years. In fact, the running correlation between May scPDSI and the JJA Z index in both the instrumental and reconstructed series varies substantially over time. Significant positive correlation prevails, but decadal episodes of both high and low correlation are evident. Even brief episodes of zero correlation between the cool and warm season are observed in the

instrumental and reconstructed data for the central United States, when all predictive skill would have been lost. These decadal variations in seasonal persistence suggest that land-surface feedbacks may not be the only drivers of the correlation between May soil moisture and the subsequent summer atmospheric moisture balance.

The variability shared by the reconstructions probably does not arise from biological growth persistence and likely reflects forcing from the physical climate system. The two reconstructions are produced using not only different tree-ring chronologies but they also represent separate tree species. The predictors for each reconstruction represent the strongest seasonal signal in the trees, without any correlation with the alternate season falling outside the range of climatological persistence in the region. The relationship between the two reconstructions largely mirrors that of the instrumental data and because of this separation of seasons, information that may have been muddled in an integrated drought variable such as summer PDSI can be extracted from these selected high quality seasonal proxies. Fluctuations in the correlation between the reconstructions in the pre-instrumental era appear to largely represent the time-varying relationship between spring and summer moisture availability.

The AMO has been implicated in the development of drought and pluvial conditions over the central United States, and our results suggest that the AMO may also influence the level of moisture persistence from the cool to warm season. Persistent atmospheric pressure fields over the interior United States appear to be more common during years of warmer North Atlantic SSTs associated with the AMO. The new cool and warm season reconstructions also suggest that multidecadal variability in moisture persistence has been an important feature of climate over the study area during the past 330-years. Warm North Atlantic SSTs might therefore change the

probability of cool to warm season moisture persistence and have some modest value for seasonal climate prediction over the central United States.

ACKNOWLEDGEMENTS

We appreciate the constructive discussions had about the manuscript with Dorian Burnette, Edward Cook, Daniel Griffin, Ian Howard, and Park Williams. We thank the Oklahoma Nature Conservancy for permission to collect tree-ring samples from the Nickel Preserve and Michael Stambaugh for permission to re-measure his tree-ring collections from Missouri and Oklahoma. Finally, Greg Pederson and two additional anonymous reviewers helped improve this manuscript. The National Science Foundation (grant #AGS-1266014) funded this study.

REFERENCES

Betts, A.K., J.H. Ball, A.C.M. Beljaars, M.J. Miller, and P.A. Viterbo, 1996. The land surface-atmosphere interaction: A review based on observational and global modeling perspectives. *Journal of Geophysical Research* **101** (D3): 7209-7225.

Blasing, T.J., D.W. Stahle, and D.N. Duvick, 1988. Tree-ring based reconstruction of annual precipitation in the south-central United States from 1750 to 1980. *Water Resources Research* **24**: 163-171.

Bloomfield, P., 2000. *Fourier Analysis of Time Series – An Introduction*. John Wiley & Sons, Inc., New York, NY.

Brubaker, K.L., D. Entekhabi, and P.S. Eagleson, 1993. Estimation of continental precipitation recycling. *Journal of Climate* **6**: 1077-1089.

Coats, S., J.E. Smeardon, R. Seager, D. Griffin, and B.I. Cook, 2015. Winter-to-summer precipitation phasing in southwestern North America: A multicentury perspective from paleoclimatic model-data comparisons. *Journal of Geophysical Research: Atmospheres* **120**.

Conover, W., 1980. *Practical nonparametric statistics* (2nd edition), Wiley, New York, NY.

Cook, B.I., 2011. On the causes and dynamics of the early twentieth-century North American pluvial. *Journal of Climate* **24**: 5043-5060.

Cook, B.I., E.R. Cook, K.J. Anchukaitis, R. Seager, and R.L. Miller, 2011. Forced and unforced variability of twentieth century North American droughts and pluvials. *Climate Dynamics* **37**: 1097-1110.

Cook, B.I., and R. Seager, 2013. The response of the North American Monsoon to increased greenhouse gas forcing. *Journal of Geophysical Research: Atmospheres* **118**: 1690-1699.

Cook, E.R., and K. Peters, 1981. The smoothing spline: A new approach to standardizing forest interior tree-ring width series for dendroclimatic studies. *Tree-Ring Bulletin* **41**: 45-53.

Cook, E.R., and A. Kairiukstis, 1990. Methods of Dendrochronology – Applications in the environmental sciences. International Institute for Applied Systems Analysis, Kluwer Academic Publishers, Dordrecht, Netherlands.

Cook, E.R., D.M. Meko, D.W. Stahle, and M.K. Cleaveland, 1999. Drought reconstructions for the continental United States*. *Journal of Climate* **12**: 1145-1162.

Cook, E.R., R. Seager, M. Cane, D.W. Stahle, 2007. North American drought: reconstructions, causes, and consequences. *Earth Science Reviews* **81**: 93-134.

Cook, E.R., P.J. Krusic, and T.M. Melvin, 2014. Program RCSigFree. Tree-Ring Lab, Lamont Doherty Earth Observatory of Columbia University, Palisades, NY.

Cook, E.R. and 58 others, 2015. Old World megadroughts and pluvials during the Common Era. *Science Advances* **1**: e1500561.

Daly, C., W.P. Gibson, M. Doggett, J. Smith, and G. Taylor, 2004. Up-to-date monthly climate maps for the conterminous United States. 14th AMS Conf. on Applied Climatology, 84th AMS Annual Meeting Combined Preprints, Seattle, WA.

De Monocal, P.B., 2001. Cultural responses to climate change during the late Holocene. *Science* **292**: 667-673.

Deser, C., M.A. Alexander, S-P. Xie, and A.S. Philips, 2010. Sea surface temperature variability: Patterns and mechanisms. *Annual Review of Marine Science* **2**: 115-143.

Dijkstra, H.A., L. te Raa, M. Schmeits, and J. Gerrits, 2006. On the physics of the Atlantic Multidecadal Oscillation. *Ocean Dynamics* **56**: 36-50.

Edmondson, J.R., 2010. The meteorological significance of false rings in eastern redcedar (Juniperus virginiana L.) from the southern Great Plains, U.S.A. *Tree-Ring Research* **66**: 19-33.

Enfield, D.B., A.M. Mestas-Nuñez, and P.J. Trimble, 2001. The Atlantic Multidecadal Oscillation and its relation to rainfall and river flows in the continental U.S. *Geophysical Research Letters* **28**: 2077-2080.

Feng, S., R.J. Oglesby, C.M. Rowe, D.B. Loope, and Q. Hu, 2008. Atlantic and Pacific SST influences on Medieval drought in North America simulated by the Community Atmospheric Model. *Journal of Geophysical Research: Atmospheres* **113**.

Feng, S., Q. Hu, and R.J. Oglesby, 2011. Influence of Atlantic sea surface temperatures on persistent drought in North America. *Climate Dynamics* **37**: 569-586.

Fisher, R.A., 1921. On the probable error of a coefficient of correlation deduced from a small sample. *Metron* **1**: 3-32.

Fritts, H.C., 1965. Tree ring evidences for climatic changes in western North America. *Monthly Weather Review* **93**: 421-443.

Fye, F.K., D.W. Stahle, and E.R. Cook, 2003. Paleoclimatic analogs to 20th century moisture regimes across the USA. *Bulletin of the American Meteorological Society* **84**: 901-909.

Fye, F.K., D.W. Stahle, E.R. Cook, and M.K. Cleaveland, 2006. NAO influence on sub-decadal moisture variability over central North America. *Geophysical Research Letters* **33**: L15707.

Ghil, M., M.R. Allen, M.D. Dettinger, K. Ide, D. Kondrashov, M.E. Mann, A.W. Robertson, A. Saunders, Y. Tian, F. Varadi, and P. Yiou, 2002. Advanced spectral methods for climatic time series. *Reviews of Geophysics* **40**: 3-1-3-41.

Graham, N.E., M.K. Hughes, C.M. Ammann, K.M. Cobb, M.P. Hoerling, D.J. Kennett, J.P. Kennett, B. Rein, L. Stott, P.E. Wigand, and T. Xu, 2007. Tropical Pacific – mid-latitude teleconnections in medieval times. *Climatic Change* **83**: 241-285.

Gray, S.T., J.L. Graumlich, J.L. Betancourt, and G.T. Pederson, 2004. A tree-ring based reconstruction of the Atlantic Multidecadal Oscillation since 1567 A.D. *Geophysical Research Letters* **31**: L12205.

Griffin, D., C.A. Woodhouse, D.M. Meko, D.W. Stahle, H.L. Faulstich, C. Carrillo, R. Touchan, C.L. Castro, and S.W. Leavitt, 2013. North American monsoon precipitation reconstructed from tree-ring latewood. *Geophysical Research Letters* **40**: 954-958.

Grosfeld, K., G. Lohmann, N. Rimbu, K. Fraedrich, and F. Lunkeit, 2007. Atmospheric multidecadal variations in the North Atlantic realm: proxy data, observations, and atmospheric circulation model studies. *Climate of the Past* **3**: 39-50.

Hao, Z., A. AghaKouchak, N. Nakhjiri, and A. Farahmand, 2014. Global integrated drought monitoring and prediction system. *Scientific Data* **1**: 14001.

Heim, R.R., 2002. A review of twentieth-century drought indices used in the United States. *Bulletin of the American Meteorological Society* **83**: 1149-1165.

Herweijer, C., R. Seager, and E.R. Cook, 2006. North American droughts of the mid to late nineteenth century: a history, simulation and implication for Mediaeval drought. *Holocene* **16**: 159-171.

Herweijer, C., R. Seager, E.R. Cook, and J. Emile-Geay, 2007. North American droughts of the last millennium from a gridded network of tree-ring data. *Journal of Climate* **20**: 1353-1376.

Hickmon, W.C., 1920. Weather and crops in Arkansas, 1819 to 1879. *Monthly Weather Review* **48**: 447-51.

Hirsch, R.M., and K.R. Ryberg, 2012. Has the magnitude of floods across the USA changed with global CO_2 levels? *Hydrological Sciences Journal* **57**: 1-9.

Hoerling, M.P., X.-W. Quan, and J. Eischeid, 2009. Distinct causes for two principal U.S. droughts of the 20th century. *Geophysical Research Letters* **36**: L19708.

Hu, Q., and S. Feng, 2004. Why has the land memory changed? *Journal of Climate* **17**: 3236-3243.

Huang, J., H.M. van den Dool, and K.P. Georgarakos 1996. Analysis of model-calculated soil moisture over the United States (1931-1993) and applications to long-range temperature forecasts. *Journal of Climate* **9**: 1350-1362.

Jolliffe, I., 2002. *Principal Component Analysis*. Springer, Dordrecht, Netherlands.

Karl, T.R., F. Quinlan, and D.S. Ezell, 1987. Drought termination and amelioration: Its climatological probability. *Journal of Climate and Applied Meteorology* **26**: 1198-1209.

Knight, O., 1954. Cherokee society under the stress of removal. *Chronicles of Oklahoma* **32**: 414-428.

Knight, J.R., C.K. Folland, and A.A. Scaife, 2006. Climate impacts of the Atlantic Multidecadal Oscillation. *Geophysical Research Letters* **33**.

Koster, R.D., M.J. Suarez, and M. Heiser, 2000. Variance and predictability of precipitation at seasonal-to-interannual timescales. *Journal of Hydrometeorology* **1**: 26-46.

Lettenmaier, D.P., E.F. Wood, and J.R. Wallis, 1994. Hydro-climatological trends in the contentinental United States, 1948-1988. *Journal of Climate* **7**: 586-607.

Lins, H.F., and J.R. Slack, 1999. Streamflow trends in the United States. *Geophysical Research Letters* **26**: 227-230.

Lyon, B., M.A. Bell, M.K. Tippett, A. Kumar, M.P. Hoerling, X.-W. Quan, and H. Wang, 2012. Baseline probabilities for the seasonal prediction of meteorological drought. *Journal of Applied Meteorology and Climatology* **51**: 1222-1237.

Mason, S.J., and O. Badour, 2008. Statistical Modelling (Ch. 7) *in* A. Troccoli, M. Harrison, D.L.T. Anderson, and S.J. Mason (Eds.) *Seasonal Climate: Forecasting and Managing Risk*. Springer Science & Business Media, Berlin, Germany.

Maurer, E.P., A.W. Wood, J.C. Adams, D.P. Lettenmaier, and B. Nijssen, 2002. A long-term hydrologically based dataset of land surface fluxes and states for the conterminous United States*. *Journal of Climate* **15**: 3237-3251.

McCabe, G.J., M.A. Palecki, and J.L. Betancourt, 2004. Pacific and Atlantic influences on multidecadal drought frequency in the United States. *Proceedings of the National Academy of Sciences of the United States of America* **101**: 4136-4141.

Meko, D.M., and C.H. Baisan, 2001. Pilot study of latewood-width of conifers as an indicator of variability of summer rainfall in the North American monsoon region. *International Journal of Climatology* **21**: 697-708.

Melvin, T.M., K.R. Briffa, K. Nicolussi, and M. Grabner, 2007. Time-varying-response smoothing. *Dendrochronologia* **25**: 65-69.

Melvin, T.M., and K.R. Briffa, 2008. A "signal-free" approach to dendroclimatic standardization. *Dendrochronologia* **26**: 71-86.

Mo, K.C., and J.N. Paegle, 2000. Influence of sea surface temperature anomalies on precipitation regimes over the southwest United States. *Journal of Climate* **13**: 3588-3599.

Mooney, J., 1979. *Calendar history of the Kiowa Indians.* Smithsonian Institution, Washington, D.C. (originally published in 1898).

Nigam, S., and A. Ruiz-Barradas, 2006. Seasonal hydroclimate variability over North America in global and regional reanalyses and AMIP simulations: varied representation. *Journal of Climate* **19**: 815-837.

Nigam, S., B. Guan, and A. Ruiz-Barradas, 2011. Key role of the Atlantic Multidecadal Oscillation in 20th century drought and wet periods over the Great Plains. *Geophysical Research Letters* **38**.

Otkins, J.A., M.C. Anderson, C. Hain, and M. Svoboda, 2015. Using temporal changes in drought indices to generate probabilistic drought intensification forecasts. *Journal of Hydrometeorology* **16**: 88-105.

Palmer, J.G., E.R. Cook, C.S.M. Turney, K. Allen, P. Fenwick, B.I. Cook, A. O'Donnell, P. Grierson, and P. Baker, 2015. Drought variability in the eastern Australia and New Zealand summer drought atlas (ANZDA, CE 1500-2012) modulated by the Interdecadal Pacific Oscillation. *Environmental Research Letters* **10**: 124002.

Palmer, W.C., 1965. *Meteorological Drought*. Research Paper, vol. 45. U.S. Weather Bureau.

Percival, D.B., and W.L.B. Constantine, 2006. Exact simulation of Gaussian time series from nonparametric spectral estimates with application to bootstrapping. *Statistics and Computing* **16**: 25-35.

Perdue, T., and M.D. Green, 2007. *The Cherokee Nation and the Trail of Tears*, Penguin Group, New York, NY.

Preisler, H.K., and A.L. Westerling, 2007. Statistical model for forecasting monthly large wildfire events in western United States. *Journal of Applied Meteorology and Climatology* **46**: 1020-1030.

Pu, B., R. Fu, R.E. Dickinson, and D.N. Fernando, 2016. Why do summer droughts in the Southern Great Plains occur in some La Niña years but not others? *Journal of Geophysical Research: Atmospheres* **121**.

Rogers, J.C., and J.S.M. Coleman, 2003. Interactions between the Atlantic Multidecadal Oscillation, El Niño/La Niña, and the PNA in winter Mississippi Valley stream flow. *Geophysical Research Letters* **30**.

St. George, S., and T.R. Ault, 2011. Is energetic decadal variability a stable feature of the central Pacific Coast's winter climate? *Journal of Geophysical Research: Atmospheres* **116**.

St. George, S., 2014. An overview of tree-ring width records across the Northern Hemisphere. *Quaternary Science Reviews* **95**: 132-150.

Schulman, E., 1942. Dendrochronology in pines of Arkansas. *Ecology* **23**: 309-318.

Seager, R., A. Tzanova, and J. Nakamura, 2009. Drought in the southeastern United States: Causes, variability over the last millennium, and the potential for future hydroclimate change. *Journal of Climate* **22**: 5021-5045.

Seager R., and M. Hoerling, 2014. Atmosphere and ocean origins of North American droughts. *Journal of Climate* **27**: 4581-4606.

Speer, J.H., T.W. Swetnam, B.E. Wickman, and A. Youngblood, 2001. Changes in Pandora moth outbreak dynamics during the past 622 years. *Ecology* **82**: 679-697.

Stahle, D.W., M.K. Cleaveland, and J.G. Hehr, 1985. A 450-year drought reconstruction for Arkansas, United States. *Nature* **316**: 530-532.

Stahle, D.W., and M.K. Cleaveland, 1988. Texas drought history reconstructed and analyzed from 1698 and 1980. *Journal of Climate* **1**: 59-74.

Stahle, D.W., F.K. Fye, E.R. Cook, and R.D. Griffin, 2007. Tree-ring reconstructed megadroughts over North America since A.D. 1300. *Climatic Change* **83**: 133-149.

Stahle, D.W., M.K. Cleaveland, H. Grissino-Mayer, R.D. Griffin, F.K. Fye, M.D. Therrell, D.J. Burnette, D.M. Meko, and J. Villanueva Diaz, 2009. Cool- and warm-season precipitation reconstructions over western New Mexico. *Journal of Climate* **22**: 3739-3750.

Stahle, D.W., and J.S. Dean, 2011. North American tree rings, climatic extremes, and social disasters. In Hughes, M.K., T.W. Swetnam, H.F Diaz (Eds.) *Dendroclimatology: Progress and Prospects*. Developments in Paleoenvironmental Research **11**: 297-327.

Stahle, D.W., J. Villanueva Diaz, D.J. Burnette, J. Cerano Paredes, R.R. Heim Jr., F.K. Fye, R. Acuna Soto, M.D. Therrell, M.K. Cleaveland, and D.K. Stahle, 2011. Major Mesoamerican droughts of the past millennium. *Geophysical Research Letters* **38**: L05703.

Stokes, M.A., and T.L. Smiley, 1968. *An introduction to tree-ring dating*. University of Chicago Press, Chicago, IL.

Sutton, R.T., and M.R. Allen, 1997. Decadal predictability of North Atlantic sea surface temperature and climate. *Nature* **388**: 563-567.

Thornton, R., 1984. Cherokee population losses during the Trail of Tears: a new perspective and a new estimate. *Ethnohistory* **31**: 289-300.

Ting, M., Y. Kushnir, R. Seager, and C. Li, 2009. Forced and internal twentieth-century SST trends in the North Atlantic. *Journal of Climate* **22**: 1469-1482.

Ting, M., Y. Kushnir, R. Seager, and C. Li, 2011. Robust features of Atlantic multi-decadal variability and its climate impacts. *Geophysical Research Letters* **38**.

Torbenson, M.C.A., D.W. Stahle, J. Villanueva Diaz, E.R. Cook, and D. Griffin, 2016. The relationship between earlywood and latewood ring-growth across North America. *Tree-Ring Research* **72**: 53-66.

Watson, E., and B.H. Luckman, 2002. The dendroclimatic signal in Douglas-fir and ponderosa pine tree-ring chronologies from the southern Canadian Cordillera. *Canadian Journal of Forest Research* **32**: 1858-1874.

Welch, B.L., 1947. The generalization of 'Student's' problem when several different population variances are involved. *Biometrika* **34**: 28-35.

Wells, N., S. Goddard, and M.J. Hayes, 2004. A self-calibrating Palmer Drought Severity Index. *Journal of Climate* **17**: 2335-2351.

Williams, A.P., R. Seager, J.T. Abatzoglou, B.I. Cook, J.E. Smerdon, and E.R. Cook, 2015. Contribution of anthropogenic warming to California drought during 2012-2014. *Geophysical Research Letters* **42**: 6819-6828.

Woodhouse, C.A., and J.T. Overpeck, 1998. 2000 years of drought variability in the central United States. *Bulletin of the American Meteorological Society* **79**: 2693-2714.

Woodhouse, C.A., J.J. Lukas, and P.M. Brown, 2002. Drought in the western Great Plains, 1845-56: Impacts and implications. *Bulletin of the American Meteorological Society* **83**: 1485-1493.

Woodhouse, CA., K.E. Kunkel, D.R. Easterling, and E.R. Cook, 2005. The twentieth-century pluvial in western United States. *Geophysical Research Letters* **32**.

Xie, S-P., and Y. Tanimoto, 1998. A pan-Atlantic decadal climate oscillation. *Geophysical Research Letters* **25**: 2185-2188.

TABLES

Table 1. Tree-ring records used for the reconstructions of seasonal moisture balance over the central United States.

Site code	Site name	Lon.	Lat.	Start	End	Species	Variable	Study
CANUSA	Canadian River	35.58	98.38	1680	1982	QUST	TRW	Stahle and Cleaveland, 1988
CBKUSA	Cedar Bluff	38.46	99.49	1353	2008	JUVI	TRW	Edmondson, 2010
DNRUSA	Nichols Ranch	32.98	99.18	1681	1995	QUST	TRW	
EPLUSA	Egypt Promised	35.51	90.95	1417	1980	TADI	TRW	Stahle *et al*., 1985
HHCUSA	Hemmed in Hollow	36.08	93.31	1359	1992	JUVI	TRW	
KEYUSA	Keystone Lake	36.21	96.22	1611	1995	QUST	TRW	
MAUUSA	Little Maumelle	34.83	92.51	1532	1985	TADI	TRW	Stahle *et al*., 1985
BSWUSA	Black Swamp	35.09	91.17	1019	1980	TADI	EW	Stahle *et al*., 1985
DEVUSA	Bayou Deview	34.51	91.17	1133	1985	TADI	EW	Stahle *et al*., 1985
SKYUSA	Sky Lake	33.16	90.29	1238	2010	TADI	EW	
CCWUSA	Clifty Canyon	36.04	92.15	1672	1980	PIEC	LW	
LAWUSA	Lake Winona	34.48	92.56	1667	1980	PIEC	LW	
MCWUSA	McCurtain County	34.18	94.39	1685	1982	PIEC	LW	
NICUSA	Nickel Preserve	36.03	94.83	1581	2015	PIEC	LW	

Table 2. Correlations between tree-ring chronology predictors of May scPDSI and JJA Z index and local (closest grid point) climate data for both the period 1921-1980. Correlations in bold indicate r > 0.50 ($p < 0.001$).

May scPDSI predictors			**r May scPDSI**	**r JJA Z**
CANUSA	QUST	TRW	**0.622**	0.317
CBKUSA	JUVI	TRW	0.419	0.368
DNRUSA	QUST	TRW	0.334	0.268
EPLUSA	TADI	TRW	**0.500**	0.325
HHCUSA	JUVI	TRW	0.302	0.216
KEYUSA	QUST	TRW	**0.583**	0.308
MAUUSA	TADI	TRW	0.444	0.246
BSWUSA	TADI	EW	**0.501**	0.289
DEVUSA	TADI	EW	**0.676**	0.193
SKYUSA	TADI	EW	**0.557**	0.279
JJA Z index predictors				
CCWUSA	PIEC	LW	0.351	**0.648**
LAWUSA	PIEC	LW	0.402	**0.564**
MCWUSA	PIEC	LW	0.128	**0.746**
NICUSA	PIEC	LW	0.456	**0.724**

Table 3. Calibration and verification statistics for the reconstructions of May soil moisture and summer atmospheric moisture balance over the central United States.

	Calibration			Verification		
Variable	**Period**	***R*2 adj.**	**Durbin-Watson**	**Period**	***r***	**RE/CE**
May scPDSI	1941-1980	0.704	1.801, p = 0.485	1895-1940	0.728	0.486/0.449
JJA *Z* index	1941-1980	0.735	2.632, p = 0.826	1895-1940	0.797	0.683/0.682
May scPDSI	1895-1980	0.628	1.472, p= 0.020	-	-	-
JJA *Z* index	1895-1980	0.679	1.794, p = 0.325	-	-	-

FIGURES

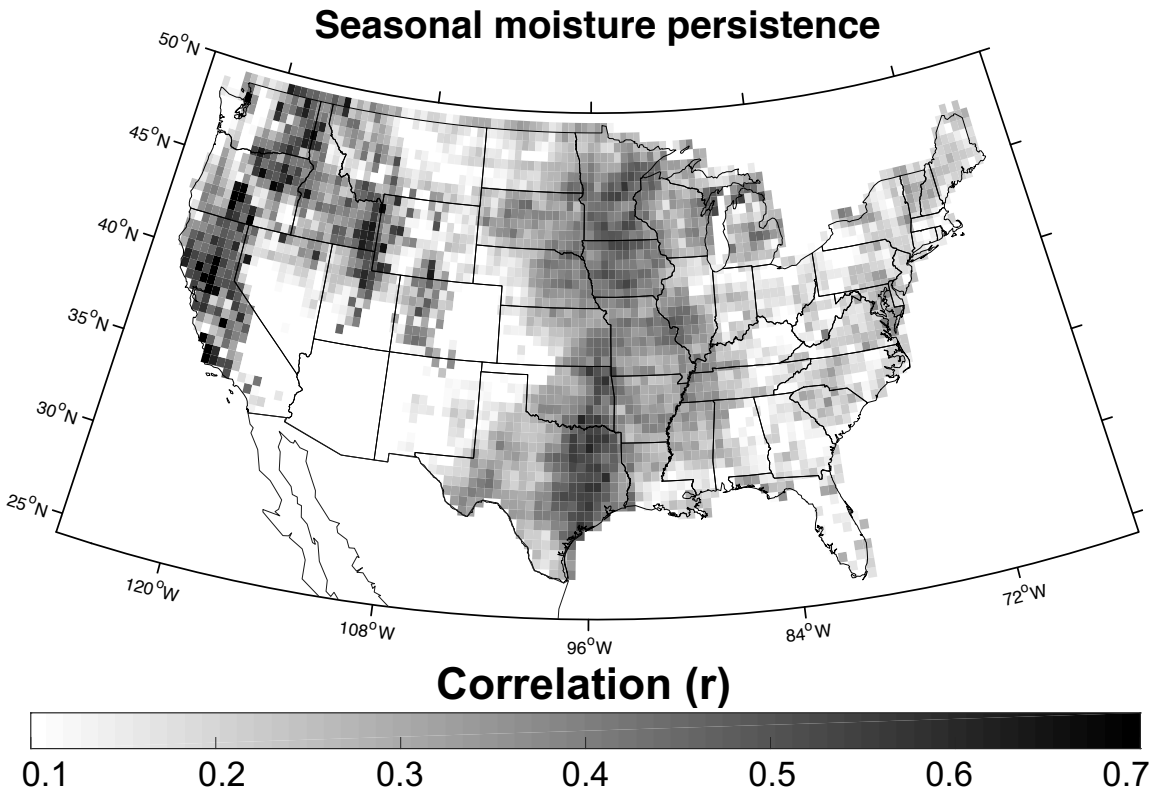

Figure 1. The correlation between the long-term soil moisture balance ending in May (May scPDSI) and the short-term atmospheric moisture balance for summer (Palmer's *Z* index for JJA) is plotted for each 0.25 by 0.25° grid point over the United States based on instrumental observations from 1895-2015.

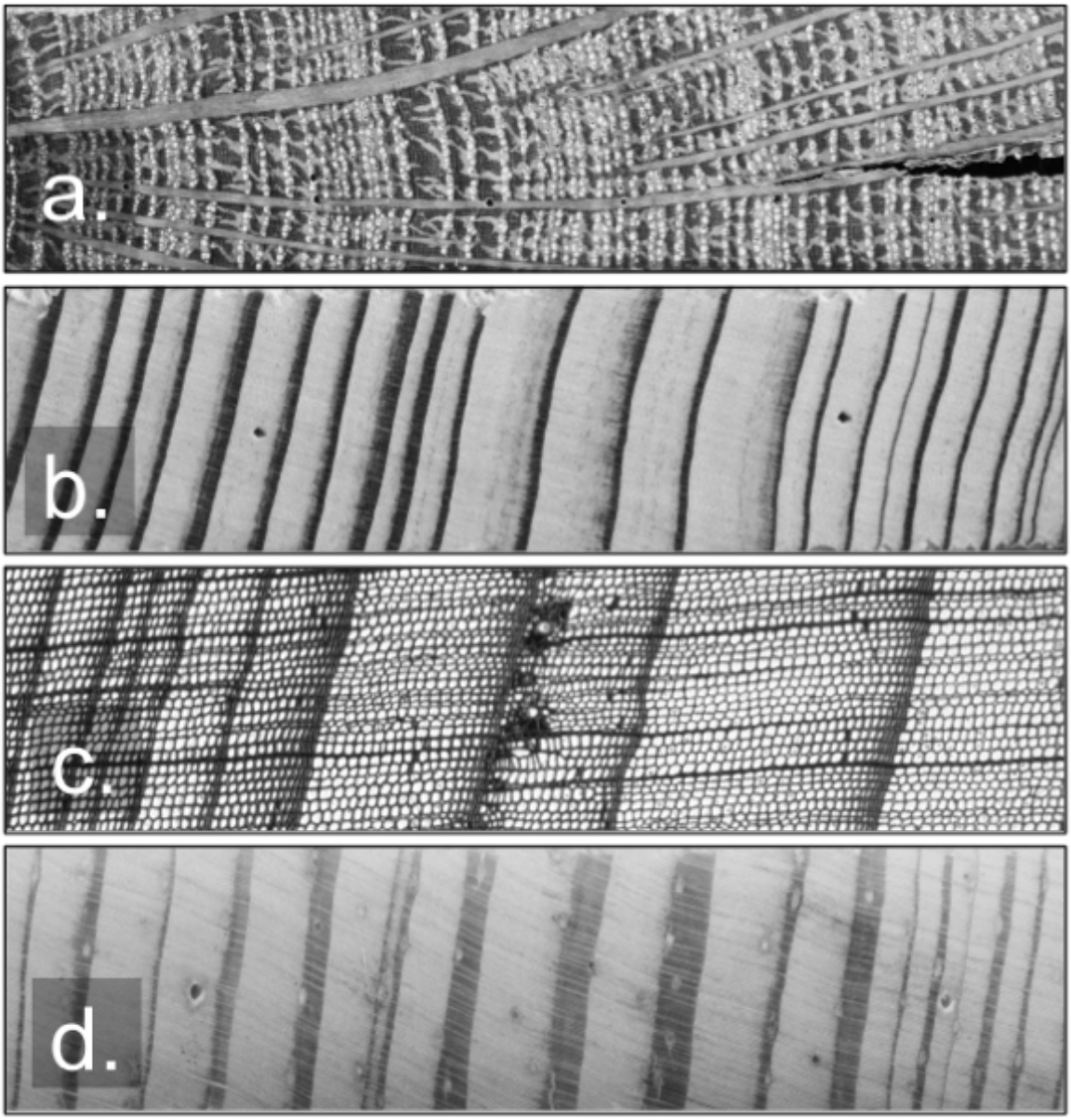

Figure 2. Photomicrographs of the annual growth rings for the tree species used for seasonal moisture reconstructions are illustrated [(a) *Quercus stellata*, (b) *Taxodium distichum*, (c) *Juniperus virginiana*, all used for the cool season; and (d) *Pinus echinata*, used for the warm season estimtes].

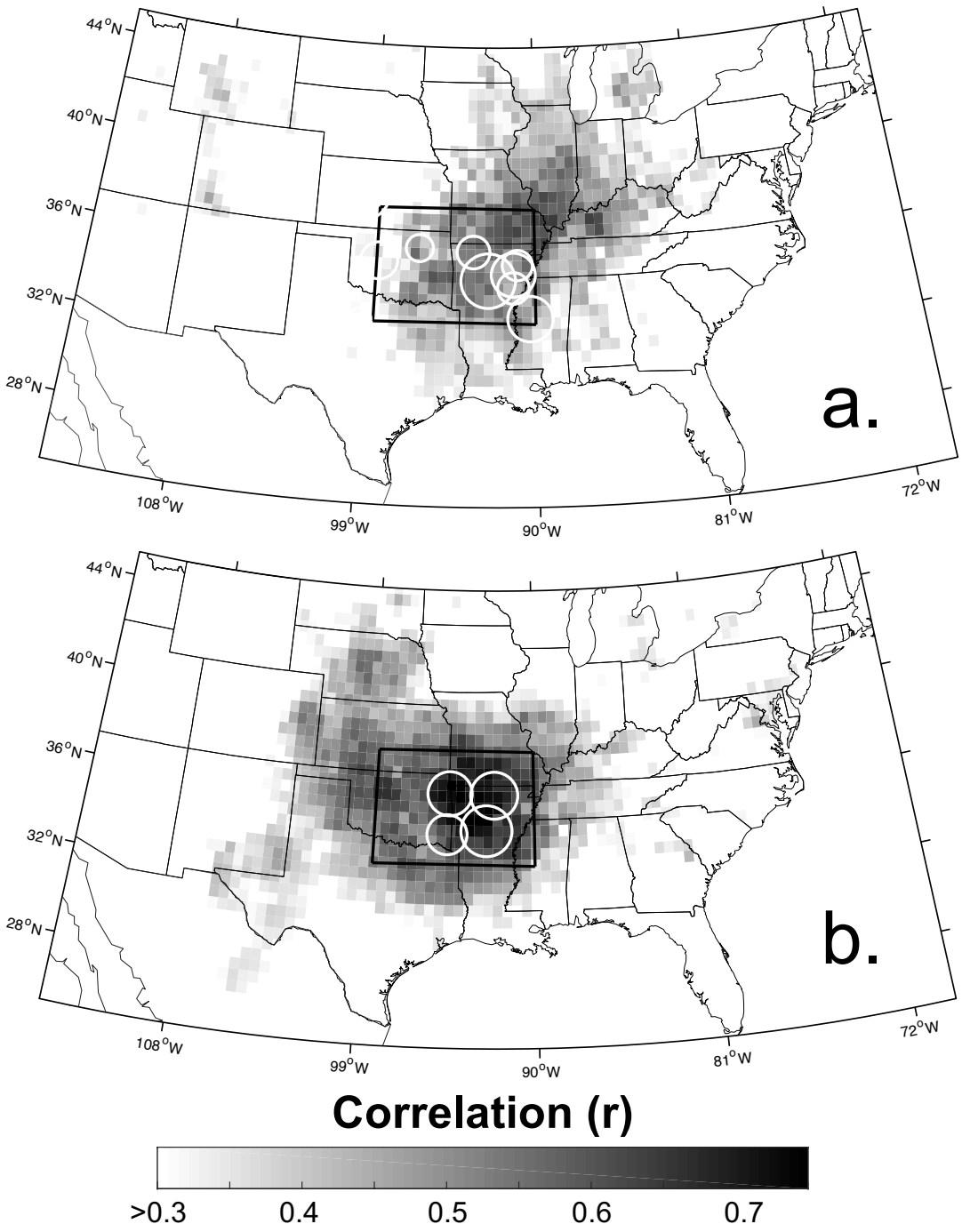

Figure 3. The spatial correlation between (**a**) the first PC time series of the cool season tree-ring network and instrumental May scPDSI for the period 1895-1980; and (**b**) the same as (**a**) for the warm season tree-ring network and the instrumental JJA Z index. Circles indicate the location of each tree-ring chronology and circle diameter is scaled to the relative loading of each chronology on PC1. The black boxes show the area of the central United States within which the regional average May scPDSI and JJA Z indices were calculated.

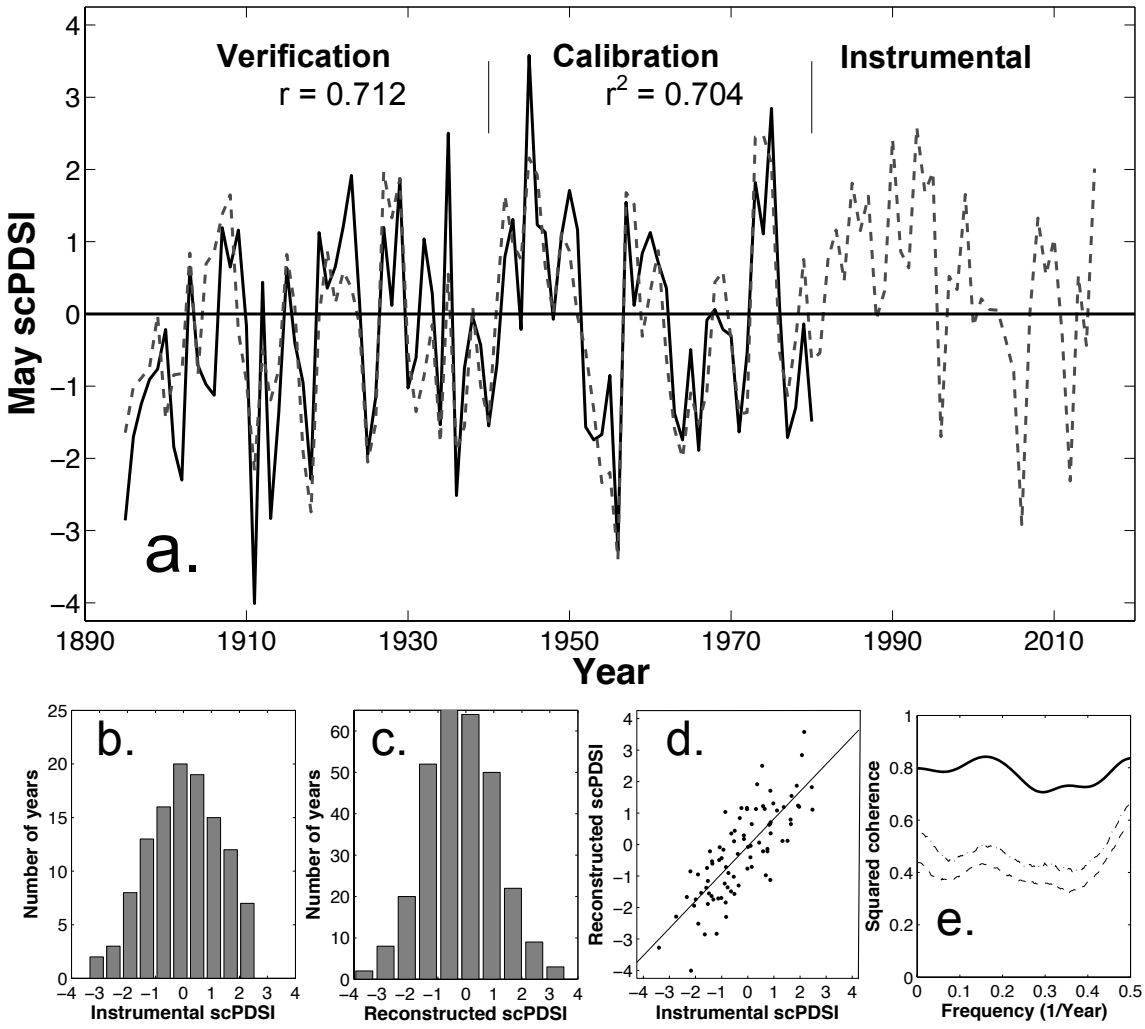

Figure 4. (**a**) The time series comparison between instrumental (dashed line) and reconstructed (solid line) regionally averaged May scPDSI for the central United States. The reconstruction was based on the cool season network of tree-ring chronologies and was calibrated for the period 1941-1980 and verified by comparison with the instrumental data from 1895-1940. The frequency distributions of scPDSI values are plotted for the instrumental observations (**b**; 1895-1980) reconstructed estimates (**c**; 1685-1980). (**d**) The scatterplot between instrumental and reconstructed May scPDSI is presented for the full overlap period (1895-1980). (**e**) The squared coherence between instrumental and reconstructed scPDSI for the period 1895-1980 is plotted (solid line; dashed lines represent the 95% and 99% confidence thresholds for significant coherence).

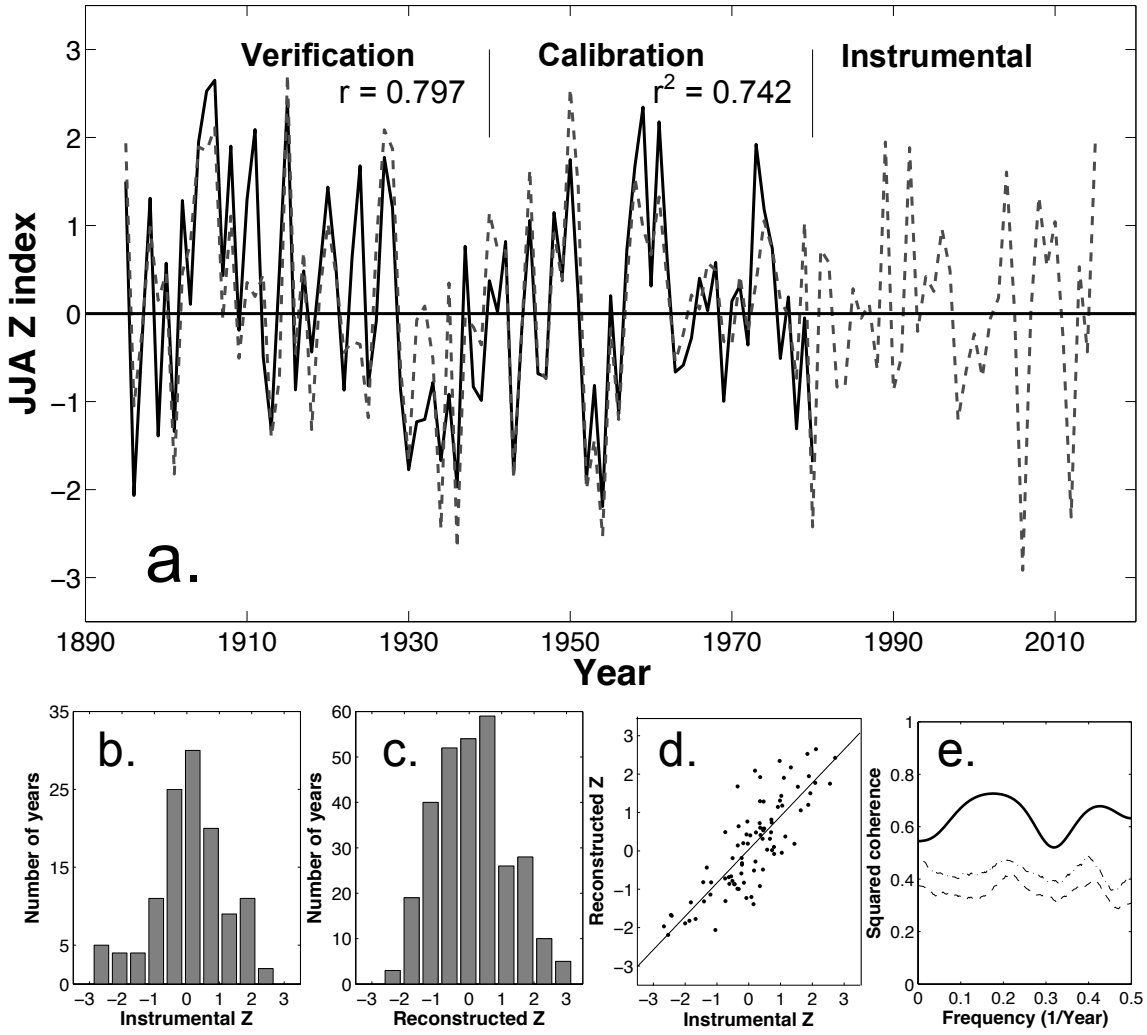

Figure 5. Same as for Figure 4 for the warm network estimation of the JJA *Z* index.

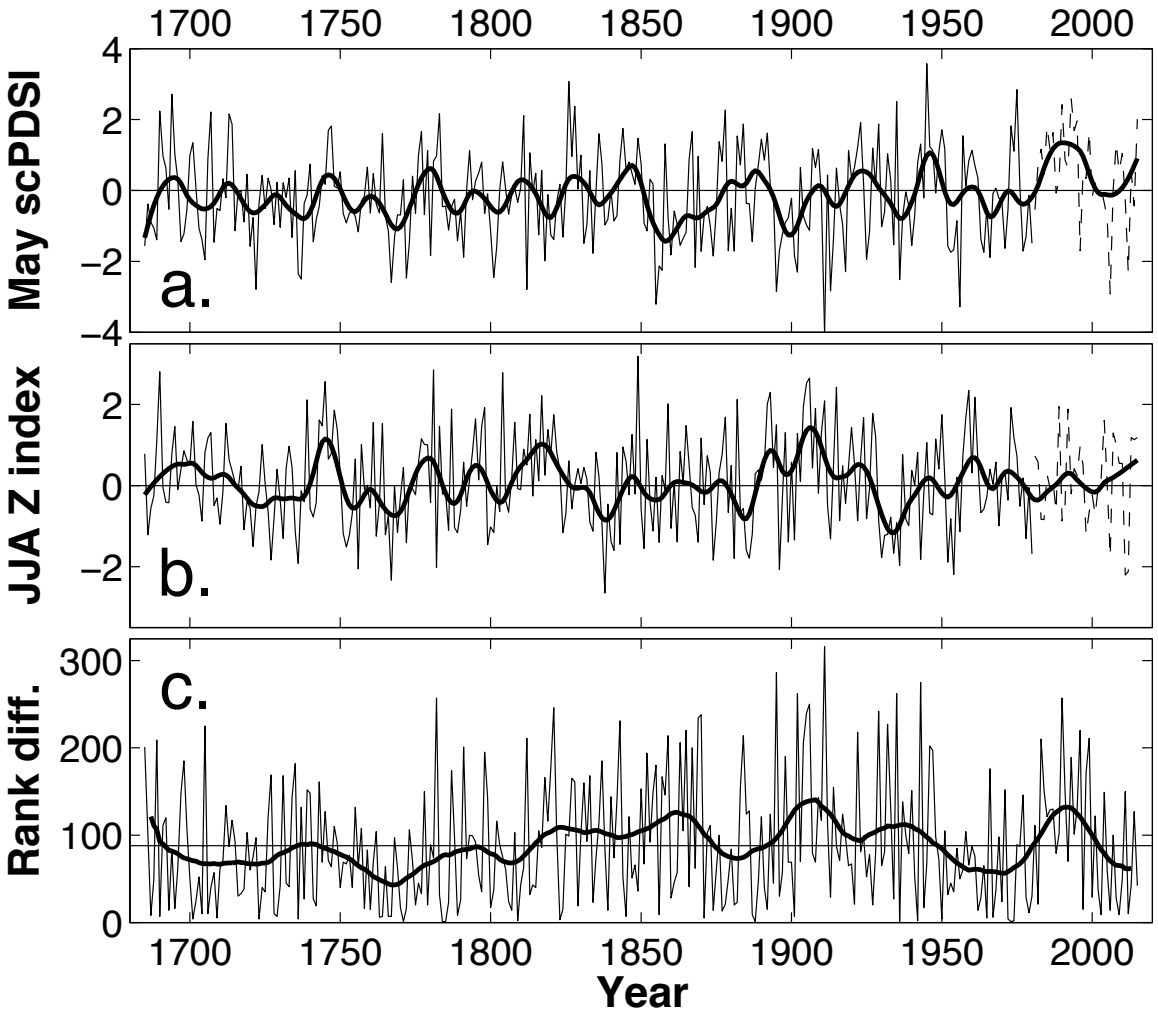

Figure 6. Moisture reconstructions for the central United States extending from 1685 to 2015 based on the tree-ring chronologies in **Table 1** and **Figure 3a,b** (**a**: May scPDSI; **b**: JJA Z index). Instrumental observations extend each seasonal reconstruction to 2015 (dashed lines). The reconstructions are fitted with a cubic spline designed to highlight the decadal variability of the time series (black curve; Cook and Peters, 1981). (**c**) Each year of the reconstructions was ranked and the absolute difference calculated to estimate the interannual change in persistence from spring to summer. A cubic spline (25 years) is fitted to the time series (black curve).

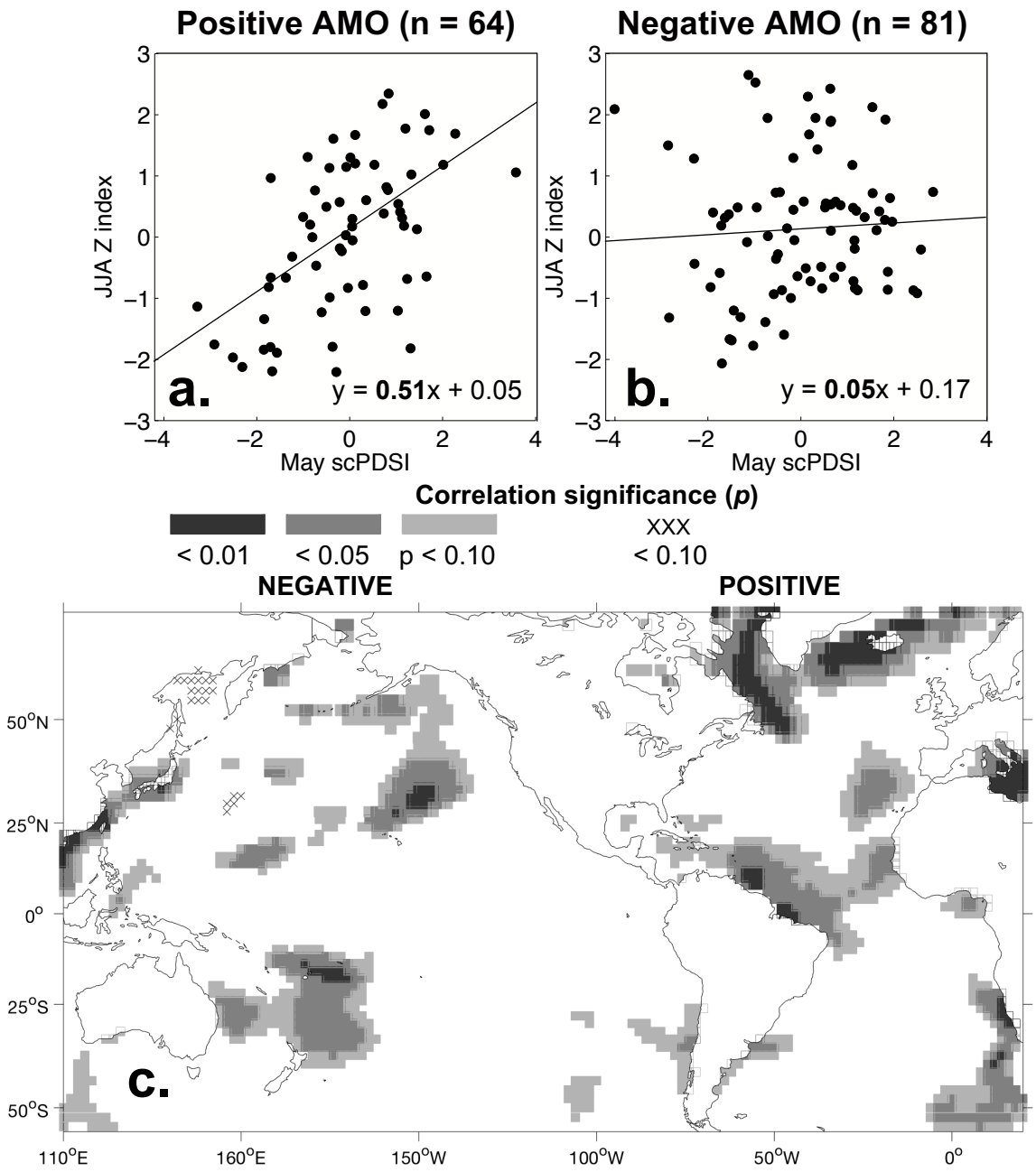

Figure 7. Scatterplots between reconstructed May scPDSI and JJA Z index during years of (**a**) negative AMO and (**b**) positive ondJFM AMO. (**c**) Correlations between detrended prior October to current March sea surface temperatures and the ranked differences time-series, 1871-2015 (**Figure 6c**).

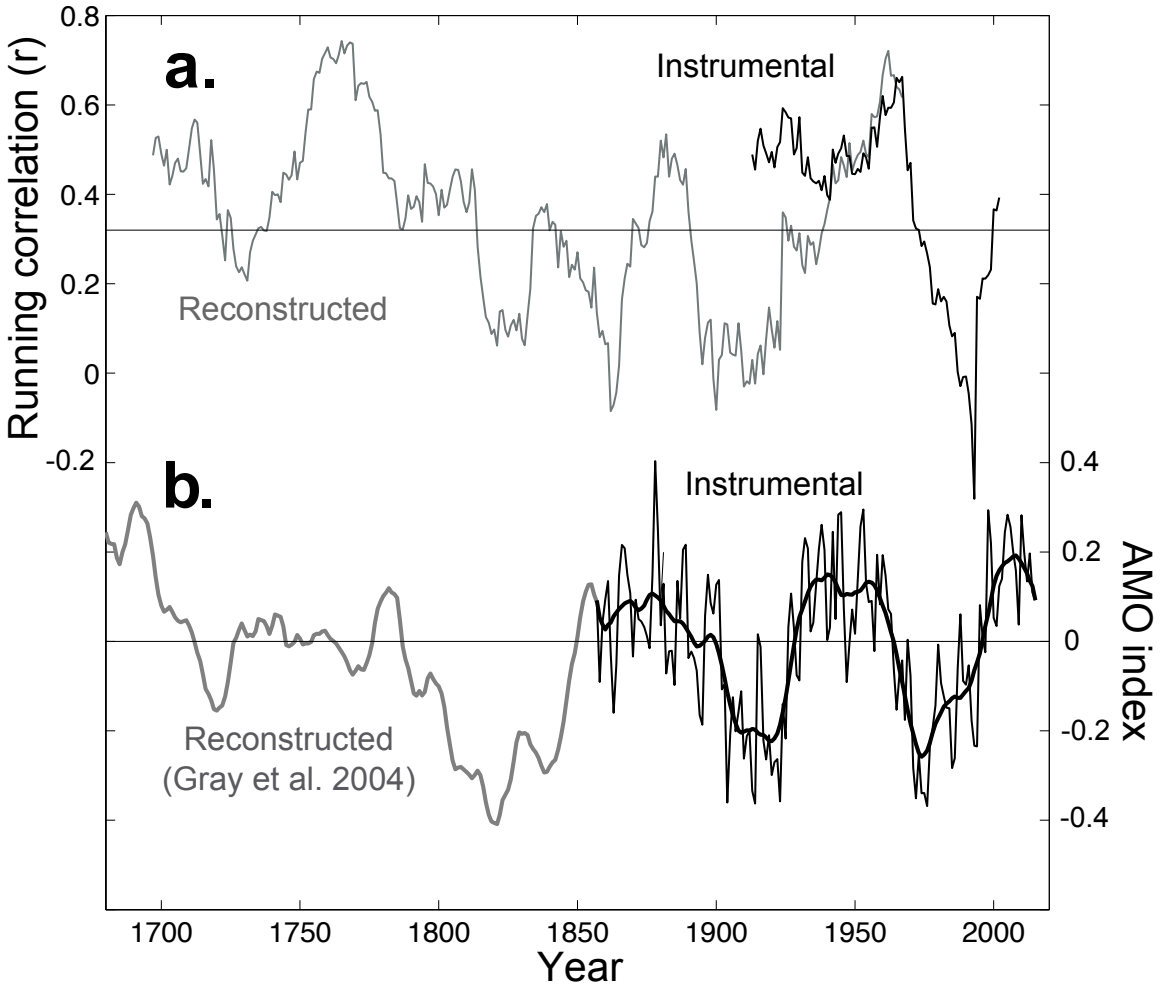

Figure 8. (**a**) The running correlation (25-year window) between the May scPDSI and the JJA Z index is plotted for the instrumental data from 1907 to 2004 (red), and for the reconstructed data from 1697 to 1968 (blue). A black line is plotted for the mean correlation between the reconstructions. (**b**) Observational AMO index for prior October to current March in black (with 10-year spline fitted in thick) and reconstructed AMO (Gray et al. 2004) fitted with a 10-year spline in grey prior to 1871.

CHAPTER 4

Multidecadal modulation of the ENSO teleconnection to precipitation and tree growth over subtropical North America

M.C.A. Torbenson[1,*], D.W. Stahle[1], I.M. Howard[1], D.J. Burnette[2], J. Villanueva-Díaz[3], E.R. Cook[4], D. Griffin[5]

[1] Department of Geosciences, University of Arkansas, AR, USA.

[2] Department of Earth Sciences, University of Memphis, TN, USA.

[3] INIFAP, Gómez Palacio, Durango, Mexico.

[4] Lamont-Doherty Earth Observatory, Columbia University, NY, USA.

[5] Department of Geography, Environment and Society, University of Minnesota, MN, USA.

Corresponding author: Max C.A. Torbenson (mtorbens@uark.edu)

Key Points:

- The ENSO teleconnection to North American hydroclimate varies in magnitude and spatial impact on multidecadal timescales.
- The strongest and most stable ENSO influence is observed in the TexMex sector of northern Mexico and the borderlands of southwestern US.
- Tree rings reproduce these temporal and spatial changes and suggest that the changes may arise in part from North Atlantic SST variations.

ABSTRACT

The teleconnection of the El Niño/Southern Oscillation (ENSO) to instrumental precipitation and temperature during the cool season over North America is strongest and most temporally stable in the TexMex sector of northern Mexico and the borderlands of southwestern United States. The ENSO impact on North American hydroclimate expands and contracts out of this region on multidecadal timescales, possibly associated with the positive and negative phases of the Atlantic Multidecadal Oscillation (AMO). A subset of tree-ring chronologies from the TexMex sector also has the strongest and most stable ENSO signal detected in the North American network, similar to the strong ENSO signal measured in instrumental climate data from the same region. This subset of chronologies is used to reconstruct the Multivariate ENSO index (MEI) as a measure of ENSO impact on North American hydroclimate during the instrumental and pre-instrumental eras. The reconstruction exhibits improved fidelity in the frequency domain and better registration of spatial changes in ENSO signal over North America when compared to an MEI reconstruction based on all ENSO-correlated tree-ring chronologies irrespective of temporal stability of correlation. When correlated with gridded instrumental and tree-ring reconstructed Palmer drought indices across North America, the stable MEI estimate reproduces the changes in spatial impact of ENSO signal measured with instrumental data and it reveals similar multidecadal changes in prehistory, potentially linked to the AMO. The Great Plains drought of the 1850s and 1860s may have been an example of this Pacific-Atlantic configuration.

INTRODUCTION

Our understanding of long-term ENSO variability, including potential decadal to multidecadal changes, is limited by relatively short meteorological and oceanographic instrumental records (Cane et al. 1993; Brown and Comrie 2004; van Oldenborgh and Burgers 2005). Due to the

relationship between ocean-atmospheric variability and regional climate, tree-ring chronologies tuned to local climate have been used as proxies to estimate pre-instrumental ENSO variability (e.g. Lough and Fritts 1990; Stahle and Cleaveland 1993; D'Arrigo et al. 2005; Li et al. 2013). Multi-proxy reconstructions of past ENSO, utilizing several different record types, have also relied heavily on North American tree-ring data (e.g. Stahle et al. 1998; Braganza et al. 2009; Gergis and Fowler 2009). Through these reconstructions, we have gained new information about long-term ENSO variability (Mann et al. 2000; D'Arrigo et al. 2005), and the interactions between ENSO and global and regional climate (Brönnimann et al. 2007), climate extremes (Gergis and Fowler 2006), volcanic eruptions (Adams et al. 2003; Wilson et al. 2010; Wahl et al. 2014), and wildfire activity (Kitzberger et al. 2007; Yocom et al. 2010). However, there are disagreements within and between reconstructions (Gergis and Fowler 2006; Wilson et al. 2010), and these differences increase the uncertainty in estimates of past ENSO variability.

The ENSO teleconnection to climate variability over subtropical North America has not been stable during the instrumental era (Cole and Cook 1998; Enfield et al. 2001; Yu et al. 2015). It has been suggested that North Atlantic sea surface temperatures (SSTs) may modulate the strength of the ENSO teleconnection to North American hydroclimatic variability (Enfield et al. 2001), and this could be a cause of some of the disagreement among tree-ring reconstructions of ENSO. The validity of any paleoclimatic reconstruction hinges on the assumption that the relationship between the proxy record and the target climate variable has remained stable over time (Lough and Fritts 1990; Grudd et al. 2002). Reconstructions of teleconnection indices do not only assume a time-stable relationship between local climate and proxy but also assume a stable relationship between local climate and the teleconnection in question. Any time-dependent relationship between the mode of ocean-atmospheric variability and the remote

predictors can exacerbate already existing sources of uncertainty in teleconnection reconstructions (Wilson et al. 2010).

In this paper, we investigate the robustness and temporal stability of ENSO signals in 447 tree-ring chronologies from subtropical North America with respect to the phases of the Atlantic Multidecadal Oscillation (AMO). Our results indicate that some chronologies that represent an important component of previous ENSO reconstructions have a time-dependent relationship with ENSO variability in the tropical Pacific. A subset of chronologies, located in the TexMex region (*per* Stahle et al. 1998) of northern Mexico, and the borderlands of New Mexico and west Texas, display a stable ENSO signal across all subperiods of analysis from 1901-1991. This stable relationship with tropical Pacific SSTs is also in agreement with the temporal and spatial correlation of ENSO with instrumental precipitation data. The subset of TexMex chronologies with a stable ENSO signal is used to estimate the waxing and waning of the ENSO teleconnection to subtropical North America on multidecadal timescales over the past 340 years.

DATA AND METHODS

Gridded precipitation and temperature data (0.5° x 0.5°, CRU TS 4.021; Harris et al. 2014) for the North American continent were compared to the extended Multivariate ENSO index (MEI; Wolter and Timlin 2011) for a common period of 1902-1991, as well as three subperiods (1902-1929; 1930-1959; and 1965-1991) based on the phasing of the AMO (*per* Enfield et al. 2001). Comparisons for a fourth subperiod (1992-2016) were calculated using the non-extended Multivariate ENSO index (MEI; Wolter and Timlin 2011). Each grid point was correlated with four-month windows of MEI spanning prior October to current May (ONDJ; NDJF; DJFM; JFMA; FMAM) with precipitation and temperature data for the same seasonal windows.

North American tree-ring chronologies from south of 42°N, publically available at the International Tree-Ring Data Bank (ITRDB; Grissino-Mayer and Fritts 1997; https://www.ncdc.noaa.gov/data-access/paleoclimatology-data/datasets/tree-ring), were screened for correlation with ENSO. A total of 447 tree-ring records, including both conifer and deciduous species, spanning at least 1871-1991 were selected for analysis. Of these 447 chronologies, 116 included earlywood width (EW), latewood width (LW), and total ring-width (TRW) variables (Torbenson et al. 2016). The other 331 records only include TRW. Chronologies were correlated with MEI for the common period 1902-1991, as well as for the three early periods. Instrumental MEI data for 1872-1901 were withheld for verification purposes. For records that contain EW, LW, and TRW, only the chronology with the highest correlation with a given ENSO variable for 1902-1991 was selected for further analysis. Records that displayed a significant local correlation with MEI were also compared to the gridded CRU precipitation and temperature variables for the same periods as with the ENSO data. The CRU climate data were spatially smoothened using the Queen's case approach (Lloyd 2010) on the nine closest grid points to the tree-ring record location.

a. Reconstruction of the regional ENSO signal

Two separate reconstructions of past ENSO influence on the study region were produced in order to estimate the impact that non-stationary ENSO response may have on reconstruction fidelity and uncertainty. All chronologies were again screened for correlation with November through February MEI for an early calibration period (1902-1959). The first reconstruction only considered chronologies that also correlate significantly ($r > 0.42$) with NDJF MEI for 1960-1991 as potential predictors. This "stable" subset of chronologies (i.e. well-correlated with MEI in both periods) was submitted to a principal components analysis (PCA; Jolliffe 2002). The

resulting PC1 was entered into a simple regression model with NDJF MEI as the target predictand, using the screening period (1902-1959) as calibration and 1960-1991 for independent verification. Because of the differing start dates of the individual predictor chronologies, three PC1 regression models (nests) were produced for periods 1869-1991, 1770-1991, and 1675-1991. This process was repeated using a late calibration (1930-1991) and early verification (1902-1929) periods. The early and late calibration reconstructions were then averaged (D'Arrigo et al. 2005) to produce a stable reconstruction of the ENSO signal in North American tree-ring chronologies from 1675-1991 (referred to as the stable reconstruction). The nests were spliced together, using the nest of maximum number of predictors for each time period.

The same reconstruction procedure was performed on the full network of chronologies, irrespective of their multidecadal variations in correlation with the NDJF MEI during the verification period (referred to as the ALL reconstruction), and includes chronologies with both stable and nonstable ENSO signals. The two reconstructions (stable and ALL) were quantitatively and qualitatively compared to the instrumental MEI data, including spectral coherence analysis (Percival and Constantine 2006) and sign tests (Cook and Kairiukstis 1990). Comparisons were also made with various other previous ENSO reconstructions (e.g. D'Arrigo et al. 2005) and early documentary records of suspected El Niño and La Niña events (Gergis and Fowler 2006). Finally, the temporal instability of ENSO influence on North American hydroclimate prior to the observational period was examined through comparing the stable reconstruction with the North American Drought Atlas (NADA; Cook et al. 1999), a gridded reconstruction of the Palmer Drought Severity Index (PDSI; Palmer 1965; Cook et al. 2010).

RESULTS

The NDJF MEI is positively correlated with instrumental winter (NDJF) precipitation across subtropical North America for the full period of analysis (1902-1991), with the highest correlations in Florida, western Cuba, and northern Mexico (**Figure 1a**; Allan et al. 1996). Winter precipitation is negatively correlated with MEI over western Canada and the Pacific Northwest. The MEI is also negatively correlated with instrumental winter mean temperature over subtropical North America and positively over most of Canada and Alaska (**Figure 1b**). The negative ENSO correlations with temperature and positive correlations with precipitation during the cool season are most strongly expressed in northern Mexico, extreme southern Texas and New Mexico (**Figure 1ab**). The ENSO teleconnections to cool season precipitation and temperature also has a strong influence on the hydroclimate response of moisture sensitive tree-ring chronologies, especially over the TexMex sector (**Figure 2**). Because the growth of most TexMex tree-ring chronologies is highly correlated with soil moisture delivered during the cool season (Stahle and Cleaveland 1993), many chronologies are also well correlated with the NDJF MEI.

a. Stability of the ENSO teleconnection to climate and tree growth

Cool season precipitation and temperature in northern Mexico and the southwestern United States are significantly correlated with ENSO during both positive and negative phases of the AMO during the instrumental era. But the spatial pattern and intensity of the ENSO teleconnection expand and contract from this TexMex sector on multidecadal timescales (**Figure 3**). California precipitation was positively correlated with the MEI during the positive phases of the AMO (1930-1959, 1992-2016; **Figure 3bd**), but not during the negative phases (1902-1929, 1965-1991; **Figure 3ac**). The winter precipitation correlation with ENSO also weakens over

Arizona, east Texas, Louisiana, and elsewhere during at least one multidecadal episode of the instrumental era (**Figure 3**). The ENSO teleconnection to winter temperature is most intense and widespread during negative phases of the AMO over subtropical North America (**Figure 3eg**). But the ENSO signal in both precipitation and temperature in the core area of the TexMex sector remains statistically significant during all four multidecadal windows of the instrumental period (**Figure 3**).

This stable and significant ENSO teleconnection to instrumental precipitation and temperature is also stable and significant in a subset of North American tree-ring chronologies located in the TexMex sector. The ENSO correlation with the chronologies is illustrated in **Figure 4** for the three multidecadal phases of the AMO (1901-1929, 1930-1959, 1965-1991; as specified by Enfield et al. (2001)). In all subperiods, the chronologies that are significantly correlated with the MEI are located primarily in northern Mexico and the southwestern United States (**Figure 2**; **Figure 4abc**). However, like the instrumental climate data, the ENSO correlation to tree growth is modulated on multidecadal timescales over California, Arizona, and east Texas. When only those tree-ring chronologies that are significantly ($r > 0.42$) correlated with the MEI during all three subperiods are mapped along with the magnitude of their correlation for their full period (1901-1991), they are all located in northern Mexico and the borderland of New Mexico and west Texas (**Figure 2**). These TexMex chronologies have one of the strongest (Stahle et al. 1998; 2016) and most stable ENSO signals yet detected in tree-ring data worldwide and they are located largely within the region of subtropical North America with the strongest and most stable hydroclimate response to ENSO (**Figure 1**, **Figure 3**).

The highest number of chronologies significantly ($r > 0.42$) correlated with NDJF MEI is recorded for the subperiod 1930-1959 ($n = 112$), while the number of significant correlations for

the other two subperiods (1902-1929 (n = 75) and 1965-1991 (n = 47)) are considerably lower (**Figure 5**). The varying response to ENSO largely reflects the changes in ENSO influence on regional precipitation (**Figure 3**). For the first subperiod (1902-1929), most tree-ring chronologies from Texas are positively and significantly correlated with MEI (**Figure 4a**). In subsequent periods, when ENSO and instrumental precipitation correlations weaken, many of these chronologies also appear to lose their MEI signal (**Figure 4bc**). However, the seasonal precipitation signal in these tree-ring chronologies does not change during these subperiods of the 20th century (**Figure 5**). Chronologies selected for the stable reconstruction are slightly more numerous than those that are stable over all three subperiods (due to the combination of two of the three subperiods for calibration) but all 18 chronologies identified above make up predictors in the stable PCA for both early and late calibration (**Table 1**).

b. Estimating past ENSO influence on North American hydroclimate with tree rings: stable vs. ALL predictors

Two sets of tree-ring chronologies were used to reconstruct the MEI. The first includes all chronologies from the North American study area that show significant correlation ($r > 0.42$) for the full period of analysis (1901-1991) with MEI (the ALL set). Between the early and late calibration periods, the combined ALL reconstruction has 104 potential predictors. The second set of tree-ring chronology predictors only include chronologies that are significantly correlated with MEI in both the calibration and verification periods (1901-1959/1930-1991 and 1901-1929/1960-1991) and the total number of predictors in the stable set of chronologies is 27 (**Table 1**). The locations of chronologies used for the ALL and stable reconstructions are mapped in **Figure 6**.

The stable reconstruction has greater calibration and verification skill than the ALL reconstruction based on statistical evaluation of the nested reconstructions in the early, late, and combined periods of analysis (**Table 2**). The largest difference between the two ENSO reconstructions occurs during the early calibration period (1901-1959) when the stable reconstruction clearly outperforms the ALL version (**Table 2**). For the ALL predictor pool, the number of chronologies that pass screening ($r > 0.42$) for the early calibration period greatly outnumbers that of the late calibration period, in all three nest windows. Chronologies that go into the stable reconstruction make up less than 30% of the ALL chronology set for the early period and less than 40% for the late calibration period. The geographical distribution of chronologies selected for the stable reconstruction is mainly located south of the US-Mexico border (**Figure 6**), especially for the late period with a well-defined region of chronologies that correlate significantly with both the calibration and verification periods (not shown).

The stable and ALL reconstructions for the MEI are compared in **Figure 7**. The two reconstructions are correlated at $r = 0.871$ for 1675-1991, but this correlation varies significantly over time. Regression residuals and the running correlation between stable and ALL are plotted in **Figure 7cd** and illustrate these differences, most notably during the mid-19th century. For the period 1675-1750, there is little to distinguish the two approaches ($r = 0.926$). In later periods, for which there are a larger set of chronologies used in the PCA for the stable reconstruction, there are periods for which the two reconstructions share less than 50% of their variance (**Figure 7d**). The residual time-series (from regressing the stable reconstruction on the ALL reconstruction; **Figure 7c**) displays large departures from the mean in the 1850s and 1860s, as well as in the 1900s and 1910s.

Spectral coherence analysis indicates that both reconstructions capture high frequency MEI variability during the 20th century (**Figure 7ef**). However, the stable reconstruction is more coherent across the entire frequency domain, especially at lower frequencies (> 10 years) where the ALL lacks significant coherence with the instrumental MEI data. This difference in the spectral fidelity of the stable reconstruction of the MEI appears to have important implications for the estimation of low frequency spatial changes in moisture variability over North America potentially linked with ENSO.

Sign tests between reconstructions and instrumental data indicate that the stable reconstruction performs marginally better in values around the mean than the ALL ENSO estimates. The stable reconstruction has 27 misses over the full period of instrumental overlap (1872-1991), while ALL has 34. For the ten most extreme instrumental El Niño and La Niña events, the stable reconstruction displays the same sign for all 20 years (**Supplementary Table 1**). The ALL reconstruction has two misses and the average difference between reconstructed and instrumental values is also higher. Overall, both reconstructions track La Niña events better than El Niño events.

DISCUSSION

The influence of ENSO variability on North American precipitation and temperature during the 20th century is most prominent in the subtropical band from Baja California to Florida, where years of positive ENSO (El Niño) favor wet and cool conditions and years of negative ENSO (La Niña) favor dry and warm conditions for NDJF (**Figure 1**). Correlations between ENSO and precipitation exceed 0.7 in northern Mexico, making the TexMex sector one of the strongest ENSO teleconnection regions on Earth (Dai and Wigley 2000). The negative correlation

between the MEI and precipitation over the Pacific Northwest is also significant (**Figure 2**) but it is subject to considerable multidecadal variability (**Figure 3**).

Because of the strong modulation of winter precipitation in the US Southwest and northern Mexico by ENSO, and the dependence of regional tree growth on soil moisture recharge by winter precipitation, the strongest ENSO signal in the North American tree-ring network can also be found in the TexMex sector (**Figure 2**; Stahle and Cleaveland 1993). Many of the strongest correlations ($r > 0.42$) are observed with Douglas-fir (*Pseudotsuga menziesii*) EW or TRW chronologies from the Sierra Madre Occidental, including the strongest single correlation recorded by an EW chronology from Puentecillas, Durango, Mexico ($r = 0.599$; 1901-1991). With the exception of a small number of *Taxodium distichum* chronologies from Florida, few tree ring chronologies outside the North American southwest have a strong and stable correlation with ENSO indices.

The time-dependent ENSO signal in instrumental hydroclimate data for North America previously described by Cole and Cook (1999) and Enfield et al. (2001) is also present in the CRU NDJF precipitation data. The highest number of significant correlations between tree-ring chronologies and NDJF ENSO is recorded for the positive phase of the AMO (1930-1959), a period when ENSO and precipitation are also widely and significantly correlated across the TexMex sector and into Arizona, southern California and Nevada. Many of these chronologies display lower or non-significant correlations for subperiods of negative AMO phasing. Only 18 of the 442 tree-ring chronologies analyzed record significant correlations with NDJF MEI for the full period of analysis and with all three subperiods. Again, the majority of these chronologies are located in the TexMex sector and 13 are based on ring-width variables from Douglas-fir. There are few differences in the number of chronologies that are significantly correlated with

local precipitation or temperature over the three subperiods (**Figure 5**). Some of the chronologies that lose significance in the earliest subperiod (1901-1929) are located in Mexico where instrumental climate data for the early 20th century are problematic (Jauregui 1978; Douglas 2007). Overall, there is nothing to suggest that trees in the US Southwest or Mexico have changed their response to local hydroclimate variability over the 20th century. Therefore, the multidecadal variability in the spatial scale of the ENSO signal to tree growth is most likely due to changes of the teleconnection to hydroclimate over North America.

Comparisons between the stable and ALL reconstructions of the MEI suggest that a regional subset of the network of over 100 chronologies has the best calibration and verification statistics. The subsequent stable reconstruction from using the 27 chronologies that display significant ENSO correlations during both positive and negative AMO phases as predictors explains over 50% of the variance for the full period (1872-1991) of instrumental MEI data overlap. Although the two reconstructions are highly correlated over the full period of reconstruction ($r = 0.871$; 1675-1991), the relationship varies greatly over time. The lowest point in the running correlation between the stable and ALL reconstructions is recorded for the 1850s and 60s, when the stable reconstruction estimates stronger La Niña conditions (the mean for 1856-1868 in stable is -0.601 but only -0.302 in ALL). Several of the differences in this period occur during years when other multiproxy reconstructions indicate strong or very strong La Niña events (Gergis and Fowler 2009).

a. Pre-instrumental variability of ENSO influence

The relationship between ENSO and precipitation variability across North America does not appear to have been stationary during the observational era (**Figure 3**). Comparing the stable reconstruction with the NADA reveals changing patterns prior to the instrumental record, similar

to those recorded for precipitation and soil moisture during the instrumental era (Cole and Cook 1999). The stable reconstruction reproduces the teleconnection pattern of instrumental MEI (**Figure 8a**) with great fidelity (**Figure 8b**) for the verification period 1872-1900, with positive correlations extending into the Central Plains. Although the stable ENSO reconstruction cannot be considered independent from the NADA over the TexMex region (as the predictors are highly correlated with PDSI), spatial changes in correlations are recorded beyond the search radius of the NADA (450 km; Cook et al. 1999).

The correlations between ENSO and reconstructed PDSI are not significant in eastern Texas during 1872-1900, and also weak in western Arizona. Correlation analyses for 28-year periods during the pre-instrumental era also indicate change in the spatial pattern and intensity over North America (**Figure 8c-i**). For example, the influence of ENSO on summer PDSI in eastern Texas has fluctuated between periods of strong and weak ENSO influence. The shifting magnitude of negative ENSO correlations with precipitation is also recorded during the pre-instrumental era (**Figure 8**). There is little significant negative correlation during 1731-1758 (**Figure 8g**) while negative correlations are present from northern California to the Canadian border and beyond during 1843-1871 (**Figure 8c**) and 1787-1814 (**Figure 8e**).

Spatial expansion and contraction of significant ENSO correlation from the core region in northern Mexico occur on multidecadal timescales during the instrumental and pre-instrumental era since at least 1675 (**Figure 8**). Correlations between the stable reconstruction and the NADA is significant during the 1872-1900 verification period for a large region north of the US Southwest, entering South Dakota and Wyoming (**Figure 8ab**), and similar patterns are estimated for 1815-1842 and 1843-1871 (**Figure 8cd**). Expansion occurs westward during 1731-1758 (**Figure 8g**) during which positive correlations are recorded for all of California, analogous

to the precipitation correlations recorded for the middle of the 20th century and the most recent decades (**Figure 3**).

b. The role of Atlantic variability on spatial ENSO precipitation influence

The magnitude of correlations between ENSO and winter precipitation, and subsequent summer PDSI, has not remained static across western North America over the 20th and early 21st centuries. Possible interactions between the Pacific and Atlantic oceans have previously been suggested as drivers of drought in North America (e.g. McCabe et al. 2004; d'Orgeville and Peltier 2007; Ruprich-Robert 2018). Yu et al. (2015) proposed that the positive phase of the AMO is associated with an intensification of the subtropical high. Winter-to-spring atmospheric pressure conditions are more consistent across the southwest and the Great Plains during years of positive AMO and could explain why the influence of ENSO on precipitation spreads northeastwards from the core TexMex region. No similar pattern is recorded for the Pacific Decadal Oscillation (PDO; Mantua et al. 1997), instead, increased differences in pressure change over western United States are associated with the PDO (Yu et al. 2015). Similar results on the relationship between warmer North Atlantic SSTs and drought-driven wildfire activity were found by Kitzberger et al. (2007), for which synchronous fires from the southwest to South Dakota and the upper Colorado River basin were associated with the positive phase of the AMO.

The AMO reconstruction of Gray et al. (2004) records overall negative values for the 18th century. For subperiods between 1703-1786, the positive correlations between the stable MEI reconstruction and the NADA are confined to the core TexMex region. However, some changes are recorded over eastern Texas, including lessened correlations during 1731-1758 (**Figure 8g**), a period during which the AMO reconstruction is positive, albeit weak (0.074). Reconstructed persistence between May soil moisture and JJA atmospheric moisture balance over the central

United States, thought to be driven by positive AMO, reach a high point around 1750 (Torbenson and Stahle 2018). This change in ENSO influence over Texas is analogous to the positive AMO phase of 1930-1965. Similar drops in correlation over eastern Texas are present for 1675-1702, occurring during the strong positive AMO phase estimated for the end of the 17th century (Gray et al. 2004).

One of the most severe decadal droughts of the past 500 years in the Central Plains occurred during the 1850s and 60s (Stahle and Cleaveland 1988; Woodhouse and Overpeck 1998), termed the 'Civil War drought' (Herweijer et al. 2006; Stahle et al. 2011). The differences in estimated MEI between the stable and ALL reconstructions (**Figure 7c**) suggest stronger and more persistent La Niña conditions for the period based on the stable estimates. ENSO influence also appears to have expanded into the Great Plains during the 'Civil War drought', with positive correlations into Missouri and the confluence region of the Ohio and Mississippi rivers (**Figure 8c**). Reconstructed AMO (Gray et al. 2004) indicates the strongest positive AMO phase of the 19th century during this period and this combination of Pacific and Atlantic conditions may have contributed to the severity of moisture deficits during the 1850s and 60s. This configuration appears to have continued through the end of the 19th century, recorded by both instrumental and reconstructed MEI (**Figure 8ab**). Although no exact 'Civil War drought' analogue exists for the instrumental period, positive correlations between ENSO and precipitation during the positive AMO phase of 1930-1959 extends to South Dakota and Nebraska. The mid 19th century drought appears to have been most extreme during the cool season (Torbenson and Stahle 2018; Howard et al. 2019) and the stable reconstruction of the MEI suggest that recurrent La Niña conditions may have played a prominent role in this episode of multidecadal dryness.

Our results suggest that the low frequency swings in spatial influence of ENSO on North American hydroclimate recorded for the observational era also occurred in centuries past. Although there are several sources of uncertainty associated with each reconstruction used in this analysis, the results are indicative of Pacific-Atlantic teleconnections similar to those that have been reported elsewhere (e.g. Cole and Cook 1999; Kitzberger et al. 2007; Yu et al. 2015). Because the recorded changes are multidecadal in nature and seem to conform with the sign changes of instrumental and possibly reconstructed AMO indices, these low frequency changes in the regions of subtropical North America influenced by ENSO may be driven in part by SST variability in the North Atlantic that are associated with atmospheric pressure changes over western United States.

CONCLUSIONS

The spatial pattern of ENSO forcing on cool-season precipitation and temperature, and the subsequent growing season soil moisture balance over North America has varied over the 20th and 21st centuries. The strongest and most stable ENSO signal apparent in the instrumental precipitation and temperature observations, and the North American tree-ring network, is located in the subtropical TexMex sector of northern Mexico and the borderlands of the US Southwest. The region is not well represented by instrumental weather observations before 1950, but moisture sensitive tree-ring chronologies from the area indicate a strong and stable correlation with ENSO indices during the late 19th and early 20th centuries when regional weather observations are most limited.

Correlations between the stable ENSO reconstruction and gridded drought for pre-instrumental periods display changes in magnitude and spatial influence outside of the core ENSO region, analogous to those recorded in the 20th and early 21st century instrumental data.

The non-stationarity of ENSO signal recorded for the instrumental period in Arizona, southern California, and Texas, appears to have been a feature of ocean-atmospheric interactions over the past 350 years. The changes in strength and spatial scale of ENSO teleconnection to North America hydroclimate could be linked to North Atlantic SST variability. The positive phase of AMO during the mid- and late 19th century coincides with strong negative MEI values. The 'Civil War drought' of the mid-19th century may therefore be an example of interaction between persistent La Niña conditions and positive AMO resulting in prolonged cool-season moisture deficits over the Great Plains. These results need to be tested in observations and simulations but understanding the expected extent and magnitude of ENSO influence outside of the TexMex sector may be enhanced based in part on the state of the SST field in the North Atlantic.

ACKNOWLEDGEMENTS

We thank two anonymous reviewers, the editor, and assistant editor, for constructive feedback that helped improve this manuscript. We appreciate everyone who have contributed to the ITRDB for making their data publically available. The National Science Foundation (grant #AGS-1266014) and Inter-American Institute for Global Change Research (CRN #2047) funded this study. Lamont-Doherty Earth Observatory contribution no. XXXX. Both reconstructions will be available for public access through the NOAA NCEI Paleoclimatology data bank upon publication.

REFERENCES

Allan, R.J., Lindesay, J., & Parker, D. (1996). *El Niño/Southern Oscillation & Climatic Variability*. CSIRO Publishing, Clayton, Australia.

Braganza, K., Gergis, J.L., Power, S.B., Risbey, J.S., & Fowler, A.M. (2009). A multiproxy index of the El Niño-Southern Oscillation, A.D. 1525-1982. *Journal of Geophysical Research* **114**: D05106. https://doi.org/10.1029/2008JD010896

Brönnimann, S., Xoplaki, E., Casty, C., Pauling, A., & Luterbacher, J. (2007). ENSO influence on Europe during the last centuries. *Climate Dynamics* **28**: 181-197. https://doi.org/10.1007/s00382-006-0175-z

Brown, D.P., & Comrie, A.C. (2004). A winter precipitation 'dipole' in the western United States associated with multidecadal ENSO variability. *Geophysical Research Letters* **31**: L09203. https://doi.org/10.1029/2003GL018726

Cane, M.A., Fairbanks, R.G., & Shen, G.T. (1993). Recent variability in the Southern Oscillation: Isotopic results from a Tarawa atoll coral. *Science* **260**: 1790-1793. https://doi.org/10.1126/science.260.5115.1790

Cole, J.E., & Cook, E.R. (1998). The changing relationship between ENSO variability and moisture balance in the continental United States. *Geophysical Research Letters* **25**: 4529-4532. https://doi.org/10.1029/1998GL900145

Cook, E.R., & Kairiukstis, L. (1990). *Methods of Dendrochronology*, Springer, New York.

Cook, E.R., Meko, D.M., Stahle, D.W., & Cleaveland, M.K. (1999). Drought reconstructions of the continental United States. *Journal of Climate* **12**: 1145-1162. https://doi.org/10.1175/1520-0442(1999)012<1145:DRFTCU>2.0.CO;2

Cook, E.R., Seager, R., Heim Jr., R.R., Vose, R.S., Herweijer, C., & Woodhouse, C. (2010). Megadroughts in North America: placing IPCC projections of hydroclimatic change in a long-term paleoclimate context. *Journal of Quaternary Science* **25**: 48-61. https://doi.org/10.1002/jqs.1303

D'Arrigo, R., Cook, E.R., Wilson, R.J., Allan, R., & Mann, M.E. (2005). On the variability of ENSO over the past six centuries. *Geophysical Research Letters* **32**: L03711. https://doi.org/10.1029/2004GL022055

d'Orgeville, M., & Peltier, W.R. (2007). On the Pacific Decadal Oscillation and the Atlantic Multidecadal Oscillation: Might they be related? *Geophysical Research Letters* **34**: L23705. https://doi.org/10.1029/2007GL031584

Dai, A., & Wigley, T.M.L. (2000). Global patterns of ENSO-induced precipitation. *Geophysical Research Letters* **27**: 1283-1286. https://doi.org/10.1029/1999GL011140

Douglas, A.V. (2007). Summer precipitation variability over Mexico. AGU Joint Assembly, Acapulco, Mexico. May 2007.

Enfield, D.B., Mestas-Nuñez, A.M., & Trimble, P.J. (2001). The Atlantic multidecadal oscillation and its relation to rainfall and river flows in the continental U.S. *Geophysical Research Letters* **28**: 2077-2080. https://doi.org/10.1029/2000GL012745

Gergis, J.L., & Fowler, A.M. (2006). How unusual was late 20th century El Niño-Southern Oscillation (ENSO)? Assessing evidence from tree-ring, coral, ice-core and documentary palaeoarchives, A.D. 1525-2002. *Advances in Geosciences* **6**: 173-179. https://doi.org/10.5194/adgeo-6-173-2006

Gergis, J.L., & Fowler, A.M. (2009). A history of ENSO events since A.D. 1525: implications for future climate change. *Climate Change* **92**: 343-387. https://doi.org/10.1007/s10584-008-9476-z

Gray, S.T., Graumlich, L.J., Betancourt, J.L., & Pederson, G.T. (2004). A tree-ring based reconstruction of the Atlantic Multidecadal Oscillation since 1567 A.D. *Geophysical Research Letters* **31**: L019932. https://doi.org/10.1029/2004GL019932

Grissino-Mayer, H.D., & Fritts, H.C. (1997). The International Tree-Ring Data Bank: an enhanced global database serving the global scientific community. *The Holocene* **7**: 235-238. https://doi.org/10.1177/095968369700700212

Grudd, H., Briffa, K.R., Karlén, W., Batholin, T.S., Jones, P.D., & Kromer, B. (2002). A 7400-year tree-ring chronology in northern Swedish Lapland: natural climatic variability expressed on annual to millennial timescales. *The Holocene* **12**: 657-665. https://doi.org/10.1191/0959683602hl578rp

Harris, I., Jones, P.D., Osborn, T.J., & Lister, D.H. (2014). Updated high resolution grids of monthly climatic observation – the CRU TS3.10 dataset. *International Journal of Climatology* **34**: 623-642. https://doi.org/10.1002/joc.3711

Herweijer, C., Seager, R., & Cook, E.R. (2006). North American droughts of the mid to late nineteenth century: a history, simulation and implication for Mediaeval drought. *The Holocene* **16**: 159-171. https://doi.org/10.1191/0959683606hl917rp

Howard, I., Stahle, D.W., & Feng, S. (in press). Separate tree-ring reconstructions of spring and summer moisture in the northern and southern Great Plains. *Climate Dynamics*. https://doi.org/10.1007/s00382-018-4485-8

Jauregui, E. (1979). Algunos aspectos de las fluctuaciones pluviometricas en Mexico en los ultimos cien anos. *Boletin del Instituto Geográfica* UNAM **9**: 39-63.

Jolliffe, I.T. (2002). *Principal Component Analysis*. Springer, New York.

Kitzberger, T., Brown, P.M., Heyerdahl, E.K., Swetnam, T.W., & Veblen, T.T. (2007). Contingent Pacific-Atlantic Ocean influence on multicentury wildfire synchrony over western North America. *Proceedings of the National Academy of Sciences of the United States of America* **104**: 543-548. https://doi.org/10.1073/pnas.0606078104

Lloyd, C. (2010). *Spatial data analysis*. Oxford University Press, Oxford, UK.

Lough, J.M., & Fritts, H.C. (1990). Historical aspects of El Niño/Southern Oscillation – Information from tree rings. *Elsevier Oceanography Series* **52**: 285-321. https://doi.org/10.1016/S0422-9894(08)70039-4

Li, J., Xie, S.P., Cook, E.R., Morales, M.S., Christie, D.A., Johnson, N.C., et al. (2013). El Niño modulations over the past seven centuries. *Nature Climate Change* **3**: 822-826. https://doi.org/10.1038/nclimate1936

Mann, M.E., Bradley, R.S., & Hughes, M.K. (2000). Long-term variability in the El Niño Southern Oscillation and associated teleconnections. In *El Niño and the Southern Oscillation: Multi-scale Variability and Its Impacts on Natural Ecosystems and Society*, H.F. Diaz and V. Markgraf (Eds.), Cambridge University Press, Cambridge, UK.

Mantua, N.J., Hare, S.R., Zhang, Y., Wallace, J.M., & Francis, R.C. (1997). A Pacific interdecadal climate oscillation with impacts on salmon production. *Bulletin of the American Meteorological Society* **78**: 1069-1079. https://doi.org/10.1175/1520-0477(1977)078<1069:APICOW>2.0.CO;2

McCabe, G.J., Palecki, M.A., & Betancourt, J.L. (2004). Pacific and Atlantic Ocean influences on multidecadal drought frequency in the United States. *Proceedings of the National Academy of Sciences of the United States of America* **101**: 4136-4141. https://doi.org/10.1073/pnas.0306738101

Palmer, W.C. (1965). Meteorological drought. *Weather Bureau Research Paper No. 45*. U.S. Department of Commerce, Washington, DC.

Percival, D.B., & Constantine, W.L.B. (2006). Exact simulation of Gaussian time series from nonparametric spectral estimates with application to bootstrapping. *Statistics and Computing* **16**: 25-35. https://doi.org/10.1007/s11222-006-5198-0

Ropelewski, C.F., & Halpern, M.S. (1986). North American precipitation and temperature patters associated with ENSO. *Monthly Weather Review* **114**: 2352-2362. https://doi.org/10.1175/1520-0493(1986)114<2352:NAPATP>2.0.CO;2

Ruprich-Robert, Y. (2018). Impacts of the Atlantic Multidecadal Variability on North American summer climate and heat waves. *Journal of Climate* **31**: 3679-3700. https://doi.org/10.1175/JCLI-D-17-0270.1

Stahle, D.W., & Cleaveland, M.K. (1988). Texas drought history reconstructed and analyzed from 1698 to 1980. *Journal of Climate* **1**: 59-74. https://doi.org/10.1175/1520-0442(1988)001<0059:TDHRAA>2.0.CO;2

Stahle, D.W., & Cleaveland, M.K. (1993). Southern Oscillation extremes reconstructed from tree-rings of the Sierra Madre Occidental and the southern Great Plains. *Journal of Climate* **6**: 129-140. https://doi.org/10.1175/1520-0442(1993)006<0129:SOERFT>2.0.CO;2

Stahle, D.W., D'Arrigo, R.D., Krusic, P.J., Cleaveland, M.K., Cook, E.R., Allan, R.J., et al. (1998). Experimental dendroclimatic reconstruction of the Southern Oscillation. *Bulletin of the American Meteorological Society* **79**: 2137-2152. https://doi.org/10.1175/1520-0477(1998)079<2137:EDROTS>2.0.CO;2

Stahle, D.W., Cook, E.R., Burnette, D.J., Villanueva, J., Cerano, J., Burns, J.N., et al. (2016). The Mexican Drought Atlas: Tree-ring reconstructions of the soil moisture balance during the late pre-Hispanic, Colonial, and modern Eras. *Quaternary Science Reviews* **149**: 34-60. https://doi.org/10.1016/j.quascirev.2016.06.018

Torbenson, M.C.A., Stahle, D.W., Villanueva Díaz, J., Cook, E.R., & Griffin, D. (2016). The relationship between earlywood and latewood ring-growth across North America. *Tree-Ring Research* **72**: 53-66. https://doi.org/10.3959/1536-1098-72.02.53

Torbenson, M.C.A., & Stahle, D.W. (2018). The relationship between cool and warm season moisture over the central United States, 1685-2015. *Journal of Climate*. https://doi.org/10.1175/JCLI-D-17-0593.1

van Oldenborgh, G.J, & Burgers, G. (2005). Searching for decadal variations in ENSO precipitation teleconnections. *Geophysical Research Letters* **32**: L023110. https://doi.org/10.1029/2005GL023110

Wahl, E.R., Diaz, H.F., Smerdon, J.E., & Ammann, C.M. (2014). Late winter temperature response to large tropical volcanic eruptions in temperate western North America: relationships to ENSO phases. *Global and Planetary Change* **122**: 238-250. https://doi.org/10.1016/j.gloplacha.2014.08.005

Wahl, E.R., Diaz, H.F., Vose, R.S., & Gross, W.S. (2017). Multicentury evaluation of recovery from strong precipitation deficits in California. *Journal of Climate* **30**: 6053-6063. https://doi.org/10.1175/JCLI-D-16-0423.1

Wilson, R., Cook, E., D'Arrigo, R., Riedwyl, N., Evans, M.N., Tudhope, A., & Allan, R. (2010). Reconstructing ENSO: the influence of method, proxy data, climate forcing and teleconnections. *Journal of Quaternary Science* **25**: 62-78. https://doi.org/10.1002/jqs.1297

Wolter, K., & Timlin, M.S. (2011). El Niño/Southern Oscillation behaviour since 1871 as diagnosed in an extended multivariate ENSO index (MEI.ext). *International Journal of Climatology* **31**: 1074-1087. https://doi.org/10.1002/joc.2336

Woodhouse, C.A., & Overpeck, J.T. (1998). 2000 years of drought variability in the central United States. *Bulletin of the American Meteorological Society* **79**: 2693-2714. https://doi.org/10.1175/1520-0477(1998)079<2693:YODVIT>2.0.CO;2

Yocom, L.L., Fulé, P.Z., Brown, P.M., Cerano, J., Villanueva-Diaz, J., Falk, D.A., & Cornejo-Oviedo, E. (2010). El Niño-Southern Oscillation effect on a fire regime in northeastern Mexico has changed over time. *Ecology* **91**: 1660-1671. https://doi.org/10.1890/09-0845.1

Yu, J.-Y., Kao, P.-K., Paek, H., Hsu, H.-H., Hung, C., Lu, M.-M., & An, S.-I. (2015). Linking emergence of the central Pacific El Niño to the Atlantic Multidecadal Oscillation. *Journal of Climate* **28**: 651-662. https://doi.org/10.1175/JCLI-D-14-00347.1

TABLES

Table 1. Tree-ring chronologies used as predictors in the stable reconstruction of MEI. The final two columns indicate if the chronology was used in early and/or late calibration model.

State	Site code	Site name	Species	Variable	Start date	Lat.	Lon.	Early calib.	Late calib.
CH	MDG	Guacamayas	PSME	EW	1598	30.33	-108.37		X
CH	TUT	Tutuaca	PSME	EW	1534	28.37	-108.16		X
DU	AVE	Arroyo Verde	PSME	EW	1770	25.03	-106.04	X	X
DU	CGD	Cienega Guadalupe	PIPO	EW	1675	25.04	-106.18	X	X
DU	CHU	Cerro Huehuento	PSME	EW	1552	24.05	-105.44	X	X
DU	CUE	Cueveci	PSME	EW	1770	23.30	-104.32	X	X
DU	CVS	Cuevacillas	PSME	EW	1747	25.09	-106.23	X	X
DU	PUE	Puentecillas	PSME	EW	1573	24.19	-105.55	X	X
DU	TAH	Tarahumara	PSME	EW	1724	25.34	-106.20	X	X
NM	FCU	Filmore Canyon	PIPO	EW	1306	32.20	-106.34		X
NM	SMT	San Mateo	PSME	EW	816	33.43	-107.27	X	X
CH	CAC	Cañon del Cobre	PSME	TRW	1770	28.01	-107.49	X	X
CH	CIA	Creel Airstrip	PSME	TRW	1739	27.42	-107.37		X
CH	MOH	Cerro Mohinara	PSME	TRW	1681	25.56	-107.01	X	X
CO	CHK	Chokecherry	PIED	TRW	1450	37.33	-105.34	X	
CO	WMC	Wet Mountains	PSME	TRW	1336	37.54	-105.09	X	
CU	COA	Coahuilón	PSME	TRW	1675	25.14	-103.55	X	X
CU	HUA	Huachichil	PICM	TRW	1552	25.12	-100.50	X	X
DU	BAR	Cerro Barajas	PSME	TRW	1651	26.24	-106.05	X	X
DU	BAY	Bayas	PSME	TRW	1845	23.27	-104.50	X	X
DU	BDG	Barrial Guadalupe	TAMU	TRW	1869	25.59	-103.14	X	X
NL	CHO	Chona	PICM	TRW	1573	24.44	-100.07	X	X
NM	LAT	Las Tablas	PIED	TRW	1520	36.32	-106.01	X	
NM	SAN	Sandia Mountain	PIFL	TRW	290	35.15	-107.30	X	
SL	VER	Rio Verde	TAMU	TRW	1724	21.41	-99.47	X	X
TA	SAB	Rio Sabinas	TAMU	TRW	1534	23.09	-99.09		X
TX	BSC	Big Bend	PSME	TRW	1473	29.15	-103.18	X	X

Table 2. Common calibration and verification statistics for the stable and ALL reconstructions. Ver. RE = verification reduction of error; Ver. CE = verification coefficient of efficiency. Lower part shows correlations of respective reconstruction with instrumental MEI data.

Early calibration (1901-1959), verification 1960-1991

	r2	**Ver. R**	**Ver. RE**	**Ver. CE**	***n***
Nest 1 stable	0.546	0.709	0.467	0.457	22
Nest 2 stable	0.508	0.698	0.444	0.434	20
Nest 3 stable	0.429	0.653	0.367	0.356	13
Nest 1 ALL	0.533	0.493	0.253	0.239	78
Nest 2 ALL	0.486	0.495	0.257	0.243	66
Nest 3 ALL	0.445	0.453	0.218	0.204	50

Late calibration (1930-1991), verification 1901-1929

	r2	**Ver. R**	**Ver. RE**	**Ver. CE**	***n***
Nest 1 stable	0.452	0.761	0.561	0.558	23
Nest 2 stable	0.433	0.739	0.525	0.522	21
Nest 3 stable	0.397	0.723	0.496	0.492	13
Nest 1 ALL	0.366	0.430	0.026	0.020	59
Nest 2 ALL	0.350	0.419	0.017	0.011	54
Nest 3 ALL	0.334	0.407	0.010	0.004	45

	Early calib. (1901-1959)		*Late calib. (1930-1991)*		*Combined*	
	ALL	**stable**	**ALL**	**stable**	**ALL**	**stable**
1872-1900	0.588	0.633	0.430	0.625	0.525	0.638
1901-1929	0.736	0.754	0.430	0.761	0.597	0.768
1930-1959	0.759	0.737	0.719	0.748	0.752	0.750
1965-1991	0.479	0.699	0.589	0.615	0.553	0.658
1872-1991					0.598	0.706

FIGURES

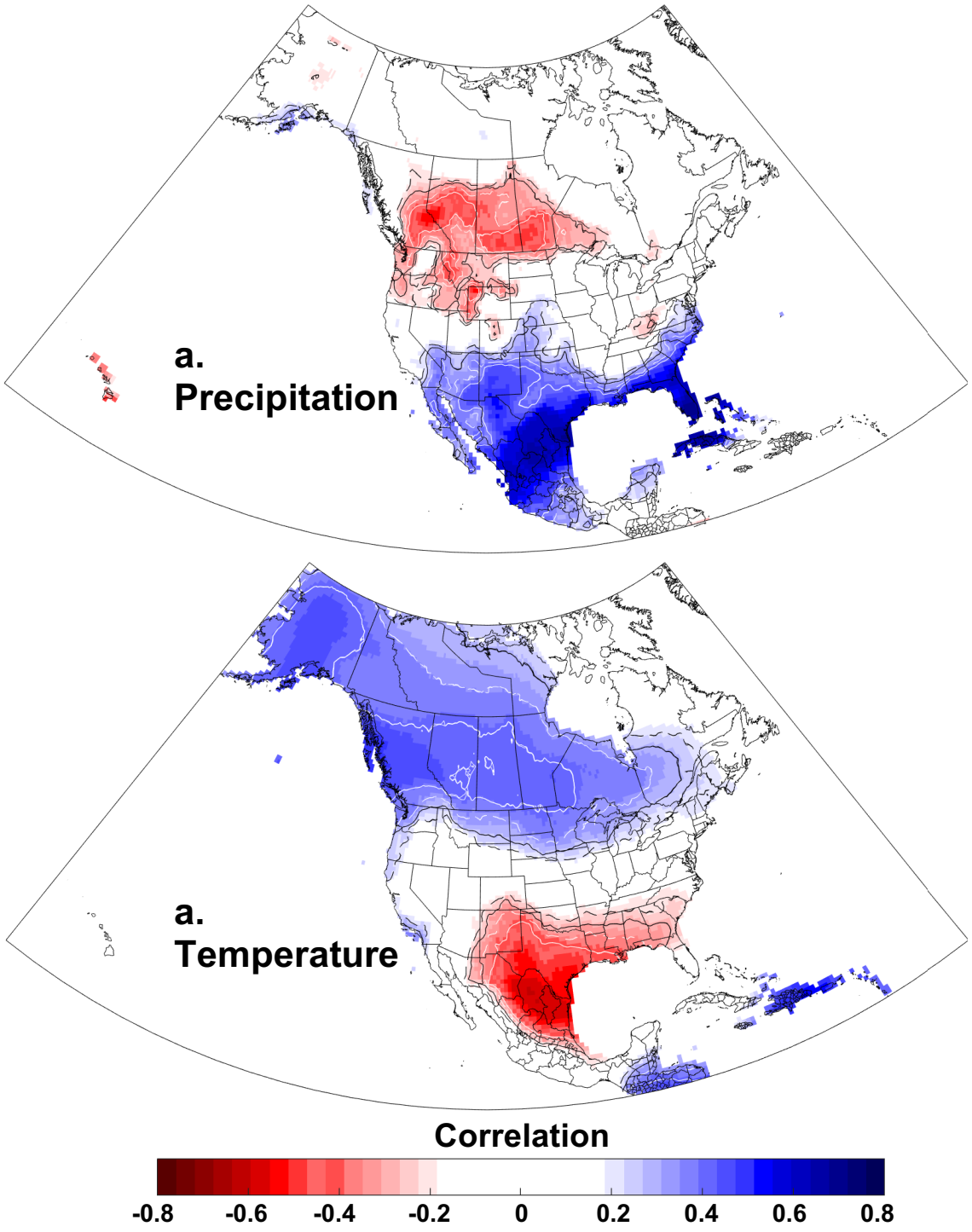

Figure 1. Local correlations between instrumental NDJF extended MEI and instrumental NDJF (a) precipitation and (b) temperature for the period 1901-1991. Contours: black dashed $p < 0.05$; black solid $p < 0.01$; white dashed $p < 0.001$; white solid $p < 0.0001$.

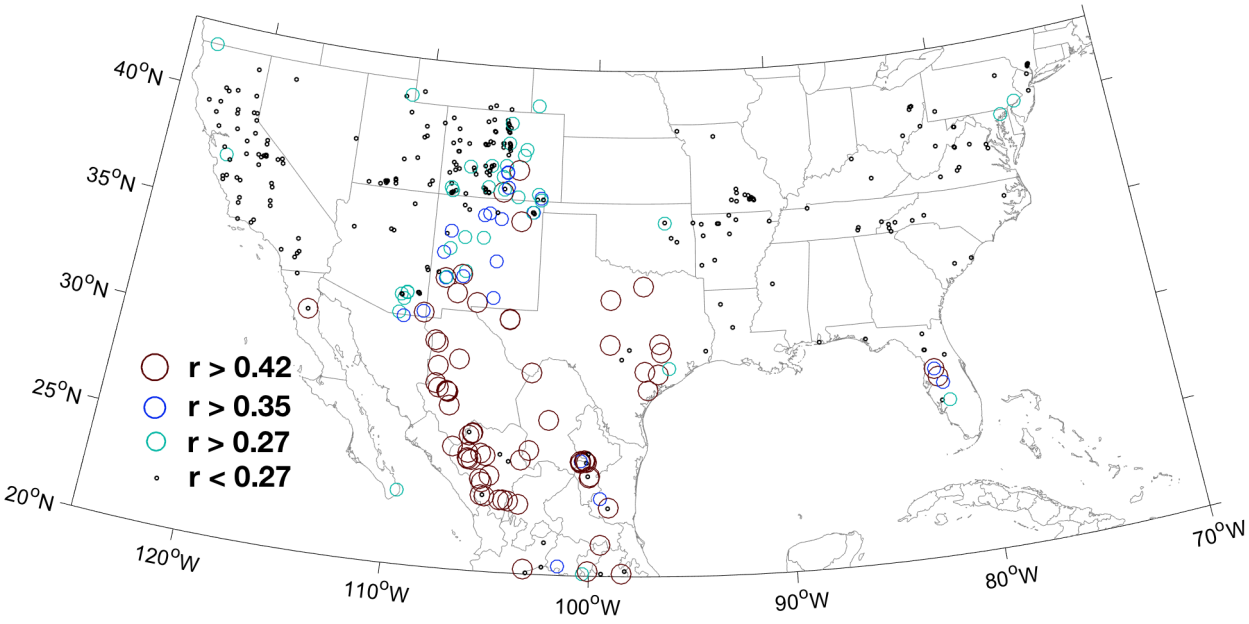

Figure 2. Magnitude of correlation between individual tree-ring chronologies and the NDJF extended MEI for the period 1901-1991.

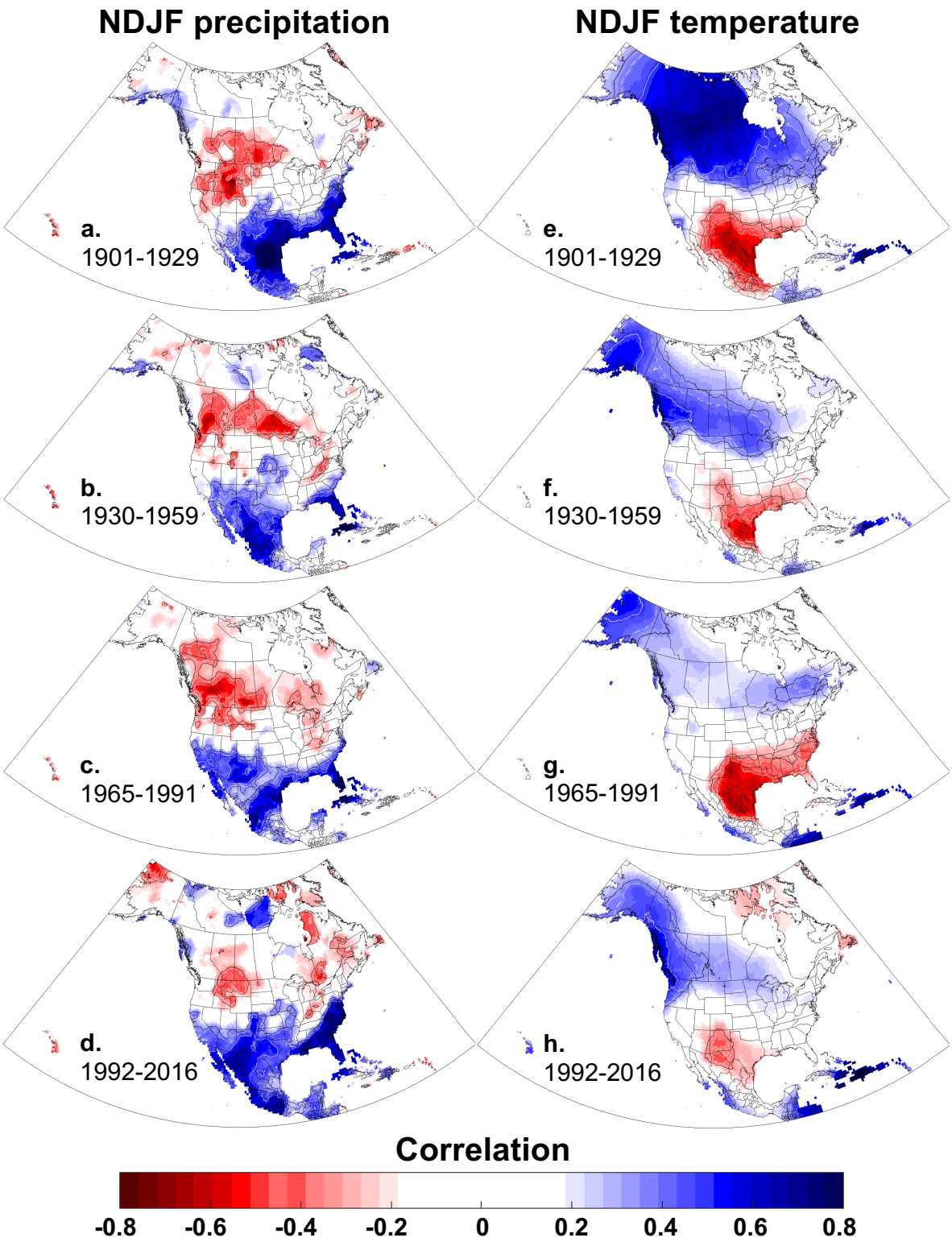

Figure 3. Local correlations between instrumental NDJF extended MEI and instrumental NDJF precipitation and temperature for different subperiods. Correlations for 1992-2016 (**d** and **h**) are computed using MEI, not extended MEI. Contours: black $p < 0.10$; white dashed $p < 0.05$; white solid $p < 0.01$.

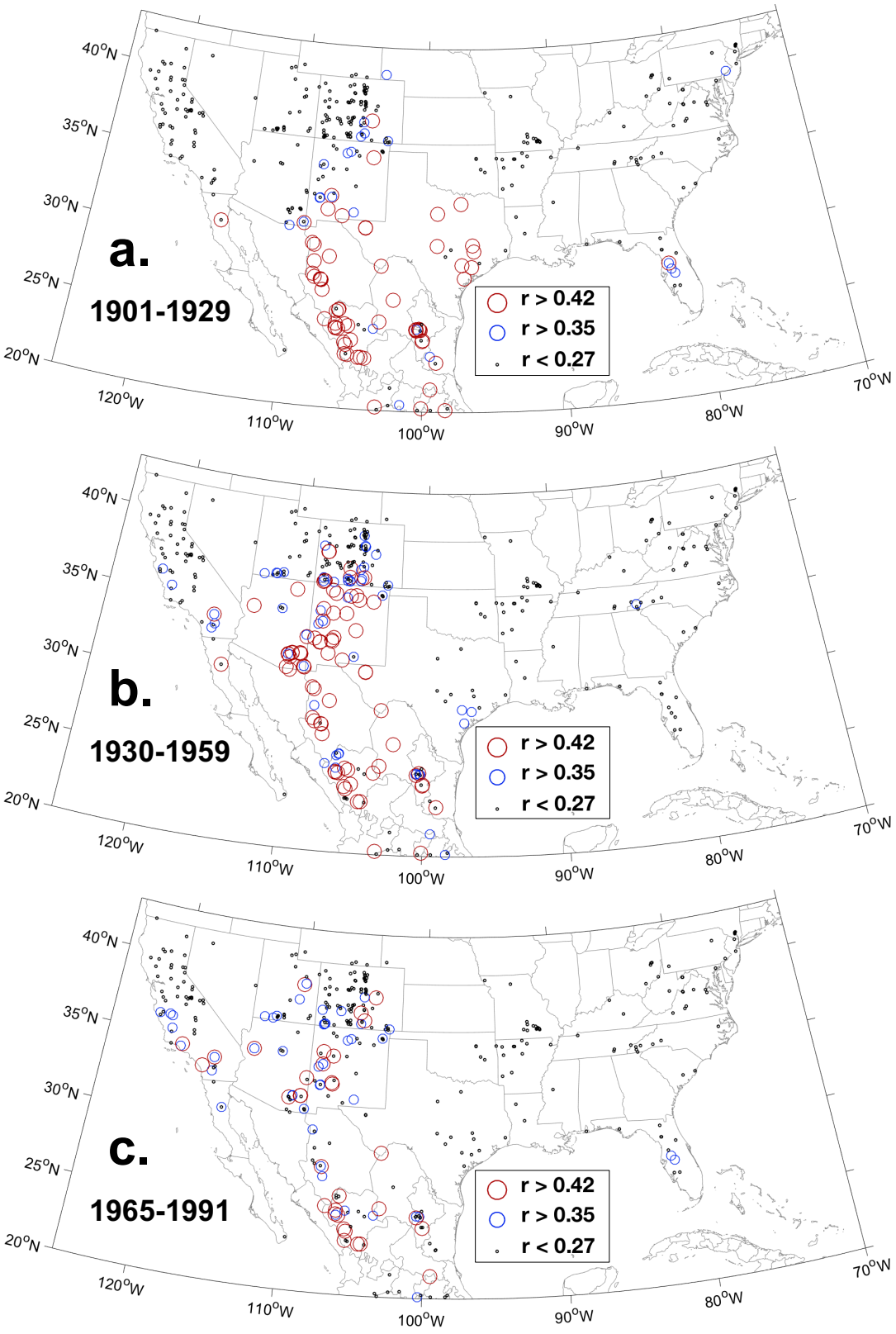

Figure 4. Same as for Figure 2 but for subperiods: (**a**) 1901-1929; (**b**) 1930-1959; and (**c**) 1965-1991.

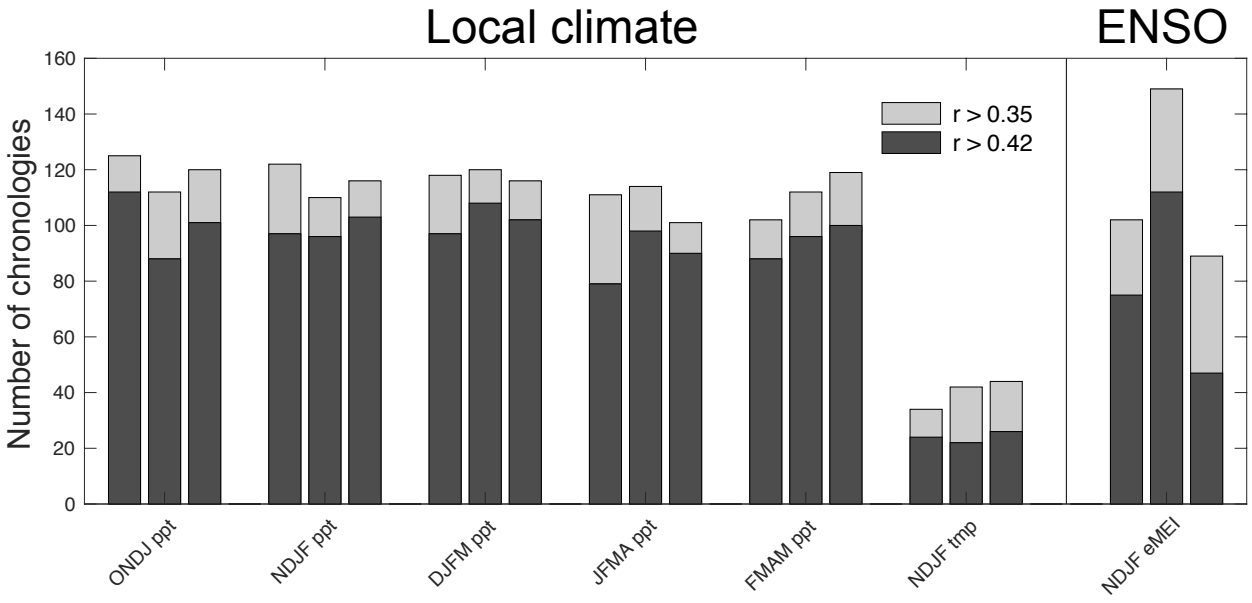

Figure 5. Barplot showing the number of chronologies from the study area that are significantly correlated with local precipitation, local temperature, and extended MEI for subperiods 1901-1929 (left bar), 1930-1959 (center bar), and 1965-1991 (right bar).

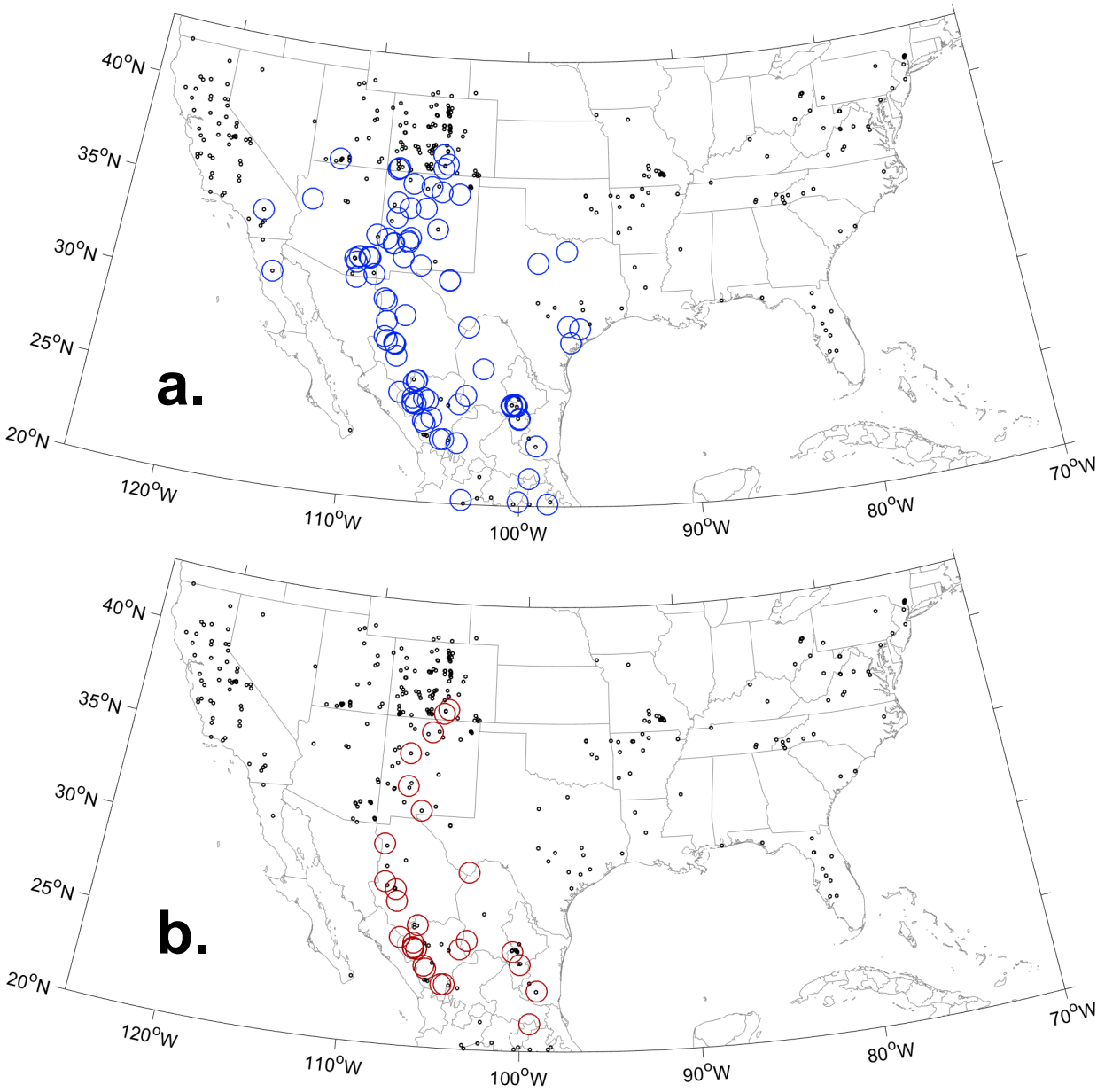

Figure 6. Locations of chronologies used for (**a**) the ALL (blue circles); and (**b**) stable (red circles) reconstructions of MEI. Black dots indicate all tree-ring chronologies screened.

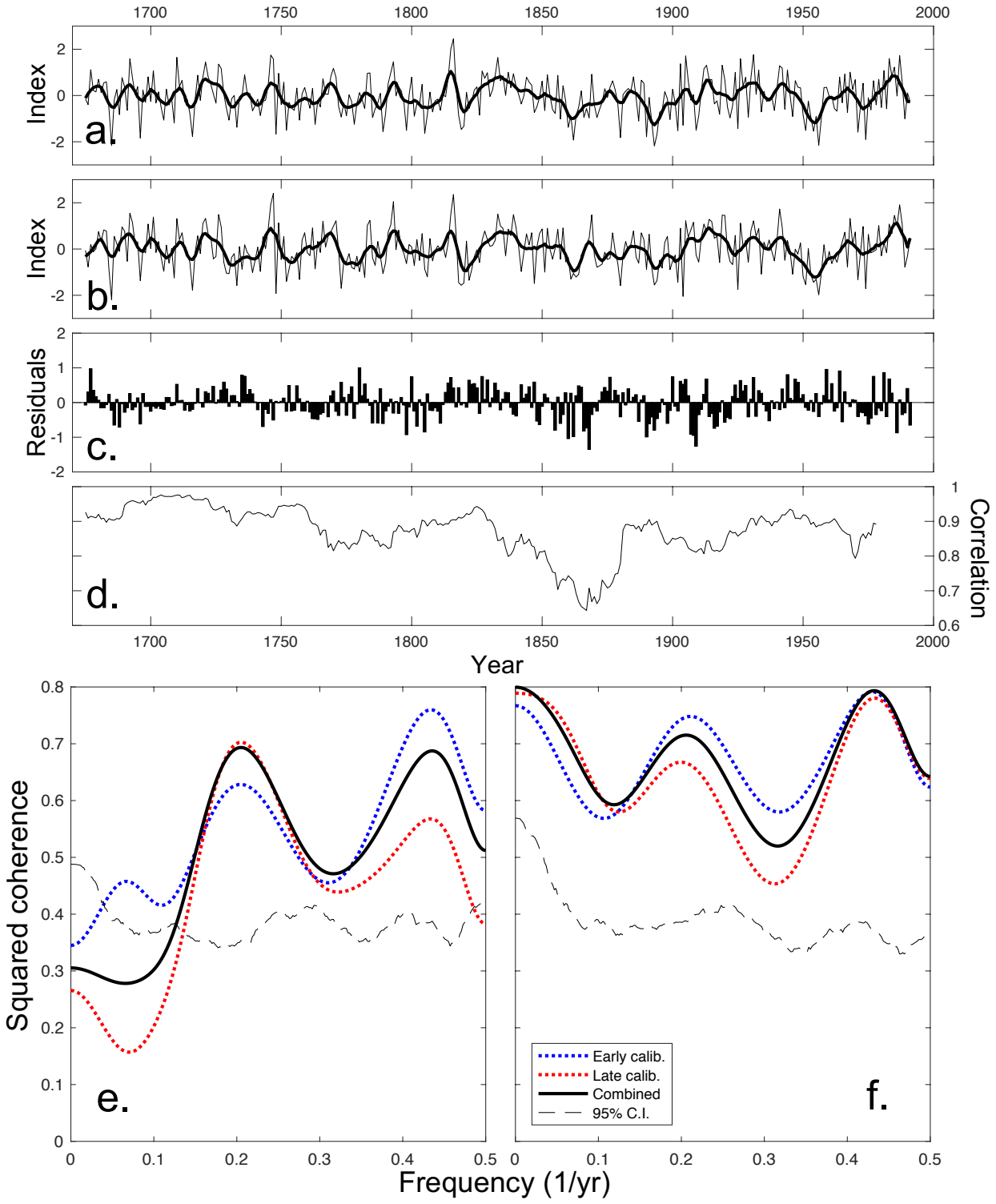

Figure 7. Reconstructions of MEI from (**a**) ALL; and (**b**) stable networks of tree-ring chronologies for 1675-1991. The residuals from linear regression is plotted in (**c**) and the running correlation (15-year window) is plotted in (**d**). The squared coherence between instrumental and reconstructed MEI for the period 1901-1991 is plotted for (**e**) ALL and (**f**) stable.

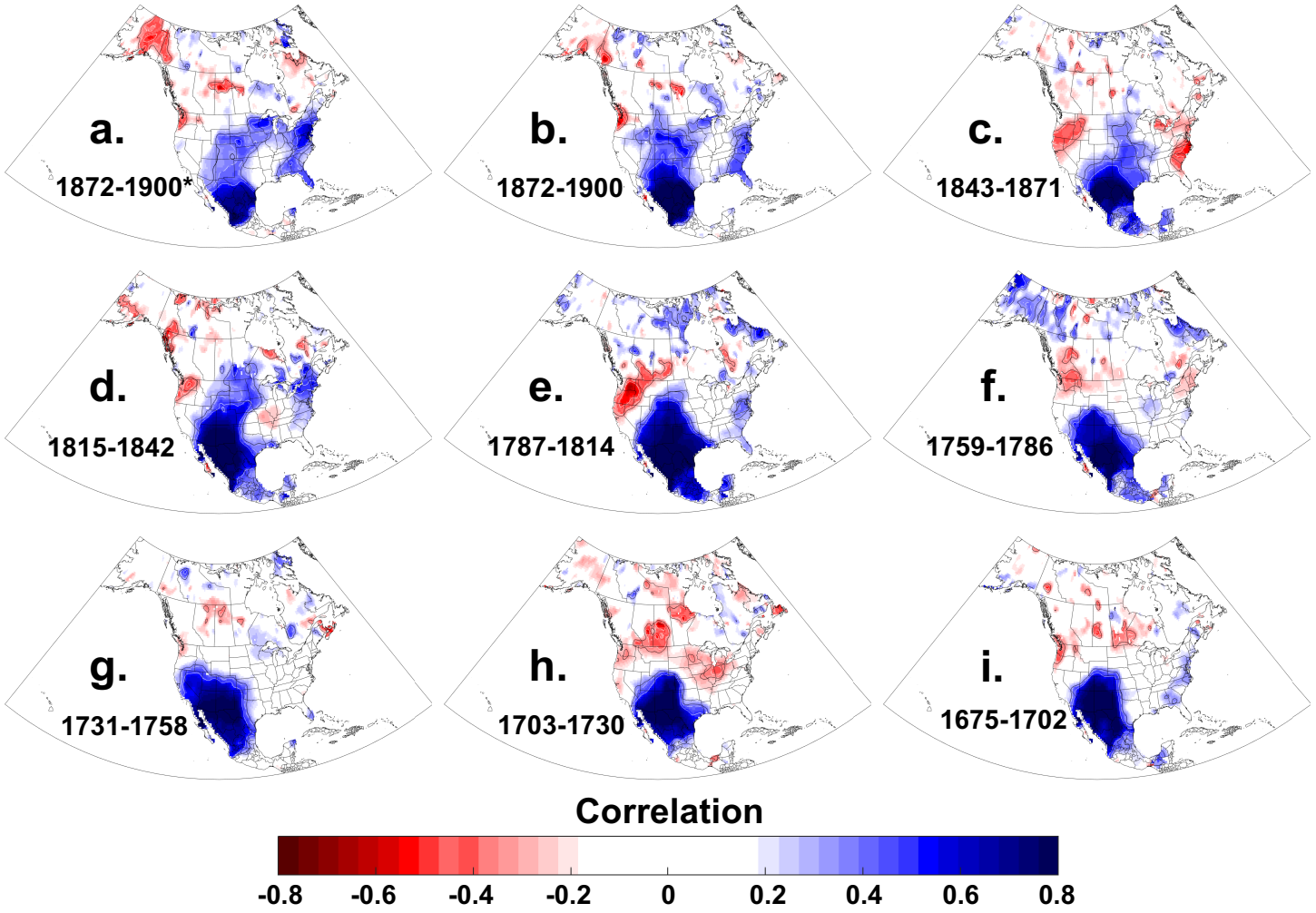

Figure 8. Local correlations between (**a**) instrumental NDJF MEI and the NADA; and (**b**-**h**) the stable reconstruction and the NADA for 28-year periods. Contours: black $p < 0.10$; white dashed $p < 0.05$; white solid $p < 0.01$.

CHAPTER 5

CONCLUSIONS

The North American tree-ring network, developed by numerous contributors over the past 50 years, represents one of the greatest sources of paleoclimate information in existence. Many of the chronologies produced several decades ago continue to provide new insights into pre-instrumental climate variability as EW and LW measurements of existing collections are being produced and analyzed (e.g. Griffin et al. 2013; Howard et al. 2018; Torbenson and Stahle 2018). The relationship between EW and LW growth is highly variable across the continent and even within a single species. Higher correlations suggest less independent LW variability, which may indicate less of an independent and separate climate signal. It may also affect the time-series properties of the adjusted LW chronologies, including the magnitude of low-frequency variability. Douglas-fir displays the largest range of correlations (from r = 0.166 to r = 0.891) of any species. The lowest correlations in Douglas-fir can be found in Mexico and correlations increase with latitude, reaching its highest in northern Arizona and Colorado. A potential explanation for this apparent spatial bias in the EW-LW relationship is the seasonal climatology of the region and the temporal evolution of monsoon rainfall, for which the start of monsoon rainfall occurs earlier in central Mexico (and therefore could provide a larger and separate portion of growing season moisture) than in the states north of the border.

The lowest average correlation between EW and LW for any conifer species is recorded for shortleaf pine in the central United States. The distribution of shortleaf pine overlaps with post oak in this region, another species that displays relatively low EW-LW correlations. Post oak chronologies make up important predictors in the reconstruction of May scPDSI. The independent variability in shortleaf pine LW is strongly connected to summer rainfall and this relationship facilitated the exceptionally strong reconstruction of JJA Z index. By extending the

limited instrumental record to cover the past 330+ years, with fidelity in the inter-seasonal relationship of the reconstructed moisture variables, it is possible to revisit studies on persistence and potential forecasting skill (e.g. Karl et al. 1987) with a much larger sample depth. The relationship between spring soil moisture and atmospheric moisture balance in the succeeding three months have fluctuated significantly during the instrumental period, varying on multidecadal timescales. The same low-frequency swings are recorded in the relationship between the reconstructions and appear to be a consistent part of the ocean-atmosphere dynamics since the 1680s. These results could have a practical application in summer rainfall prediction for the central United States and highlight the importance of high-quality paleoclimate extension of hydroclimate variables. Further investigation into the time-dependency and potential forecasting skill associated with AMO phasing is required, perhaps most urgently through climate model exercises.

The AMO also appears to play an important role in the magnitude and spatial expression of ENSO influence on North American winter precipitation. Tree growth in western North America is often limited by winter precipitation due to the large fraction of annual rainfall falling in the cool season, and the moisture-sensitive tree-ring network subsequently record the ENSO-signal changes registered in the instrumental data. Limiting predictor selection to only chronologies that remain significantly correlated with ENSO, regardless of phasing of the AMO, produces a statistically stronger reconstruction that also retains spectral properties closer to that of the instrumental data. Non-stationary signals may be a factor in other teleconnections and a similar approach could potentially yield reconstructions with increased fidelity.

Overall, the paleoclimatic data presented in this dissertation suggest that large-scale ocean-atmosphere teleconnections may have a more complex impact on North American

hydroclimate than just simple correlations with precipitation. Chapter 3 and 4 illustrate the potential role that the AMO plays in the persistence structure of seasonal moisture, as well as how it may influence other teleconnections on regional hydroclimate. Although the notion of Pacific-Atlantic teleconnection interactions is not new (e.g. McCabe et al. 2004), these results indicate that their role is complex and multifaceted. Longer records of seasonally-resolved hydroclimate are needed to gain a greater understanding of these phenomena and tree-ring based reconstructions represent the best proxies available to us.

REFERENCES

Ault, T.R., S. St. George, J.E. Smerdon, S. Coats, J.S. Mankin, C.M. Carrillo, B.I. Cook, and S. Stevenson, 2018. A robust null hypothesis for the potential causes of megadrought in western North America. *Journal of Climate* **31**: 3-24.

Bradley, R.S., 1985. *Quaternary Paleoclimatology: Methods of Paleoclimatic Reconstruction*. Chapman and Hall, London, UK.

Brauer, A., C. Endres, C. Günter, T. Litt, M. Stebich, and J.F.W. Negendank, 1999. High resolution sediment and vegetation responses to Younger Dryas climate change in varved lake sediments from Meerfelder Maar, Germany. *Quaternary Science Reviews* **18**: 321-329.

Cleaveland, M.K., 1986. Climatic response of densitometric properties in semiarid site tree rings. *Tree-Ring Bulletin* **46**: 13-29.

Cook, B.I., E.R. Cook, K.J. Anchukaitis, R. Seager, and R.L. Miller, 2011. Forced and unforced variability of twentieth century North American droughts and pluvials. *Climate Dynamics* **37**: 1097-1110.

Cook, E.R., 1985. A time-series analysis approach to tree-ring standardization. Ph.D. Dissertation, Department of Geosciences, University of Arizona, Tucson.

Cook, E.R., D.M. Meko, D.W. Stahle and M.K. Cleaveland, 1999. Drought reconstructions of the continental United States. *Journal of Climate* **12**: 1145-1162.

Cook, E.R., R.D. D'Arrigo, and M.E. Mann, 2002. A well-verified, multi-proxy reconstruction of the winter North Atlantic Oscillation since AD 1400. *Journal of Climate* **15**: 1754-1765.

Crawford, C.J., D.R. Griffin, and K.F. Kipfmueller, 2015. Capturing season-specific precipitation signals in the northern Rocky Mountains, USA, using earlywood and latewood tree rings. *Journal of Geophysical Research-Biogeosciences* **120**: 428-440.

D'Arrigo, R.D. and G.C. Jacoby, 1991. A 1000-year record of winter precipitation from northwestern New Mexico, USA: a reconstruction from tree-rings and its relation to El Niño and the Southern Oscillation. *The Holocene* **1**: 95-101.

D'Arrigo, R., R. Villalba, and G. Wiles, 2001. Tree-ring estimates of Pacific decadal climate variability. *Climate Dynamics* **18**: 219-224.

D'Arrigo, R., E.R. Cook, R.J. Wilson, R. Allan, and M.E. Mann, 2005. On the variability of ENSO over the past six centuries. *Geophysical Research Letters* **32**: L022055.

DeMenocal, P.B., 2001. Cultural responses to climate change during the late Holocene. *Science* **292**: 667-673.

Dogulass, A.E., 1919. *Climatic Cycles and Tree Growth, volume I*. Carnegie Institute of Washington, Washington, DC.

Douglass, A.E., 1920. Evidence of climatic effects in the annual rings of trees. *Ecology* **1**: 24-32.

Douglass, A.E., 1941. Crossdating in dendrochronology. *Journal of Forestry* **39**: 825-831.

Esper, J., E.R. Cook, and F.H. Schweingruber, 2002. Low-frequency signals in long tree-ring chronologies for reconstructing past temperature variability. *Science* **295**: 2250-2253.

Fritts, H.C., 1966. Growth-rings of trees: their correlation with climate. *Science* **154**: 973-979. https://doi.org/10.1126/science.154.3752.973

Fritts, H.C., D.G. Smith, J.W. Cardis, and C.A. Budelsky, 1965. Tree-ring characteristics along a vegetation gradient in northern Arizona. *Ecology* **46**: 393-401.

Fritts, H.C., 1976. *Tree Rings and Climate*. Academic Press, London, UK.

Gergis and Fowler 2009

Glock, W.S., 1937. *Principles and Methods of Tree-Ring Analysis*. Carnegie Institute of Washington, Washington, DC.

Gray, S.T., L.J. Graumlich, J.L. Betancourt, and G.T. Pederson, 2004. A tree-ring based reconstruction of the Atlantic Multidecadal Oscillation since 1567 A.D. *Geophysical Research Letters* **31**: L12205.

Griffin, D.R., C.A. Woodhouse, D.M. Meko, D.W. Stahle, H.L. Faulstich, C. Carrillo, R. Touchan, C.L. Castro, and S.W. Leavitt, 2013. North American monsoon precipitation reconstructed from tree-ring latewood. *Geophysical Research Letters* **40**: 954-958.

Guyette, R.P., R.M. Muzika, and D.C. Dey, 2002. Dynamics of anthropogenic fire regime. *Ecosystems* **5**: 472-486.

Harris, I., P.D. Jones, T.J. Osborn, and D.H. Lister, 2014. Updated high-resolution grids of monthly climatic observations – the CRU TS3.10 dataset. *International Journal of Climatology* **15**: 623-642.

Herweijer, C., R. Seager, E.R. Cook, and J. Emile-Geay, 2007. North American droughts of the last millennium from a gridded network of tree-ring data. *Journal of Climate* **20**: 1353-1376.

Howard, I.M., D.W. Stahle, and S. Feng (in press) Separate tree-ring reconstructions of spring and summer moisture in the northern and southern Great Plains. *Climate Dynamics*.

Jacoby, G.C., and R. D'Arrigo, 1989. Reconstructed Northern Hemisphere annual temperature since 1671 based on high-latitude tree-ring data from North America. *Climatic Change* **14**: 39-59.

Karl, T., F. Quinlan, and D.S. Ezell, 1987. Drought termination and amelioration: Its climatological probability. *Journal of Applied Meteorology* **26**: 1198-1209.

Kipfmueller, K.F., E.R. Larson, and S. St. George, 2012. Does proxy uncertainty affect the relations inferred between the Pacific Decadal Oscillation and wildfire activity in the western United States? *Geophysical Research Letters* **39**: L050645.

Kobashi, T., J.P. Severinghaus, E.J. Brook, J.-M. Barnola, and A.M. Grachev, 2007. Precise timing and characterization of abrupt climate change 8200 years ago from air trapped in polar ice. *Quaternary Science Reviews* **26**: 1212-1222.

Lloyd, C., 2010. *Spatial data analysis*. Oxford University Press, Oxford, UK.

Li, J., S.-P. Xie, E.R. Cook, M.S. Morales, D.A. Christie, N.C. Johnson, F. Chen, R. D'Arrigo, A.M. Fowler, X. Gou, and K. Fang, 2013. El Niño modulations over the past seven centuries. *Nature Climate Change* **3**: 822-826.

MacDonald, G.M., and R.A. Case, 2005. Variations in the Pacfic Decadal Oscillation over the past millennium. *Geophysical Research Letters* **32**: L022478.

McCabe, G.J., M.A. Palecki, and J.L. Betancourt, 2004. Pacific and Atlantic Ocean influences on multidecadal drought frequency in the United States. *Proceedings of the National Academy of Sciences of the United States of America* **101**: 4136-4141.

McKenzie, D., Z. Gedalof, D.L. Peterson, and P. Mote, 2004. Climatic change, wildfire, and conservation. *Conservation Biology* **18**: 890-902.

Meko, D.M., and C.H. Baisan, 2001. Pilot study of latewood-width of conifers as an indicator of variability of summer rainfall in the North American monsoon region. *International Journal of Climatology* **21**: 697-708.

Palmer, W.C., 1965. *Meteorological Drought.* Research Paper, vol. 45. U.S. Weather Bureau.

Paul, B.H., and R.O. Marts, 1931. Controlling the proportion of summerwood in longleaf pine. *Journal of Forestry* **29**: 784-796.

Rodrigo, F.S., D. Pozo-Vázquez, M.J. Esteban-Parra, and Y. Castro-Díez, 2001. A reconstruction of the winter North Atlantic Oscillation index back to A.D. 1501 using documentary data in southern Spain. *Journal of Geophysical Research-Atmospheres* **106**: 14805-14818.

St. George, S., D.M. Meko, and E.R. Cook, 2010. The seasonality of precipitation signals embedded within the North American Drought Atlas. *The Holocene* **20**: 983-988.

St. George, S., 2014. An overview of tree-ring width records across the Northern Hemisphere. *Quaternary Science Reviews* **95**: 132-150.

Salzer, M.W., M.K. Hughes, A.G. Bunn, and K.F. Kipfmueller, 2009. Recent unprecedented tree-ring growth in bristlecone pine at the highest elevations and possible causes. *Proceedings of the National Academy of Sciences of the United States of America* **106**: 20348-20353.

Schulman, E., 1942. Dendrochronology of pines of Arkansas. *Ecology* **23**: 309-318.

Speer, J.H., T.W. Swetnam, B.E. Wickman, and A. Youngblood, 2001. Changes in Pandora moth outbreaks dynamics during the past 622 years. *Ecology* **82**: 679-697.

Stahle, D.W., and M.K. Cleaveland, 1988. Texas drought history reconstructed and analyzed from 1698 to 1980. *Journal of Climate* **1**: 59-74.

Stahle, D.W., M.K. Cleaveland, and J.G. Hehr, 1988. North Carolina climate changes reconstructed from tree rings: AD 372 to 1985. *Science* **240**: 1517-1519.

Stahle, D.W., R.D. D'Arrigo, P.J. Krusic, M.K. Cleaveland, E.R. Cook, R.J. Allan, J.E. Cole, R.B. Dunbar, M.D. Therrell, D.A. Gay, M.D. Moore, M.A. Stokes, B.T. Burns, J. Villanueva-Díaz, and L.G. Thompson, 1998. Experimental dendroclimatic reconstructions of the Southern Oscillation. *Bulletin of the American Meteorological Society* **79**: 2137-2152.

Stahle, D.W., M.K. Cleaveland, H. Grissino-Mayer, R.D. Griffin, F.K. Fye, M.D. Therrell, D.J. Burnette, D.M. Meko, and J. Villanueva-Díaz, 2009. Cool- and warm-season precipitation reconstructions over western New Mexico. *Journal of Climate* **22**: 3739-3750.

Stahle, D.W., and J.S. Dean, 2011. North American tree rings, climatic extremes, and social disasters. In Hughes, M.K., T.W. Swetnam, H.F. Diaz (Eds.) *Dendroclimatology: Progress and Prospects*. Developments in Paleoenvironmental Research **11**: 297-327.

Therrell, M.D., and M.J. Trotter, 2011. Waniyetu Wówapi: Native American records of weather and climate. *Bulletin of the American Meteorological Society* **92**: 583-592.

Torbenson, M.C.A., D.W. Stahle, J. Villanueva Díaz, E.R. Cook, and D. Griffin, 2016. The relationship between earlywood and latewood ring-growth across North America. *Tree-Ring Research* **72**: 53-66.

Trouet, V., J. Esper, N.E. Graham, A. Baker, J.D. Scourse, and D.C. Frank, 2009. Persistent positive North Atlantic Oscillation mode dominated the Medieval Climate Anomaly. *Science* **324**: 78-80.

Villanueva-Díaz, J., D.W. Stahle, B.H. Luckman, J. Cerano-Parades, M.W. Therrell, M.K. Cleaveland, and E. Cornejo-Oviedo, 2007. Winter-spring precipitation reconstructions from tree rings from northeast Mexico. *Climatic Change* **83**: 117-131.

Watson, E., and B. Luckman, 2004. Tree-ring based reconstructions of precipitation for the southern Canadian Cordillera. *Climatic Change* **65**: 209-241.